Using Numerical Models for Managing Water Quality in Public Supply Wells

by

Marcelo Rodrigues de Sousa

A thesis
presented to the University of Waterloo
in fulfillment of the
thesis requirement for the degree of
Doctor of Philosophy
in
Earth Sciences

Waterloo, Ontario, Canada, 2013

AUTHOR'S DECLARATION

I hereby declare that I am the sole author of this thesis. This is a true copy of the thesis, including any required final revisions, as accepted by my examiners.

I understand that my thesis may be made electronically available to the public.

Abstract

Groundwater models can be useful tools to support decisions regarding the management of public water supply wells. Scientific progress and the availability of increasingly powerful computer resources provide a continuous opportunity for improving the way numerical models are applied for this purpose. In this thesis, numerical groundwater models were applied to address relevant questions regarding the management of water supply wells in two distinct glacial aquifers in southern Ontario, Canada. The objective is to propose science-based methods that can be applied in day-to-day practice in the context of source water protection. Three specific issues were addressed:

(1) Time lag in the unsaturated zone: A simplified method was proposed to assess the importance of the unsaturated zone in delaying the effects of changes at ground surface on water supply wells (*i.e.*, unsaturated zone time lag). This assessment is important because it influences field and modelling efforts to estimate well vulnerability to contamination and impacts due to changes in land use. The proposed method is based on estimations of travel time in the saturated and unsaturated zones, and provides a formal framework for an intuitive approach. For the studied case, the delay in the unsaturated zone was deemed to be significant, representing on average ~ 11 years or ~ 53% of the total travel time from ground surface to receptor. Travel times were estimated using approaches with different levels of sophistication, to evaluate the usefulness of simplified calculations. Such calculations lead to the same overall conclusion as more sophisticated and time-consuming approaches. However, when assuming limited knowledge of soil properties, common at earlier stages of most investigations, these simplified techniques generated inconclusive results.

(2) Uncertainty in capture zone delineation: A simple method was proposed to address the issue of uncertainty in capture zone delineation. This method considers uncertainty at two different scales: local (parametric) and global (conceptual). Local-scale uncertainty is addressed by using backward transport simulation to create capture probability plumes, with probabilities ranging from 0 to 100%. Global-scale uncertainty is addressed by considering more than one possible representation of the groundwater system (*i.e.*, multiple model scenarios). Multiple scenario analysis accounts for more than one possible representation of the groundwater system, and it incorporates types of uncertainty that are not amenable to stochastic treatment (*e.g.*, uncertainty due to conceptual model, to different model codes and boundary condition types). Finally, the precautionary principle is used to combine capture probability plumes generated by different scenarios. As a result, two maps are generated: One

for wellhead protection, and another for selection of priority areas for implementation of measures to improve water quality at the supply well. For the studied case, three models with different spatial distributions of recharge but with similar calibrations were considered, exemplifying the issue of non-uniqueness. The two maps obtained by the proposed method were significantly different, indicating that recharge distribution represents a major source of uncertainty in capture zone delineation.

(3) Effects of agricultural Beneficial Management Practices (BMPs) in supply wells: A numerical model framework was used to estimate the effects of measures to reduce nitrate leaching to groundwater from agricultural activities (*i.e.*, Beneficial Management Practices, or BMPs). These measures were implemented in 2003 (~ 10 years ago) at the Thornton well field (Woodstock, Ontario, Canada) to improve well water quality. This case study is based on extensive field work characterization from previous research, and allows the discussion of practical issues related with data collection and interpretation (*e.g.*, different techniques for generating mass loading distributions were compared). Regional flow was simulated in a 3D larger-scale saturated flow model, while variably-saturated flow and transport were simulated in a 3D smaller-scale, more refined grid. A vertical 1D model was used to define the discretization in the unsaturated zone of the variably-saturated flow and transport model. Results indicate that the adoption of BMPs in selected areas can be an effective strategy to improve water quality in supply wells impacted by non-point source contaminants. For the Thornton well field, the currently adopted BMPs are estimated to reduce concentrations from ~ 9.5 to ~ 7.5 mg NO_3-N/L. Water quality at the wells are predicted to respond after 5 to 10 years after implementation of BMPs, and are expected to stabilize after 20 to 30 years Management scenarios with further reductions in nitrate concentration are expected to further reduce concentrations by ~ 0.4 to ~ 0.8 mg NO_3-N/L. The proposed framework can be adapted to design and evaluate BMPs for similar problems and for other non-point source contaminants.

Some insights were common to all three issues discussed and can be useful to practitioners involved in source water protection studies: (1) Reliable recharge estimations are essential for the management of water supply wells; and (2) The use of multiple models should be encouraged to increase the understanding of different aspects of the system, assess uncertainty and provide independent checks for model predictions.

Acknowledgements

First of all, I would like to thank my supervisors Dr. Dave Rudolph and Dr. Emil Frind for all the guidance, friendship and support I received since I started my studies in Waterloo. If my work was not better or not done sooner is solely due to my own limitations. Dave and Emil provided me with absolutely everything I needed throughout my time in Waterloo. The resulting experience completely changed my life for the better and, for that, I am forever grateful. I hope I can still have the pleasure and the privilege to keep working with both in the future.

I would like to thank my committee: Dr. Jon Paul Jones, Dr. Andre Unger and Dr. Neil Thomson, from the University of Waterloo, and Dr. René Lefebvre, from the Institut National de la Recherche Scientifique (INRS). Special thanks to J.P. Jones for all the help to get me started and for the guidance throughout my studies. Also, I would like to thank Dr. Unger and Dr. Soon-Young Yu for giving me an opportunity. I wouldn't have been accepted as a student in Waterloo if it weren't for the chance you both gave me.

I would like to thank current and past members of the Rudolph Group: Dr. Brewster Conant Jr., Dr. Rengina Rahman, Jackie Brook, Dr. Steve Frey, Michael Frind, Odum Idika, Jason Cole, Dr. Claus Haslauer, Jamie Koch, Dr. Ed Cey, Kate Critchley, Joanna Passmore, Andrew Wiebe, Orin Regier, Jane Shaw, Loren Bekeris and Cailin Hillier. It was a pleasure to share the trenches with you. A big "Thank you" to my officemates: Steve Frey, Xiaomin Wang, Ismail Hussain, Ali Shafiei and Ed Cey. I have learned a lot from you and made friends for life. Thanks to Chris Neville for stimulating conversations and to Linda Truscott (Oxford County) and Michelle Fraser (Stantec) for providing me with data.

Finally, I would like to thank my friends and family for the unwavering support, patience and love. Many times throughout the past few years I did not give you enough attention and time. Please forgive me for the long silences. My plan now is to catch up and not drop the ball ever again. Thank you, Juliana Freitas, for everything.

Funding for this research was provided by the Region of Waterloo, Oxford County, Natural Sciences and Engineering Research Council of Canada (NSERC), Ontario Ministry of the Environment (MOE), the Canadian Water Network (CWN), Natural Resources Canada (NRCan) and the R.N. Farvolden Endowment Scholarship.

Dedication

I dedicate this work to three people who deeply changed my life by being great at what they do:

Dilermano "Manim" Honório de Arruda

Fernando Rebouças Stucchi

Bernhard "Beni" Müller

My goal is to inspire others as you inspired me.

Table of Contents

List of Figures

List of Tables

Chapter 1
Introduction

1.1 Background

In order to manage groundwater resources, it is important to understand the behavior and distribution of groundwater and its contaminants in the subsurface. Some examples of questions that have to be addressed for the proper management of groundwater resources are: How much water is stored in a given aquifer? How fast is it moving? How vulnerable is a water supply well to a contaminant source at ground surface?

To address some of these questions, groundwater models can be useful tools. Groundwater models are defined as any system that attempts to represent groundwater behavior (Prickett, 1979) and can be used to make predictions, entertain "what-if" scenarios, test hypotheses, assess uncertainty and support the design of field experiments and remediation efforts (Oreskes et al., 1994). Ultimately, models can be used for decision-making, decision support and deliberation (van den Belt, 2004; van den Brink et al., 2008).

In the context of water management, an important field is source water protection, which represents measures to promote safe and sustainable drinking water supplies. Numerical models are commonly used in source water protection applications, and their use is even explicitly prescribed in some regulatory guidelines, such as for the Province of Ontario (Province of Ontario, 2004; 2006).

Within source water protection activities, decisions related to the water supply well itself are critical. Pumping wells are the means by which groundwater is made readily available for human use and represent a major intervention into the natural groundwater system (Narasimhan, 2009). Some management aspects related to water supply wells are: (1) definition of areas to be protected to preserve water quantity and quality at supply wells; (2) decisions related to the operation, decommission and installation of wells; and (3) design of interventions to improve conditions at water supply wells impacted by contamination.

When numerical models are applied to support such decisions, their application involves some challenges. Some of these challenges are specific to groundwater models, such as controlling oscillations and numerical dispersion, dealing with long run times and deciding how to numerically represent processes. Others are more general and are related to the management of dynamic and heterogeneous natural systems using sparse data and imperfect representations of reality. This is the

case for many subsurface hydrology applications, as well as other fields of knowledge, such as long-term climate prediction. Examples of such challenges are: dealing with prediction uncertainty and expert bias, deciding which processes to consider in the analysis and developing ways to incorporate predictions into the decision-making process. The improvement of the use of numerical models can be made by finding better ways to describe and address these challenges and limitations.

Within this context, the goal of this thesis is to investigate possible ways to improve how numerical models are applied in source water protection problems. Although general statements about the application and limitations of models can be straightforward, how these limitations manifest in practical problems may be less intuitive. For example, it is trivial to acknowledge that model results are uncertain, but it is more complicated to quantify uncertainty and define how it should be incorporated in a given case (Pappenberger and Beven, 2006). Another example: It is trivial to state that models are simplified representations of reality, but it is less straight-forward to decide how much simplification is warranted for a given problem (Schoups et al., 2006; Doherty, 2011). Therefore, in an attempt to draw more applied and useful contributions, existing source water protection case studies are discussed, with the focus on the protection of water quality of large production water supply wells.

1.2 Objectives

As part of this thesis, three specific objectives were pursued. The first pertains to how the unsaturated zone is incorporated in numerical groundwater models. The simulation of unsaturated groundwater flow is non-linear and, consequently, much more computationally demanding than groundwater flow simulation in the saturated zone. Also, it requires the characterization of soil hydraulic parameters above the water table, which is not usually part of hydrogeological investigations. Some commonly used model codes ignore unsaturated zone flow (e.g., MODFLOW, Harbaugh et al., 2000). This simplification may be justified in some cases, but it may also result in significant errors in the analysis. In this context, the first objective of this thesis is to devise a method for deciding whether to consider the unsaturated zone in models.

The second objective relates to how uncertainty is incorporated in capture zone delineation. Capture zone is the estimated area which contributes to the flow to a given well. This area is often utilized to define land use restrictions to protect the quantity and quality of water that flows to a supply well. Groundwater numerical models are often applied to delineate capture zones, which are affected by significant uncertainty. Many techniques exist to address this problem, but their application is often not incorporated into common practice. These techniques are generally affected by two problems: (1) multiple model runs are often required, which is not practical for models that require long runs; and (2) usually only parameter uncertainty is taken into account (i.e., conceptual model uncertainty is not addressed). The second objective of this thesis is to propose a novel method to address uncertainty in capture zone delineation that avoid these two common limitations.

Finally, the last objective of this thesis pertains to the use of models to design strategies to improve water quality in supply wells. The case study of the Thornton well field (Woodstock, ON) is used to exemplify how numerical models can be applied to support groundwater management decisions. In this case study, beneficial management practices (BMPs) were implemented to reduce nitrate concentrations on supply wells. Therefore, the third and last objective of this thesis is to demonstrate the use of models to simulate the effects of BMPs in the water quality of supply wells.

1.3 Thesis organization

This thesis has five chapters, with chapters two through four discussing the specific goals previously described. These chapters were written in manuscript format, prepared as stand-alone manuscripts for submission to scientific journals. Chapters 2 and 3 are already published, as follows:

- Sousa, M.R., Jones, J.P., Frind, E.O., Rudolph, D.L. (2013) A simple method to assess unsaturated zone time lag in the travel time from ground surface to receptor, Journal of Contaminant Hydrology, Volume 144, Issue 1, January 2013, Pages 138-151 (Chapter 2);
- Sousa, M.R., Frind, E.O., Rudolph, D.L. (2013) An integrated approach for addressing uncertainty in the delineation of groundwater management areas, Journal of Contaminant Hydrology, Volume 148, May 2013, Pages 12-24 (Chapter 3).

Chapter 2

A simple method to assess unsaturated zone time lag in the travel time from ground surface to receptor

2.1 Introduction

The time taken by a solute to be transported in groundwater is important for many different practical applications. Contaminant sources - potential or existing - are often located near or at ground surface, above the water table. In these situations, the unsaturated zone may significantly affect solute transport, as it acts as a dynamic reservoir for contaminants, dampening and delaying the response at the water table to changes at ground surface (*e.g.*, Baran et al., 2007). This effect is referred as the time lag in the unsaturated zone (Cook et al., 2003, Jackson et al., 2006, Fenton et al., 2011) and it depends on a complex interaction between many different factors such as: type and properties of the porous medium, contaminant properties (*e.g.*, reactions, interactions with porous medium) and hydrological conditions (*e.g.*, precipitation, evapotranspiration, slope and runoff conditions).

An appreciation of the time lag is important for managing groundwater resources and has been the focus of many studies, such as Cook et al. (2003), Jackson et al. (2008), Iital et al. (2008), Kronvang et al. (2008), Lerner and Harris (2009), Fenton et al. (2011), Tosaki et al. (2011) and Sophocleous (2011). For example, an understanding of time lag is necessary to define monitoring and remediation strategies for aquifers or groundwater receptors (*e.g.*, wells, streams, lakes) impacted by contamination.

This issue has moved to the forefront in light of the European Union Water Framework Directive (Official Journal of the European Communities, 2000), which states that good ecological status should be achieved in all groundwater and surface water bodies by 2015. Some researchers have pointed out that this goal may not be reached due to long time lags between improvement measures and changes in water quality (Meals et al., 2010, Baily et al., 2011, Fenton et al., 2011, French et al., 2005, Wayland et al., 2002).

Numerical modelling has proven to be an invaluable tool in estimating contaminant impacts on groundwater resources, particularly in cases where partially saturated conditions are present. However, explicitly incorporating the unsaturated zone in all modelling efforts significantly increases complexity and may not always be warranted. The unsaturated flow equation is highly nonlinear and

its solution represents a much heavier computational burden than solving for saturated flow, especially for three-dimensional (3D), large-scale problems (*e.g.*, basin- or regional-scale). Excessively long execution times may have a detrimental impact on the quality of the model calibration and overall results. For example, Hill (2006) suggests that model execution times should be limited to approximately 30 minutes to allow a reasonable number of model runs for calibration, sensitivity analysis and optimization.

In addition to the heavier computational burden, the overall complexity of the problem and the difficulty in defining unsaturated soil parameters are also much higher. This may lead to more expensive and time consuming field data collection and interpretation, while not necessarily resulting in more accurate model predictions. Therefore, in most large-scale practical problems, it is reasonable to simulate unsaturated flow only if it is justifiably relevant to the question being addressed.

A common-sense approach would be to first estimate the travel time in the saturated zone, and then estimate the travel time in the unsaturated zone by some approximate technique, such as SAAT ("Surface to Aquifer Advection Time"; Province of Ontario, 2006). This will provide the total travel time, as well as the proportion of the total travel time spent in the unsaturated zone. The latter would be of interest in determining where to place the emphasis in more detailed calculations, if necessary.

The objective of this paper is to present a systematic method to support the decision of whether to explicitly account for the time lag in the unsaturated zone in earlier stages of hydrogeological investigations, providing a formal framework for the common-sense approach. This method can also be used to roughly estimate the total travel time between locations at or near ground surface and a given groundwater receptor. A series of different calculation techniques for the saturated and unsaturated zone travel times, as well as the errors involved in simplified calculations, are discussed. Finally, the method is illustrated by means of a field case. The results show that a systematic approach not only provides a framework to support a decision regarding the time lag in the unsaturated zone, but also gives much more insight than a simple common-sense estimate.

2.2 Description of method

Consider the conceptual cross-section indicated on Fig. 2.1. We propose that the decision of whether to explicitly account for the unsaturated zone or not can be supported by two values: (1) the advective travel time in the unsaturated zone t_u [T]; and (2) the estimated fraction of the travel time spent in the unsaturated zone t_r [-], which ranges between 0 and 1 and can be estimated as follows:

$$t_r = \frac{t_u}{t_u + t_s} \tag{2.1}$$

where t_u [T] is the estimated advective travel time in the unsaturated zone (*i.e.*, from ground surface to the water table) and t_s [T] the estimated advective travel time in the saturated zone (*i.e.*, from the water table to the groundwater receptor), using consistent time units.

The values of t_u and t_r represent, respectively, the absolute and relative errors in the estimation of the total travel time if the time lag in the unsaturated zone is neglected. In other words, if the unsaturated zone is ignored, the total travel time from a source at ground surface to a receptor is estimated as t_s , instead of $t_s + t_u$. Therefore, the total travel time would then be underestimated by t_u (*i.e.*, absolute error) or by t_r percent of the total travel time (*i.e.*, relative error). The decision of whether to consider the unsaturated zone can then be based on whether neglecting these two travel times (t_r and t_u) is deemed acceptable.

For example, let's suppose that for a given location of interest it is estimated that t_u ~ 5 yr and t_r ~ 0.1. The question is then: "Is it reasonable to underestimate travel time by possibly 5 years, which amounts to 10% of the total travel time?". This question should be asked in the context of other uncertainties, and of the potential cost of more detailed analysis.

For the example presented in Fig. 2.1, the fraction t_r can help support the decisions of ignoring the time lag in the unsaturated zone for point A, while explicitly taking into account for point B. For a source located at point A, ignoring the unsaturated zone would result in an error of ~ 2% in the total travel time. This error may be considered negligible when compared to other uncertainties usually involved in such problems. For point B, on the other hand, the travel time in the unsaturated zone represents ~ 50% of the total travel time. For this latter case, the unsaturated zone demands more

attention and arguably needs to be taken into account in further modelling and field efforts. In other situations, the value of t_u may be the dominant factor for the decision. For example, the same 50 percent of the travel time in the unsaturated zone (*i.e.*, $t_r \sim 0.5$) may be considered "negligible" if the travel time t_u is ~ 0.5 yr and "relevant" if it is ~ 15 yr. This means that the time lag in the unsaturated zone can be disregarded only if both t_u and t_r are acceptably small for the specific situation at hand.

In some cases, the estimated values of t_r and t_u may not lead to a conclusive assessment. The alternatives in these ambiguous situations are: (1) ignore the unsaturated zone time lag as a first approximation and revisit the evaluation once more information is collected or a saturated model is developed; (2) pre-emptively account for the time lag in the unsaturated zone, assuming it is relevant; or (3) refine estimates of advective travel times by collecting more data or using more accurate estimation techniques, and re-evaluate the problem. The proposed method is summarized on the decision tree presented on Fig. 2.2.

2.3 Techniques for estimating advective travel time

A practical issue regarding the application of this method is the level of accuracy required in the estimation of advective travel times in the saturated (t_s) and unsaturated (t_u) zones. Different techniques can be used, ranging in complexity from calibrated variably-saturated groundwater numerical models to simplified "back-of-the-envelope" calculations. For the context of this work, simplified calculations are defined as techniques that can be implemented by hand or using spreadsheets, and which can provide a quick but rough approximation of more rigorous approaches. Simplified approaches may be useful for practitioners, as long as applied in the right context and with full understanding of their embedded simplifying assumptions. Some techniques for estimating the unsaturated and saturated travel times are described in the following sections.

2.3.1 Advective travel time in the unsaturated zone (t_u)

The advective travel time in the unsaturated zone depends directly on groundwater recharge, which in turn depends on a combination of intrinsic soil properties and hydrologic conditions. A reasonable estimate of the average annual recharge (*i.e.*, averaged over an entire hydrological cycle) is critical for the application of this method. Ideally, this estimation should be done using field-based techniques, as presented by Scanlon et al. (2002), for example.

Given an estimate of the annual average recharge R [L/T] and assuming vertical flow in the unsaturated zone, the average downward groundwater velocity (v) at a point located at an elevation z above the water table can be estimated by dividing the Darcy flux (recharge R, in this case) by the soil porosity. For flow in the unsaturated zone, the porosity term can be multiplied by saturation to account for partially-saturated media. The obtained equation is:

$$v(z) = \frac{R}{n_{ef}(z) \cdot S(z)} \tag{2.2}$$

where R is groundwater recharge [L/T], S is the water saturation [-] and n_{ef} is the effective porosity [-]. Both S and n_{ef}, and consequently v, may vary depending on the elevation above the water table (z), as a function of soil properties and flow conditions. Note that the effective hydraulic conductivity is implicitly taken into account in Equation 2.2 through the recharge magnitude (R).

Using Equation 2.2, the advective travel time in the unsaturated zone (t_u) can be calculated as:

$$t_u = \int_0^L \frac{1}{v(z)}\, dz \quad \rightarrow \quad t_u = \int_0^L \frac{n_{ef}(z) \cdot S(z)}{R}\, dz \tag{2.3}$$

where L is the thickness of the unsaturated zone [L], which can be estimated using data from observation wells. Recharge R and effective porosity n_{ef} are commonly estimated either from field data or the literature. Therefore, different techniques for assessing the advective travel time t_u only differ in the way the saturation term ($S(z)$) of Equation 2.3 is evaluated.

Three different alternatives to estimate the saturation term $S(z)$ are compared: (1) one-dimensional (1D) variably-saturated modelling; (2) van Genuchten equation assuming no-flow; and (3) tabulated values from the "Surface to Aquifer Advection Time" (SAAT) vulnerability technique (Province of Ontario, 2006).

2.3.1.1 One-dimensional variably-saturated numerical model

The first alternative to estimate the saturation term $S(z)$ is to use a 1D numerical model to solve the steady-state flow equation for variably-saturated media, as follows:

$$\frac{\partial}{\partial z}\left(K(\psi)\frac{\partial h}{\partial z}\right) = 0 \tag{2.4}$$

where h is the hydraulic head [L] and K is the vertical hydraulic conductivity for a variably-saturated medium [L/T], represented as a function of pressure head ψ [L]. Vertical groundwater flow is imposed by assigning a recharge rate at the top of the column (*i.e.*, ground surface) and a constant head $h = z$ (therefore, $\psi = 0$) at the bottom of the column, representing the average water table position, as shown in Fig. 2.3.

Saturation is commonly represented as a function of the pressure head ψ, and is determined iteratively in conjunction with vertical distributions of hydraulic head and hydraulic conductivity in

the unsaturated zone. For the problem in question, the van Genuchten equations for representing saturation (S) and hydraulic conductivity (K) as functions of pressure head ψ (van Genuchten, 1980) were used, as follows:

$$S(\psi) = \begin{cases} S_r + \dfrac{1 - S_r}{\left(1 + |A \cdot \psi|^n\right)^m} & \text{for } \psi < 0 \\ 1 & \text{for } \psi \geq 0 \end{cases} \tag{2.5}$$

$$K(\psi) = \begin{cases} K_s \cdot S_e^{\lambda}\left[1 - \left(1 - S_e^{1/m}\right)^m\right]^2 & \text{for } \psi < 0 \\ K_s & \text{for } \psi \geq 0 \end{cases} \tag{2.6}$$

where: $S(\psi)$ = saturation [-] at pressure head ψ [L], S_r = residual saturation [-], S_e = effective saturation = $(S - S_r)/(1 - S_r)$, K_s = saturated hydraulic conductivity [L/T], A = an empirical coefficient related to the inverse of air-entry pressure [L^{-1}], n = an empirical coefficient related to pore-size distribution [-], λ = empirical pore-connectivity parameter [-], assumed to be 0.5 for most soils (Mualem, 1976), and $m = 1 - 1/n$. For this paper, the simulations were performed using the code Hydrogeosphere (Therrien et al., 2005) although many other commercially available models could also be used.

This technique is considered to be the most accurate in the context of this paper. The other two alternatives to be discussed are simplified calculations that can be performed by hand or using a spreadsheet.

2.3.1.2 "No-flow" van Genuchten

The first simplified technique is to calculate the saturation profile in the unsaturated zone by applying the van Genuchten equation while assuming no-flow conditions in the unsaturated zone. Assuming no-flow is obviously not strictly correct, since estimating advective travel time only makes sense if there is some flow through the soil profile (*i.e.,* recharge R is different than zero). However, this assumption allows an approximate calculation of the saturation profile without the need for simulating unsaturated flow but taking into account different soil properties and their position in relation to the water table. The estimated saturation profile is then incorporated into Equation 2.3 to determine the advective travel time. This approach always underestimates the saturation value and the advective travel time in the unsaturated zone t_u when compared with the numerical model approach, and therefore can be used to provide a lower bound for the advective travel time in the unsaturated zone.

The approximate saturation profile is obtained by assuming that the hydraulic head (h) equals zero throughout the entire unsaturated soil column, as follows:

$$h = 0 \rightarrow \psi + z = 0 \rightarrow \psi = -z \tag{2.7}$$

where z is the elevation above the water table. With this assumption, Equation 2.5 can be rewritten as:

$$S(\psi) = \begin{cases} S_r + \dfrac{1 - S_r}{\left(1 + \left|A \cdot z\right|^n\right)^m} & for\ z > 0 \\ 1 & for\ z \le 0 \end{cases} \tag{2.8}$$

From Equation 2.8, the saturation term in Equation 2.3 can be calculated in a simple spreadsheet, for example using the trapezoidal rule to evaluate the integral term.

2.3.1.3 Surface to Aquifer Advection Time (SAAT)

The second simplified technique to estimate t_u consists of using tabulated values for mobile moisture content depending only on the soil texture (Table 2.1), as proposed in the SAAT (Surface to Aquifer Advection Time) vulnerability approach (Province of Ontario, 2006). These tables can be elaborated on a site-specific basis, depending on the available data. The travel time in the unsaturated zone is then estimated as follows:

$$t_u = \frac{\overline{\theta} \cdot L}{R} \tag{2.9}$$

where $\overline{\theta}$ is the average mobile moisture content [-].

2.3.2 Advective travel time in the saturated zone (t_s)

For the travel time in the saturated zone, two techniques were evaluated: (1) particle tracking associated with a calibrated 3D model, considered the most accurate within the context of this paper, and (2) a simplified calculation based on the direct application of Darcy's law with some simplifying assumptions.

2.3.2.1 Particle tracking

This technique requires initially the development and calibration of a 3D flow model. Then, particle tracking techniques can be applied to trace the expected pathway between the water table at the source and the groundwater receptor, as well as the timeframe for arrival. This is usually achieved by placing particles at the water table and tracking them forward along the groundwater flow system.

For this work, particle tracking was performed using the code FEFLOW (Diersch, 2006), although many other commercially available codes could also be used. Particle tracking in FEFLOW is based on the 4th-order Runge-Kutta method, which is highly accurate for situations in which there is no sharp contrast in hydraulic conductivity along the flow path. An alternative more suited for general application is the Pollock method (Pollock, 1994), which is embedded in groundwater codes such as MODFLOW (Harbaugh et al., 2000). A similar approach suitable for finite element models is

WATRAC (Frind and Molson, 2004), which is linked to WATFLOW (Molson et al., 2002). However, the approach adopted by FEFLOW was considered adequate for the problem in question.

2.3.2.2 Straight-line approximation

The second technique is based on approximating the 3D travel path in the saturated zone by a straight line (Fig. 2.4). A series of simplifying assumptions are made: (1) flow is steady-state in a homogeneous, unconfined aquifer; (2) the flow path in the saturated zone can be approximated by a horizontal straight line between the source and the receptor; and (3) the hydraulic gradient is uniform along the flow path. Under these assumptions, if Darcy's equation is applied between the water table beneath the source and the groundwater receptor, we have:

$$q = -K \cdot i \rightarrow |q| = |K \cdot i| \tag{2.10}$$

where q is the Darcy flux [L/T], K is the hydraulic conductivity [L/T] and i is the hydraulic gradient [-], assumed to be simply the hydraulic head difference between the water table elevations at the source and the receptor (Δh) divided by the horizontal distance D (*i.e.*, $i = \Delta h$ / D). It is also known that:

$$|q| = |v| \cdot n_{\text{ef}} \tag{2.11}$$

and:

$$|v| = \frac{D}{t_{\text{s}}} \tag{2.12}$$

where v is the average linear horizontal velocity [L/T] and n_{ef} is the effective porosity. If we substitute Equations 2.11 and 2.12 into the expression of Darcy's equation (Equation 2.10), and

isolate the t_s term, the final expression for estimating the advective travel time in the saturated zone (t_s) becomes:

$$t_s = \frac{D^2 \cdot n_{ef}}{K \cdot \Delta h} \tag{2.13}$$

Although the assumptions for deriving Equation 2.13 above are commonly violated for most practical applications, this approach can still be useful. The errors associated with these simplifying assumptions can be relatively small in comparison with the uncertainty related to the unknown hydraulic conductivity field, which can be the major source of uncertainty in many cases. This technique was developed for unconfined aquifers, but it can also be adapted for situations in which the aquifer of interest is confined. In these cases, saturated flow can be considered vertical in the aquitard and horizontal in the aquifer.

2.4 Limiting cases

To compare the presented alternatives for calculating the travel time in the unsaturated zone (t_u), these techniques were applied to four cases which should bracket a wide variety of common field applications. Two arbitrary soil types were considered: a fine-grained (sandy silt) and a coarse-grained (coarse sand) material. The annual recharge used in the calculation was based on examples taken from the literature: 119 mm/yr for a sandy silt soil from a site located in the Yakima County, Oregon (Fisher and Healy, 2008) and 925 mm/yr for a coarse sand soil from a site in Abbotsford, British Columbia (Chesnaux and Allen, 2008). These significantly different recharge rates represent distinct overall recharge conditions, not only related to soil characteristics, but also to climate, precipitation, topography, land use, *etc*.

These two combinations of soil type and recharge (*i.e.*, (1) sandy silt with 119 mm/yr of recharge; (2) coarse sand with 925 mm/yr of recharge) were applied to both a "thick" (30m) and a "thin" (1m) unsaturated zone. The van Genuchten empirical coefficients and hydraulic conductivity in the unsaturated zone (Table 2.2) were estimated based on the soil texture description and pedo-transfer functions (Schaap et al., 1999).

The estimated advective travel times for these limiting cases are shown on Table 2.3. The error with respect with the numerical modelling approach is smaller for thinner unsaturated zones. The "no flow" van Genuchten approximation tends to perform better for the coarser soil case, in which hydraulic gradients are smaller and hence more similar to the assumption implied in its derivation (*i.e.*, no vertical hydraulic gradient). The performance of the SAAT technique depends on the representativeness of the defined average moisture content, so no generalizations can be made regarding its performance in comparison with 1D numerical model estimations. The results shown in Table 2.3 were calculated using the mobile moisture content values shown in Table 2.1.

Both the "no-flow" van Genuchten approach and the SAAT approach can be used to roughly estimate advection travel times in the unsaturated zone, with varied levels of success based on the four studied limiting cases. Errors can be substantial, such as in the case of the "thick" unsaturated zone with fine grained material, but depending on the context of the project, these approximations can provide reasonable approximations of 1D model results, as shown for the "thin" unsaturated zone case.

2.5 Example application: Thornton well field site

The Thornton well field site, situated near the City of Woodstock, ON, is located within a complex glacial aquifer system in southern Ontario, Canada. This well field currently provides approximately 6,000 m^3/day of water to Woodstock (County of Oxford, 2011) and it is surrounded mostly by agricultural areas. An increasing trend in groundwater nitrate concentrations in the production wells has been observed over the last few decades and, in order to address this water quality issue, nutrient management practices have been implemented since 2003 in a farmland located within the estimated capture zone of the supply wells (Haslauer, 2005). Previous studies were conducted to characterize the site hydrogeology (Padusenko, 2001; Haslauer, 2005) and to estimate recharge and nitrate mass loadings before and after implementation of nutrient management practices (Bekeris, 2007; Koch, 2009).

A numerical model was proposed to evaluate the time frame that would be required for nitrate concentrations to change in the supply wells in response to changes in nutrient application practices. For the proper development of this numerical model and future investigation efforts, it is important to have an appreciation of the importance of the unsaturated zone on the overall problem.

To assess the time lag in the unsaturated zone for the Thornton well field, the method described in Section 2 was applied. As commonly observed in many non-point source problems, soil properties, topography and land use practices are variable across the area of interest. To account for this variability, Equation 2.1 was applied to nine different test locations within the farmland in which changes in land use were implemented (Fig. 2.5).

For each of these test locations, observation wells were used to estimate the average water table position. The soil texture in the unsaturated zone was determined from soil cores (Fig. 2.6). Average recharge values were estimated using applied conservative tracers (Bekeris, 2007; Koch, 2009). Estimated annual recharge and average depth to the water table are presented in Table 2.4. The van Genuchten empirical coefficients and hydraulic conductivity in the unsaturated zone were taken from Table 2.2.

To compare different approaches, the assessment of the unsaturated zone importance was made using alternative combinations of techniques to estimate t_u , t_s and consequently t_r , namely: (1) Numerical modelling; (2) Simplified calculations using a narrower range of K values; and (3) Simplified calculations using a wider range of K values. Approach (1) is considered more accurate

and labor intensive, while (2) and (3) are simplified approximations that can be quickly performed by practitioners. These approaches are summarized in Table 2.5 and are described in the following:

- Numerical modelling: The numerical modelling approach estimates the advective travel time in the unsaturated (t_u) and saturated (t_s) zones using, respectively, a 1D variably saturated model and particle tracking from a calibrated saturated 3D numerical model.
- Simplified calculation with narrower range of K values: For the simplified estimation of the travel time in the saturated zone, two different sets of hydraulic conductivity (K) values were used. The first set uses a narrower range of K values (7×10^{-4} m/s and 2×10^{-4} m/s) taken from the same spatially variable K distribution used in the saturated model for the aquifer in which the pumping wells are screened. This distribution was based on the slug tests and additional field data which were incorporated into a numerical model and adjusted to achieve calibration. The objective of considering this first set of K values is to compare simplified estimations with a more rigorous technique (particle tracking), assuming the same knowledge regarding the hydraulic conductivity distribution.
- Simplified calculation with wider range of K values: The second set of values is similar to what a practitioner would encounter in the preliminary stages of a hydrogeological assessment. For this case, a broader range of K values is used (1×10^{-3} m/s and 1×10^{-5} m/s), based on a series of slug tests performed in the aquifer unit in which the supply wells are screened.

2.5.1 Results for the Thornton well field

To illustrate the differences between the alternative techniques discussed in this paper, Fig. 2.7 shows a comparison of the saturation profiles calculated for test location 6 (Fig. 2.6) using different approaches to estimate travel time in the unsaturated zone (t_u). Fig. 2.7 shows water saturation *vs.* elevation above the water table, where three different soil textures are identified: clayey sand, medium sand and silty sand, listed from ground surface to the water table. The saturation obtained using the SAAT technique is calculated through the expression:

$$S = \frac{\theta}{n} \tag{2.14}$$

where θ is the volumetric water content, assumed as the average mobile moisture content $\overline{\theta}$, shown on Table 2.1, and n is the total porosity, assumed as the effective porosity n_{ef}, presented in Table 2.2. Therefore, the SAAT saturation values do not depend on the elevation above the water table, remaining constant and uniform for each soil texture. The saturation values from the 1D numerical model were obtained using Hydrogeosphere, using a model setting as indicated in Fig. 2.3. These saturation values depend not only on soil parameters, but also on recharge and elevation above the water table. Finally, the saturation values for the "no-flow" van Genuchten case were obtained using Equation 2.8, which depends solely on soil parameters and elevation above the water table. These saturation values do not depend on recharge, since no-flow conditions are assumed in the derivation of Equation 2.8. Saturation values obtained by this technique are smaller than or equal to those obtained using a numerical model. Fig. 2.8 shows a comparison between pathways calculated by particle tracking and those assumed in the straight-line approximation for estimating travel time in the saturated zone (t_s).

The obtained results for all test locations are presented in Table 2.6. For the unsaturated zone, the simplified techniques underestimated travel times when compared with estimates using 1D modelling. For the saturated zone, the same tendency is observed for the narrow range of hydraulic conductivity. For this case, underestimated travel times in both the saturated (t_s) and unsaturated (t_u) zones compensate for each other in the calculation of the relative travel time t_r. For the case when a broader range of K values is assumed, estimated travel times in the saturated zone spanned over a very wide range (from ~ 1 yr to several decades). Consequently, t_r varied from small (~ 0.01 to ~ 0.05) to high (~ 0.4 to ~ 0.9) values.

Results for relative travel time t_r are shown in Fig. 2.9. For the simplified estimations, only the maximum and minimum t_r values are plotted, with the intention of assessing the ability of simplified calculations to provide bounds for predictions made using numerical models (*i.e.*, 1D numerical modelling combined with particle tracking). The results using the ranges of K values $7x10^{-4}$ to $2x10^{-4}$ m/s (*i.e.*, narrower range); and $1x10^{-3}$ to $1x10^{-5}$ m/s (*i.e.*, broader range) are shown in Figs. 2.9a and 2.9b, respectively.

The results presented in Fig. 2.9 and Table 2.6 are summarized in Table 2.7. These results can be used to formulate an objective question that can guide the decision regarding whether to consider the time lag in the unsaturated zone. For example, assuming the results calculated by the numerical modelling approach, the key question to be addressed is: "Is it reasonable to neglect an average time

lag of ~ 11 yr (ranging from 2 yr to 32 yr) or ~ 53% (ranging from 26% to 82%) of the total time lag by disregarding the unsaturated zone?". Based on these results, it was considered unreasonable to neglect the unsaturated zone time lag for the Thornton well field. Therefore, subsequent modelling and field efforts should explicitly take the unsaturated zone into account.

The judgment regarding the consideration of the unsaturated zone would arguably be the same for the simplified approach with the narrow range of *K* values. So, for this case, the increased accuracy from a more sophisticated approach would not lead to a different decision, provided the same level of knowledge regarding the hydraulic conductivity field.

For the case when a broader range of *K* values was used, the situation is significantly different. The maximum and minimum estimations cover a very wide range of values, as can be seen in Table 2.7 and Fig. 2.9b. In practical terms, this means that the time lag in the unsaturated zone could be either "relevant" or "negligible" and that there is a high uncertainty regarding the role of the unsaturated zone in the overall problem. If the broad-range results were the only available information, the results would be inconclusive to support any firm decisions. In this case, the protocol for inconclusive cases could be used.

2.6 Discussion

For the application of this method, some practical considerations should be kept in mind. A major one is that there are no straightforward and general threshold values of t_r and t_u which distinguish between "negligible" and "relevant" time lags in the unsaturated zone. These threshold values should be defined on a case-by-case basis. The criteria to be used depend on many factors, such as the objective of the analysis, the solutes of interest and whether they undergo reactions, and whether ignoring the unsaturated zone is a conservative assumption.

Despite all the subjectivity and fuzziness that are inherent to this decision for most practical cases, the calculation of t_r and t_u provides a quantitative basis for discussion. It can be useful as a screening tool for a preliminary assessment of the importance of the unsaturated zone. Also, it helps to justify, communicate and document modelling decisions, which facilitates model audits, reconstruction and reproducibility (Refsgaard and Henriksen, 2004).

Practitioners may be more inclined to ignore the unsaturated zone for situations in which underestimating the travel time leads to conservative predictions. This is usually the case when the focus is the protection of ground water receptors (*e.g.*, estimating arrival times of potential contaminants from ground surface to a supply well for source water protection purposes). In other situations, ignoring the time lag in the unsaturated zone is not a conservative assumption. An example is the design of mitigation measures to improve water quality at impacted groundwater receptors (*e.g.*, estimating changes in water quality following reductions on contaminant loading at ground surface). In these cases, the unsaturated zone acts as a storage for contaminants that are gradually released to the water table. Ignoring the unsaturated zone, in these cases, may result in overly optimistic predictions of the time required for improvements in groundwater quality.

Baily et al. (2011) mentions that managing the expectations of policy makers regarding realistic timeframes for improvements in water quality is a challenge. This approach can be used for a quick and simplified estimation of the time required for water quality improvements in groundwater receptors following measures taken to reduce contaminant loading to aquifers. The simplicity and swiftness of application of this method can be beneficial in interactions with a wider community. However, it is important to keep in mind that the primary objective of this method is to guide a technical decision within a wider scope of work. It does not attempt to accurately estimate the actual time expected for water quality improvements.

It is important to keep in mind that the development of a numerical model can not only constrain the range of hydraulic conductivity values through calibration and validation, and hence reduce the uncertainty of estimations, but can also bring other insights that go beyond simply the ability to make predictions. Therefore, simplified techniques are intended to provide a useful first estimate of the advective travel time, and not be a replacement for a more detailed numerical model.

The uncertainty associated with the estimation of the hydraulic conductivity field, recharge and stratigraphy, or even uncertainties in the conceptual model should be taken into account in the analysis. It is reasonable to neglect the high complexity and computational burden associated with the unsaturated zone if its expected effect on the travel time is small in comparison to other uncertainties in the problem. This is often the case in preliminary stages of site characterization. Unfortunately, for most practical situations, all other uncertainties involved are not known *a priori*, so the decision between "relevant" and "negligible" is subjective to a certain extent.

A possible way to address the issue of parameter uncertainty and variability, both in time and space, is to use ranges of values, as presented in the Thornton well field case study. Although in this case study only hydraulic conductivity ranges were considered, a similar approach can be applied to any parameter in the analysis. Alternatively, more rigorous but more costly approach to address uncertainty in travel time estimations is Monte Carlo analysis, as demonstrated by Baily et al. (2011).

For inconclusive cases, provisionally ignoring the unsaturated zone is more adequate for preliminary stages of work and for larger and more complicated problems. Assuming the time lag is significant in inconclusive cases is more appropriate for cases in which the computational burden associated with accounting for the unsaturated zone is smaller. The following questions may help to guide the decision: What are the potential consequences of underestimating the total travel time from ground surface to receptor? What are the expected costs and time required for: (1) pre-emptively accounting for the unsaturated zone? and (2) developing further studies to better estimate the travel time in both the saturated and unsaturated zones? The decision can then be based on a simple cost/benefit analysis.

2.6.1 Limitations

Haitjema (2006) argues that a "rule of thumb" should be applied only if its origin and limitations are clearly understood. The same applies to the proposed method. All techniques described in this work assume vertical downward flow between ground surface and the water table. Horizontal flow that

may take place in perched water tables is not considered. Macropores and preferential flow paths that may play an important role (Beven and Germann, 1982) are not taken into account.

Vertical flow through the capillary fringe is also assumed, which is not always the case. Some studies discuss lateral flow and contaminant transport in the capillary fringe, such as Freitas and Barker (2011) and Berkowitz et al. (2004). However, the error associated with this assumption is expected to be small for situations in which the thickness of the capillary fringe is small in comparison with the depth of the water table.

This method assumes steady-state flow conditions. This is a reasonable assumption for situations in which the travel time from source to receptor encompasses many hydrological cycles, dampening the influence of seasonal variations.

Advection is assumed to be the main transport process between source and receptor. In cases in which dispersion is expected to play a major role, this method should not be applied. Although this method is most suited for conservative solutes because reactions are not explicitly considered, it can still be useful for situations involving reactive components. For example, the retardation factor can be used to correct advective travel times to account for sorption. Another option is to use travel time estimates in simple calculations to evaluate contaminant decay, or to predict the fate of reactive contaminants in 1D reactive transport models. These models can then be used to assess how important it is to consider reactions in the unsaturated zone.

There may be other reasons for considering the unsaturated zone, other than the time lag in advective travel time. Some examples are situations in which perched features play an important role or problems involving groundwater interaction with atmosphere or surface water. Practitioners should keep in mind all other potentially relevant processes when developing the conceptual and numerical models.

As in many other techniques, the reliability of this method strongly depends on the hydrogeological setting and on the accuracy of estimated representative bulk values for main parameters, such as hydraulic conductivity and recharge. Therefore, it is impossible to make general statements regarding the reliability of the approach.

2.6.2 Next step: How to account for the unsaturated zone?

If the time lag in the unsaturated zone is deemed important for the overall problem, the practitioner then needs to decide how to take it into account. There are many different strategies to do so, ranging

from using sophisticated variably-saturated 3D codes to simple spreadsheets or 1D model runs to adjust predictions made using saturated models.

Although this work does not intend to address this specific question, the options provided for the preliminary assessment of the role of the unsaturated zone can also serve as a guide for the level of sophistication chosen for more detailed calculations. If we expect the unsaturated zone to play a decisive role in travel time predictions, we should consider using more accurate and sophisticated approaches, both in data collection and in numerical analysis.

Also, if the main concern is advective travel time from source to receptor, estimated t_u values (advective travel time in the unsaturated zone) can be used as a preliminary correction to adjust predictions made using saturated models. In these cases, the total travel time can be estimated by the sum of t_u and t_s.

If the unsaturated zone is expected to play an important role in only a small part of the study area, approaches that consider the unsaturated zone in only a few areas can be used. One alternative is to use 1D models or analytical solutions to account for the unsaturated zone time lag in selected locations. These results can be used to correct saturated model predictions or boundary conditions at the water table. Alternatively, the unsaturated zone can be explicitly taken into account for the whole area of interest.

2.7 Conclusion

The proposed method provides an intuitive, simple way to help practitioners to assess the role of the unsaturated zone in situations in which there is a concern with the advective travel time from ground surface to a groundwater receptor. Although this decision is expected to remain somewhat subjective in most practical cases, this method should contribute to more objective and transparent decisions. The estimation of advective travel times, required to apply the proposed method, can be made using alternative techniques, with different levels of sophistication. Simplified techniques were shown to provide a quick way to generate a rough estimate of these advection times.

For the Thornton site, when the same knowledge of the hydraulic conductivity is assumed, simplified formulations lead to the same overall decision as numerical models, regarding the need to account for the time lag in the unsaturated zone. However, this case also shows that errors associated with simplified formulations can be substantial, even when the same hydraulic conductivity distribution is assumed. Therefore, these expressions can only be used to obtain rough estimates of travel time, which may be useful in preliminary stages of the work or to independently check the order of magnitude of model results.

When a rough knowledge of the hydraulic conductivity values is assumed (through the use of a wide range of possible K values), these simplified expressions lead to inconclusive results in the Thornton case. This outcome serves as a convenient way for practitioners to quickly illustrate to non-specialists the need for a better understanding of soil hydraulic properties. It also shows that field characterization is the starting point to assess the relative importance of different processes, a fundamental step to develop a useful conceptual model.

The results for the Thornton well field site also illustrate that the importance of the unsaturated zone may vary for different locations within the same site, due to different soil properties, recharge rates, unsaturated zone thicknesses and position relative to the groundwater receptor. This fact should be taken into account when planning further field studies.

Decisions based on the proposed approach should be revisited as the conceptual and numerical models are refined. This practice is consistent with common data and time limitations faced by practitioners in the earlier phases of hydrogeological assessments, as well as with the principle of gradual and conscious incorporation of complexity in the model, considered a good modelling practice, as suggested by Hill (1998) and Bredehoeft (2010). The proposed method aims to help with

this process, by providing a clear way to document model decisions. Finally, the proposed method gives valuable insight that extends much beyond what would normally be obtained from the estimation of travel times alone.

2.8 Figures and tables

Table 2.1. Mobile moisture content ($\bar{\theta}$) for different soil textures (Province of Ontario, 2006).

Soil Texture	Mobile moisture content ($\bar{\theta}$)
Sand	0.10
Loam	0.25
Clay	0.40

Table 2.2. Adopted soil parameters (based on Schaap et al.,1999).

Soil Texture	Hydraul. conduct.	Effective porosity	Residual satur.	van Genuchten coefficient	
	K [m/s]	n_{ef} [-]	S_r [-]	A [m^{-1}]	n [-]
Clay	1×10^{-11}	0.47	0.098	1.49	1.25
Silty clay	1×10^{-10}	0.45	0.111	1.62	1.32
Clayey silt	1×10^{-9}	0.45	0.079	1.58	1.42
Sandy clay	1×10^{-8}	0.43	0.117	3.34	1.21
Gravelly clay	5×10^{-8}	0.42	0.117	3.34	1.21
Silt	8×10^{-8}	0.43	0.050	0.66	1.68
Sandy silt	5×10^{-7}	0.41	0.039	2.67	1.45
Gravelly silt	1×10^{-6}	0.41	0.039	2.67	1.45
Clayey sand	5×10^{-5}	0.40	0.049	3.48	1.75
Silty sand	5×10^{-4}	0.37	0.049	3.48	1.75
Fine sand	1×10^{-3}	0.38	0.036	2.51	3.55
Medium sand	5×10^{-3}	0.36	0.053	3.52	3.18
Coarse sand	1×10^{-2}	0.38	0.030	29.4	3.28
Gravel	5×10^{-2}	0.28	0.005	493.0	2.19

Table 2.3. Estimation of advective travel time in the unsaturated zone for arbitrary limiting cases. The absolute error with respect to the numerical modelling approach is shown in parentheses.

Unsat. thickness	Approach	Sandy silt R = 119 mm/yr		Coarse sand R = 925 mm/yr	
		Time	Abs. error	Time	Abs. error
Thick (30 m)	1D num. model	71 yr	–	0.7 yr	–
	"No flow" vG	28 yr	43 yr	0.4 yr	0.3 yr
	SAAT	50 yr	21 yr	3.2 yr	2.5 yr
Thin (1 m)	1D num. model	2.8 yr	–	9 d	–
	"No flow" vG	2.7 yr	0.1 yr	12 d	3 d
	SAAT	1.7 yr	1.1 yr	39 d	30 d

Table 2.4. Annual recharge estimated based on tracer experiments (from Bekeris, 2007; Koch, 2009) and depth to the water table [m] for test locations.

Location	**Annual recharge [mm/yr]**	**Depth to the water table [m]**
1	469	3.3
2	314	26.0
3	495	17.0
4	496	21.0
5	522	22.0
6	412	9.0
7	581	5.0
8	396	5.2
9	477	2.7

Table 2.5. Summary of compared approaches to estimate the fraction of the travel time spent on the unsaturated zone t_r .

Compared Approaches	Time in the unsaturated zone (t_u)	Time in the saturated zone (t_s)
Numerical modeling	1D num. model	Particle tracking
Simplified (narrow K-range)	SAAT and "no-flow" vG	Straight-line approx. (narrow K-range)
Simplified (wide K-range)	SAAT and "no-flow" vG	Straight-line approx. (wide K-range)

Table 2.6. Results for test locations using numerical modelling (in gray) and simplified estimations. The maximum and minimum bounds for (t_r) estimates using simplified techniques are underlined.

			Location								
		Technique	1	2	3	4	5	6	7	8	9
Unsat. zone travel time t_u [yr]											
1D numerical model		(A)	2.4	32.4	12.6	16.1	15.6	8.0	3.4	5.6	2.1
"No flow" van Genuchten		(B)	0.8	7.9	1.6	3.4	2.4	1.4	1.2	2.8	0.7
SAAT		(C)	1.2	13.5	4.5	6.0	4.2	2.2	1.6	4.2	0.6
Saturated zone travel time t_s [yr]											
1D numerical model		(1)	6.9	7.3	4.9	6.4	8.8	8.5	7.5	5.8	4.7
Simplified, narrow *K*-range	$K_{max} = 7\times10^{-4}$ m/s	(2)	7.0	7.4	2.1	6.0	7.3	6.7	12.3	4.8	4.1
	$K_{min} = 2\times10^{-4}$ m/s	(3)	2.0	2.1	0.6	1.7	2.1	1.9	3.5	1.4	1.2
Simplified, wide *K*-range	$K_{max} = 1\times10^{-3}$ m/s	(4)	140	149	41.6	120	147	133	246	95.7	82.5
	$K_{min} = 1\times10^{-5}$ m/s	(5)	1.4	1.5	0.4	1.2	1.5	1.3	2.5	1.0	0.8
Relative error t_r [-]											
1D numerical model		(A,1)	0.26	0.82	0.72	0.72	0.64	0.49	0.31	0.49	0.31
"No flow" vG + narrow *K*-range, K_{max}		(B,2)	0.10	0.52	0.44	0.36	0.25	0.18	0.09	0.37	0.15
"No flow" vG + narrow *K*-range, K_{min}		(B,3)	0.28	0.79	0.73	0.66	0.54	0.43	0.25	0.67	0.38
SAAT + narrow *K*-range, K_{max}		(C,2)	0.15	0.65	0.68	0.50	0.36	0.25	0.12	0.47	0.12
SAAT + narrow *K*-range, K_{min}		(C,3)	0.38	0.86	0.88	0.78	0.67	0.53	0.32	0.75	0.32
"No flow" vG + wide *K*-range, K_{max}		(B,4)	0.01	0.05	0.04	0.03	0.02	0.01	0.005	0.30	0.01
"No flow" vG + wide *K*-range, K_{min}		(B,5)	0.36	0.84	0.80	0.74	0.62	0.52	0.32	0.75	0.47
SAAT + wide *K*-range, K_{max}		(C,4)	0.01	0.08	0.10	0.05	0.03	0.02	0.01	0.04	0.01
SAAT + wide *K*-range, K_{min}		(C,5)	0.47	0.90	0.92	0.83	0.74	0.62	0.40	0.81	0.41

Table 2.7. Summary of results for the Thornton well field site.

Compared combined approaches	Relative time (t_r) Average (range)	Absolute time (t_u) Average (range)
Numerical modeling	0.53 (0.26 to 0.82)	11 yr (2 yr to 32 yr)
Simplified (narrow K-range)	0.44 (0.09 to 0.88)	3 yr (1 yr to 14 yr)
Simplified (wide K-range)	0.34 (0.005 to 0.92)	3 yr (1 yr to 14 yr)

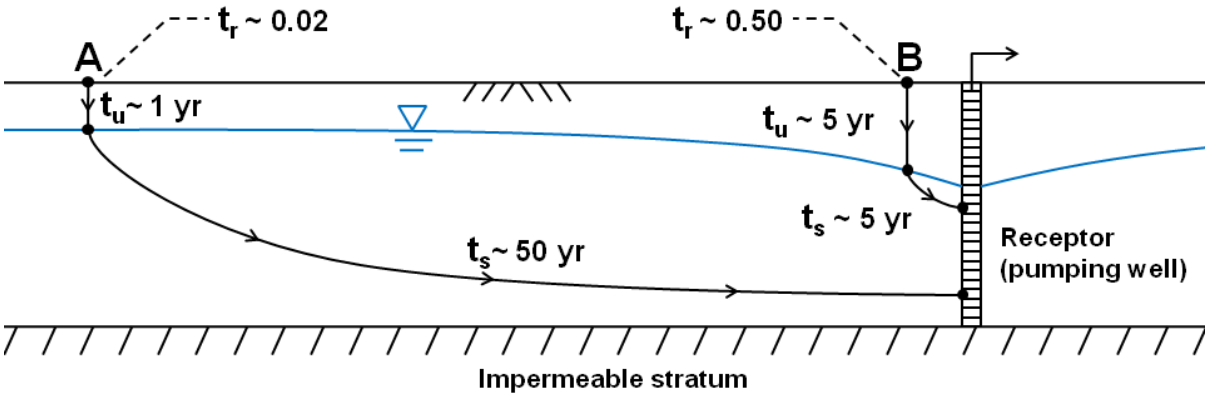

Figure 2.1. Conceptual cross-section indicating the relative importance of the time lag in the unsaturated zone. Time lag is more important for point B (t_r ~ 0.50) than for point A (t_r ~ 0.02).

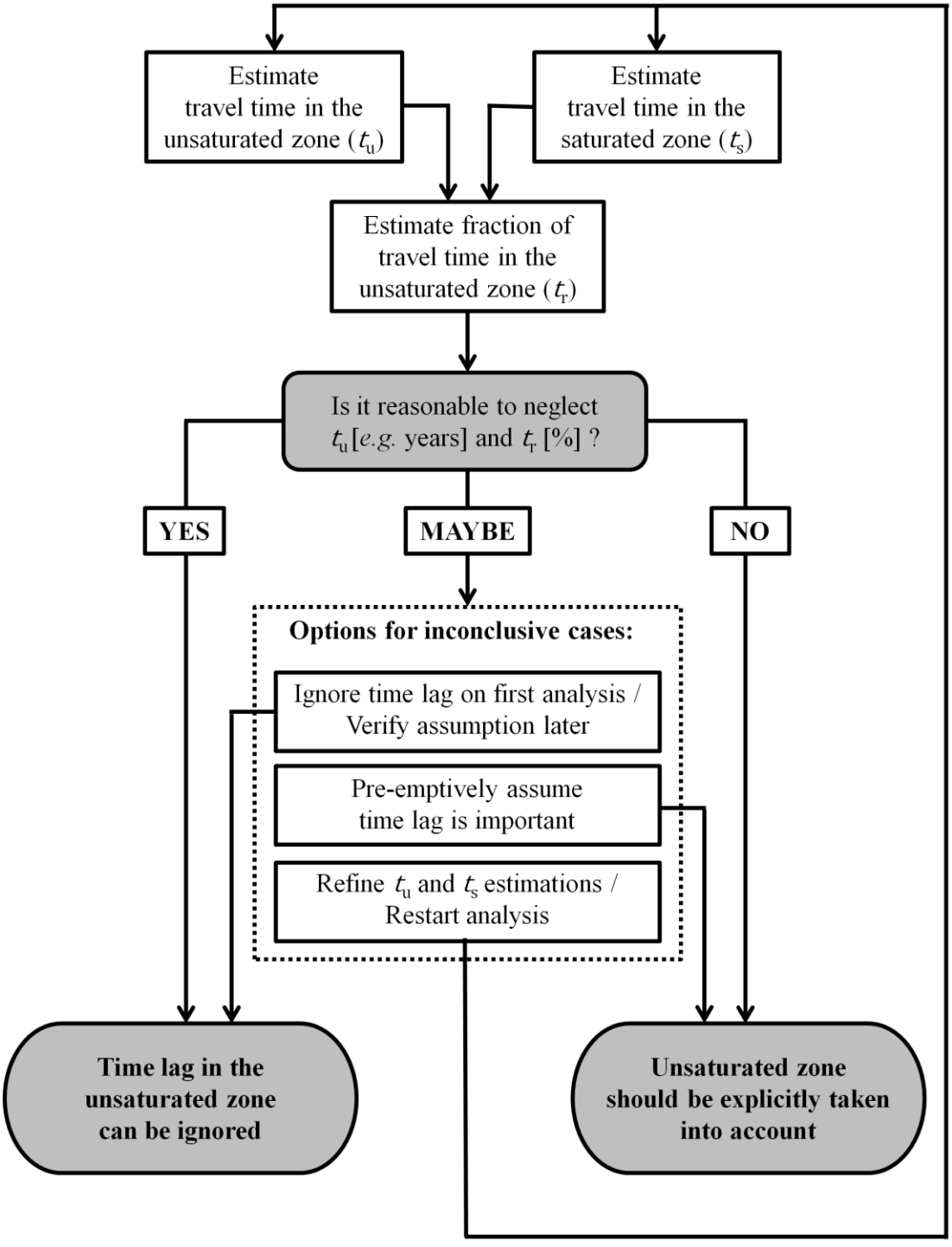

Figure 2.2. Decision tree for assessing the importance of the time lag in the unsaturated zone.

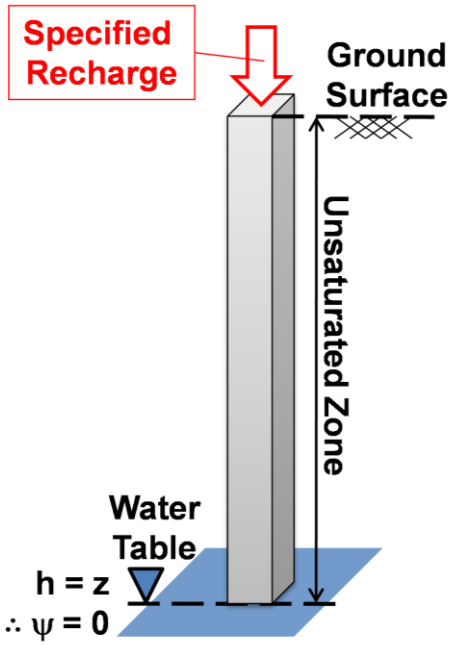

Figure 2.3. Schematic representation of the 1D model setting.

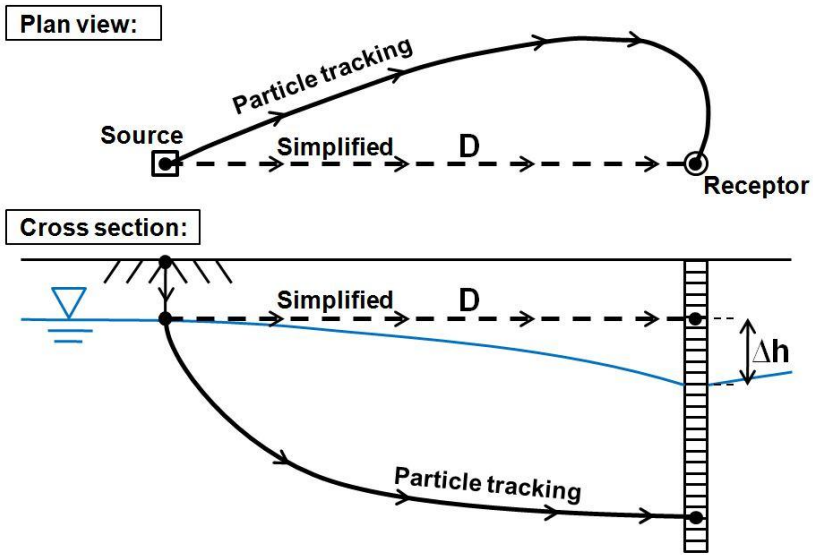

Figure 2.4. Schematic comparison between numerical modelling (particle tracking) and straight-line approximation for estimating the travel time in the saturated zone.

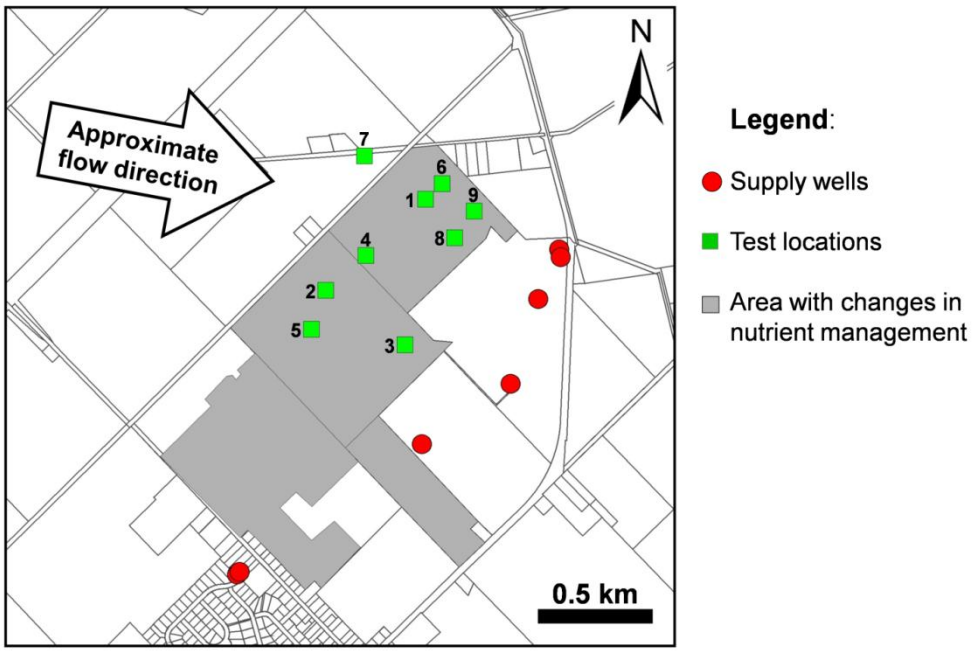

Figure 2.5. Thornton well field site showing test locations.

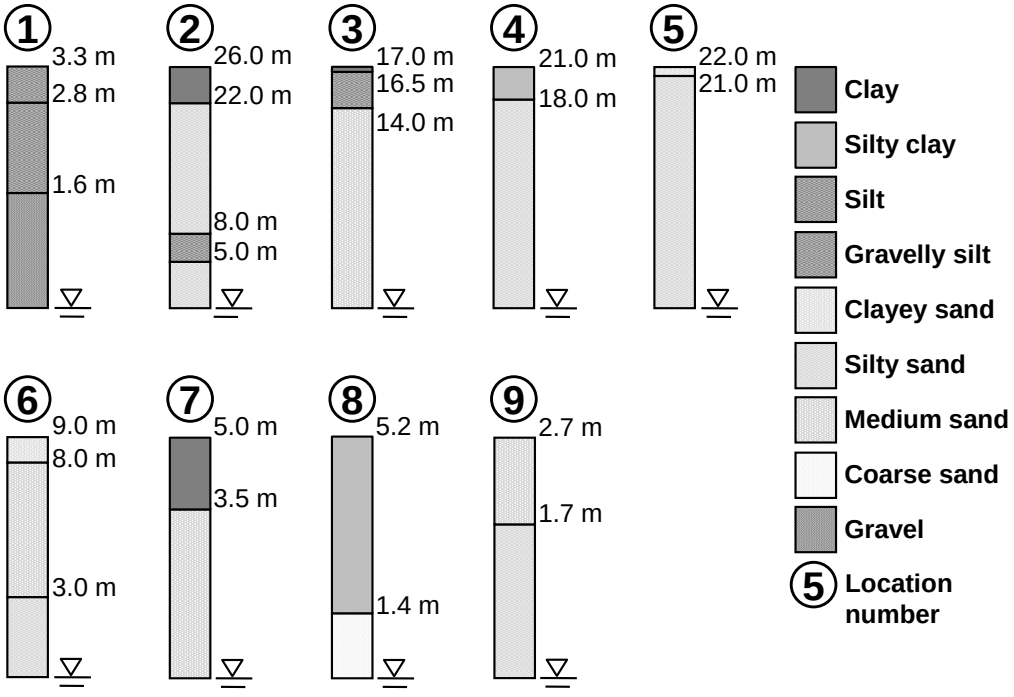

Figure 2.6. Soil texture above the water table for the test locations. Indicated elevations are above the water table. Vertical scale is different for each location.

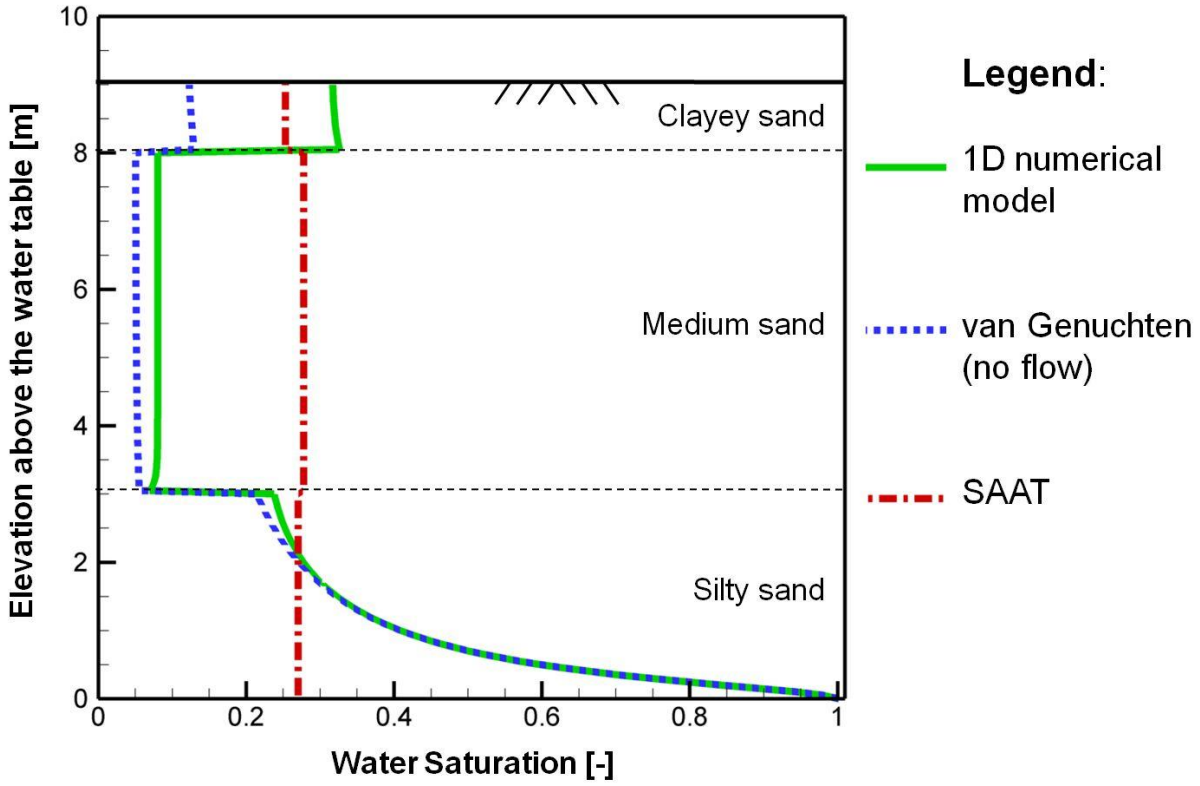

Figure 2.7. Water saturation (S) above the water table for test location 6 calculated by different techniques to estimate advective travel time in the unsaturated zone.

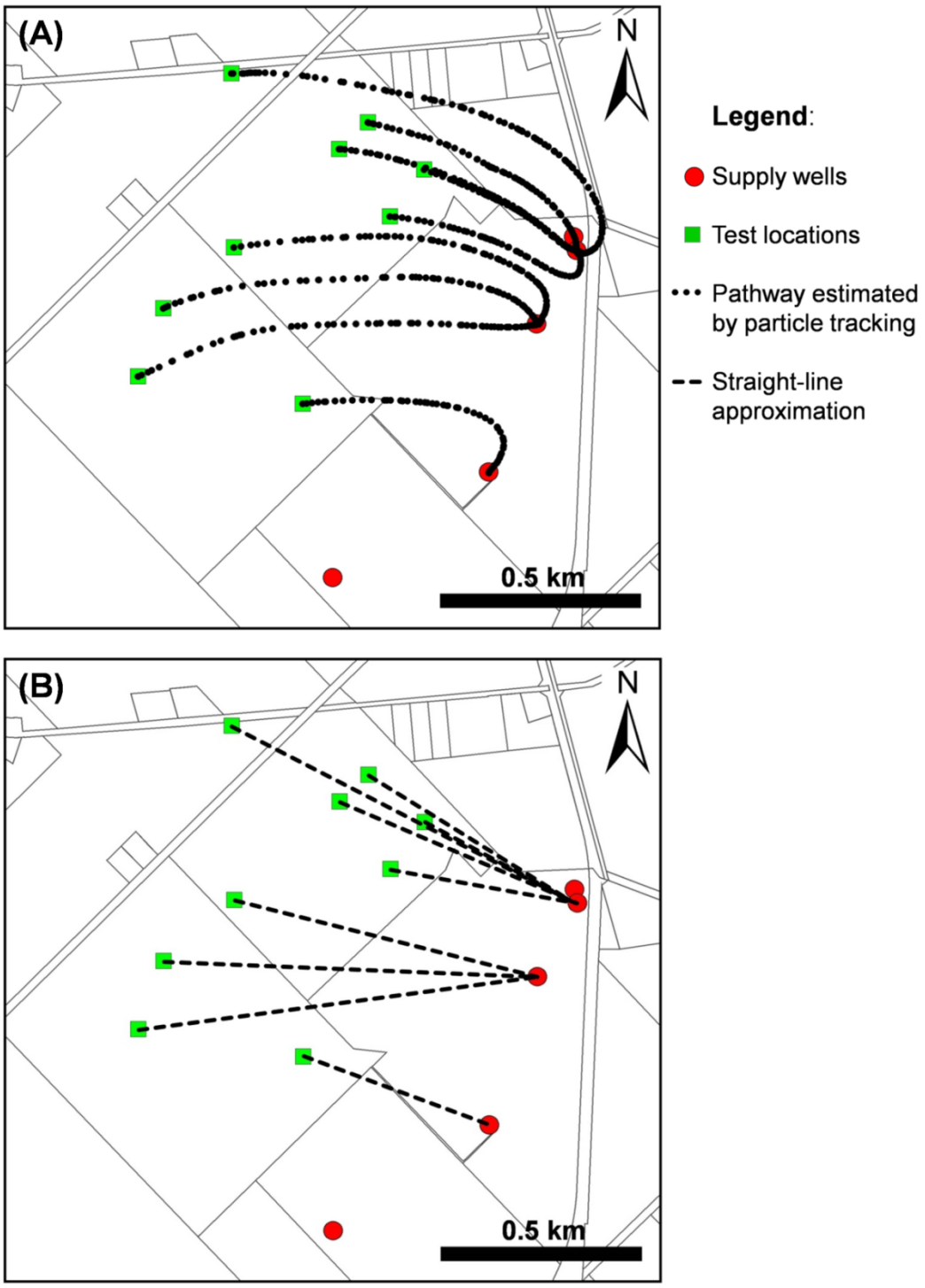

Figure 2.8. Comparison of pathways for: (A) particle tracking and (B) straight-line approximation of travel time in the saturated zone.

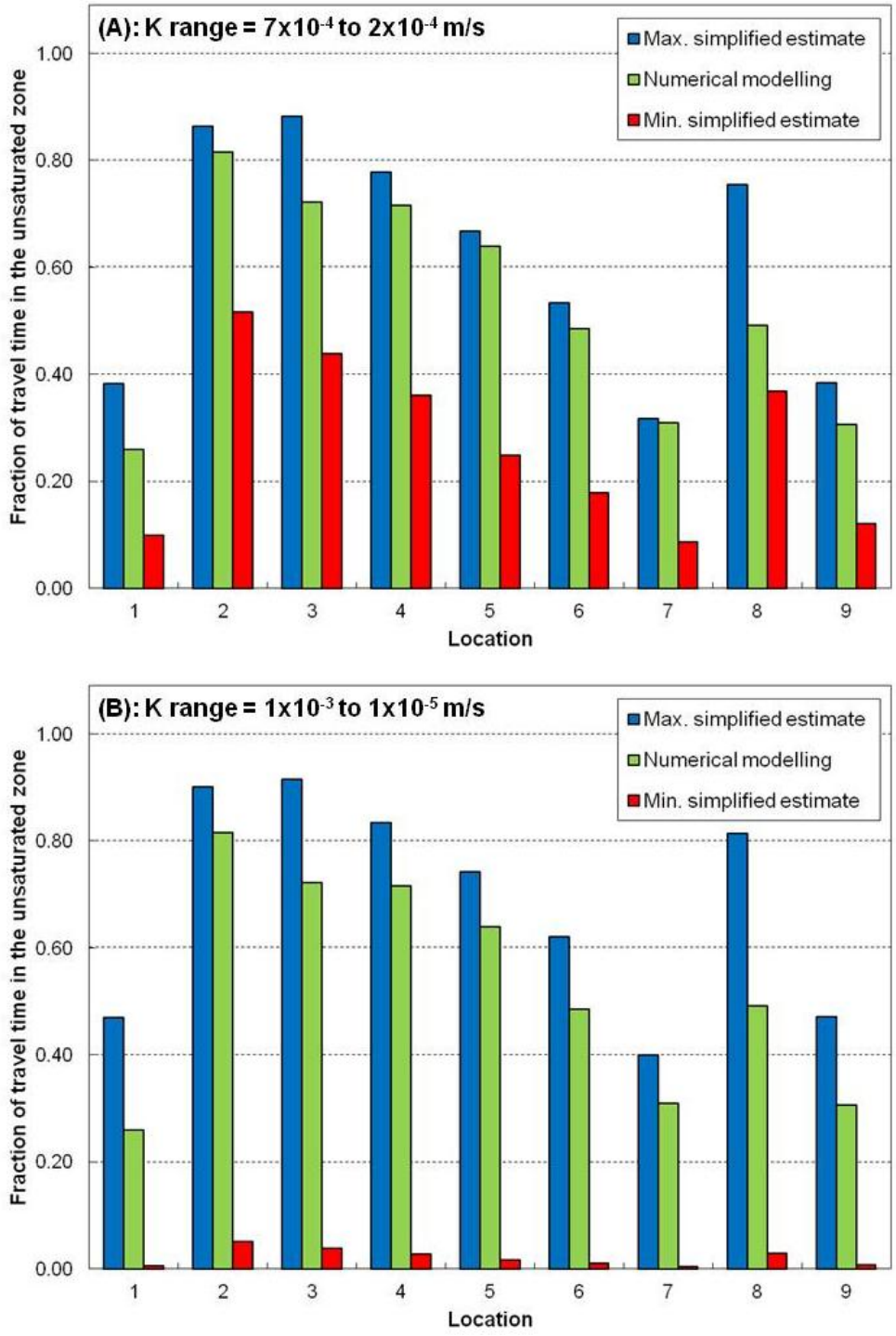

Figure 2.9. Estimated fraction of the travel time in the unsaturated zone (t_r) using numerical modelling (center bar), as well as max. and min. bounds (left and right bars, respectively) of simplified estimations using (A) narrower and (B) wider range of K values.

Chapter 3
An integrated approach for addressing uncertainty in the delineation of groundwater management areas

3.1 Introduction

Wellhead protection areas (WHPAs) serve the purpose of protecting the quantity and quality of water that flows into a well by means of restrictions imposed on land use activities within the WHPA. Most industrialized countries regulate WHPAs; for example, in the United States, the U.S. Environmental Protection Agency (US EPA, 1987; 1997) has developed guidelines for WHPA delineation, as has the Province of Ontario, Canada, through the Clean Water Act (Province of Ontario, 2004; 2006). WHPAs are usually delineated based on the estimated well capture zone, defined as the area from which the well draws its water, taking into account the travel times for water to reach the well screen.

Capture zones and WHPAs are normally delineated by means of mathematical modelling, which is subject to uncertainty due to many different factors. Hydraulic conductivity, heterogeneity, and boundary conditions are major sources of uncertainty, as is the recharge, both in terms of magnitude and spatial distribution. For capture zone delineation, uncertainties in the flow field become magnified in the delineation of the capture zone.

Uncertainty can be a barrier to the use of models, because decision makers may be reluctant to rely on uncertain model results (Poeter, 2007; Brugnach et al., 2007). Available methods to deal with uncertainty, such as the Monte Carlo approach, tend to be costly. As a result, uncertainty is not always taken into account in routine WHPA delineations. This paper presents a simple approach that should help to remove this barrier. First, uncertainty in capture zone delineation is considered at two scales — this helps in the conceptual understanding of uncertainty — and the two scales are then integrated. Second, the approach is generalized to apply to both groundwater protection and the mitigation of groundwater contamination. The main goal is to improve the understanding of the causes and effects of uncertainties, and to make uncertainty analysis more transparent for practitioners and decision makers, hopefully leading to better modelling practices and more confidence in the use of models.

3.2 Background

A well-explored approach for addressing uncertainty in capture zone delineation is by means of stochastic methods, with contributions by, among others, Varljen and Shafer (1991), Franzetti and Guadagnini (1996), van Leeuwen et al. (1998), Camp and Outlaw Jr. (1998), Vassolo et al. (1998), Wheater et al. (2000), Kunstmann and Kinzelbach (2000), Feyen et al. (2001), and Stauffer et al. (2005). The general approach consists in expressing physical parameters (*e.g.*, hydraulic conductivity) in terms of a statistical distribution, which is then used to generate capture zones expressed in terms of confidence levels or uncertainty bands.

Although stochastic methods provide a way to address uncertainty, there are some problems with this approach. Evers and Lerner (1998) pointed out that it is often impossible to characterize the statistical properties of model parameters using the available data. Also, as found by Refsgaard et al. (2005), stochastic methods in general only address uncertainty due to unknown parameter values, but usually neglect uncertainties in the model structure, including the overall problem geometry, the temporal and spatial discretization, the choice of processes being considered – hence, the governing equations to be solved – and different simplifying assumptions. A very similar argument was made by Poeter (2007).

As noted by Evers and Lerner (1998), for the stochastic approach to be applicable, the controlling parameters must be amenable to statistical description. A classical example is the work by Sudicky (1986), who sampled a sandy aquifer along a cross-section at the cm scale and developed the statistical parameters in terms of the variance of log(K) and the correlation length. Assuming that the system is "homogeneously heterogeneous", Sudicky applied the theory of Gelhar and Axness (1983) to derive effective macrodispersion coefficients that express the heterogeneity of the porous material. In a follow-up study, Frind et al. (1987) interpreted the evolution of macrodispersion as the cumulative effect of mass exchange between fast and slow streamtubes, thus providing a physical explanation for the macrodispersion theory. The heterogeneity of the material is an expression of uncertainty at the local scale of the sampling. Frind et al. (2002) applied the macrodispersion approach to delineate well capture zones in terms of capture probability, and in a different paper, Frind et al. (2006) used the same approach to develop the well vulnerability concept for estimating the impact of a contaminant source on a supply well. The fundamental theory underlying these two concepts was analyzed by Enzenhoefer et al. (2011), who used a conditional Monte Carlo simulation based on Bayes' Theorem in discussing the relationship between the macrodispersion and stochastic

(Monte Carlo) approaches, recommending the Monte Carlo approach for the well vulnerability problem.

Non-stochastic approaches have also been explored by some authors. For example, Esling et al. (2008) proposed a systematic sensitivity analysis using different recharge to hydraulic conductivity ratios. Evers and Lerner (1998) used alternative flow calibrations and backward particle tracking to define protection zones. West et al. (2011) proposed the delineation of wellhead protection areas using alternative flow scenarios associated with different weights based on technical judgement. Poeter (2007) suggested addressing predictive uncertainty by means of a reasonable set of alternative conceptual models, using multi-model averaging. Noting that geostatistical approaches are often considered first, she explained that "*to capture the full conceptual uncertainty, one must look at broader variations of the configuration of geologic units, as well as alternative initial conditions, boundary conditions, processes, scenarios, dimensionality, and perhaps even alternative algorithms*".

Pappenberger and Beven (2006) argued that uncertainty analysis is still not a common practice in many modelling exercises. Lack of available guidance for use in practical applications is pointed out as a major reason. According to these authors, what exists is a number of alternative approaches with different philosophical frameworks, all of which are more or less appropriate, depending on the problem at hand. Although the authors made this argument for hydrology, hydraulics and water resources models in general, it can also be considered a fair portrayal of groundwater models applied to capture zone delineation.

3.3 An integrated approach for addressing uncertainty

For convenience, we consider a system of two spatial scales, local and global, each with its own type of uncertainty. Local-scale uncertainty is defined as the uncertainty generated by heterogeneities within a hydrogeological unit, of the type investigated by Sudicky (1986). Local-scale uncertainty can be addressed by stochastic methods, or alternatively, it can be approximated on the basis of macrodispersion theory (Gelhar and Axness, 1983) by applying a backward transport model to generate a capture probability distribution (Frind et al., 2002; Neupauer and Wilson, 1999). The macrodispersion approximation is valid if the scale of the hydrogeological unit is much larger than the scale of the local heterogeneities within the unit.

Global-scale uncertainty (where "global" refers to the model domain) incorporates a variety of other sources of uncertainty as discussed by Poeter (2007). These include the shape of the aquifer and aquitard units, the hydraulic connections between aquifer units (*i.e.*, windows), the boundary conditions, the selection of processes to be considered and how they are represented (*i.e.*, governing equations and modelling codes), uncertainties in the conceptual model, as well as the spatial and temporal discretizations. Sources of global-scale uncertainties are generally less amenable to stochastic treatment because often they cannot be described by parameters or parameter distributions. This type of uncertainty can be addressed by scenario analysis involving multiple model representations of the natural system (Poeter, 2007).

The concept of multi-model analysis may appear controversial within the context of conventional modelling practice, which aims to identify the "best" model among possible alternatives. Indeed, for many straight-forward situations, a best model can usually be defined without difficulty. On the other hand, in more complex situations, it may not be possible to unambiguously define the one "best" or "right" model – only a number of possible candidates. In such cases, the question is what to do with these alternatives.

Thus the scenario analysis leads to the problem of combining a multitude of model predictions in a meaningful way for decision-making. Statistical methods for ranking and averaging multiple model predictions in numerical groundwater models were developed and applied by Burnham and Anderson (2002), Neuman (2003), Ye et al. (2004), Poeter and Anderson (2005), Poeter and Hill (2007), Ye et al. (2008) and Singh et al. (2010). Another way to combine different model predictions is by means of the precautionary approach. This approach is well known to policy makers and regulators, and is

usually applied to make decisions under uncertainty in situations where there is a potential risk to the public or the environment and a conservative (*i.e.*, risk-averse) stance is justified.

We propose a three-part approach to address uncertainty in capture zone delineation: (1) express local-scale uncertainty in terms of macrodispersion and apply backward transport to generate a capture probability distribution; (2) express global-scale uncertainty by using a reasonable number of alternative scenarios or conceptual models of the real system; and (3) use the precautionary approach to combine the multiple scenarios into a capture zone. By expressing the result of each scenario run in terms of a probabilistic distribution and combining these distributions, the two uncertainty scales are effectively integrated. At this stage, two types of groundwater management areas can be defined, depending on whether the underlying objective is protection of the groundwater resource or mitigation of existing contamination. The components comprising the proposed approach are explained in more detail in the following.

3.3.1 Local-scale uncertainty: Capture probability

At the scale of the individual stratigraphic unit, the porous material may be considered homogeneously heterogeneous (*i.e.*, statistically stationary) (Sudicky, 1986). The macrodispersion approach (Gelhar and Axness, 1983) applies, and a well capture zone can be expressed in terms of capture probability (Frind et al., 2002; Neupauer and Wilson, 1999). Frind et al. (2002) compared the capture probability approach to the standard particle tracking approach, which is currently the industry standard for delineating well capture zones, showing that capture probability produces more realistic capture zones than particle tracking, with less need for subjective judgement.

To implement the capture probability approach, a standard advective-dispersive transport model in backward mode (with the sign on the advective term reversed) is applied to solve for capture probability with respect to the well. The simulation process can be compared to the tracking of particles upgradient from a well, except that a dispersion term is added to represent local-scale uncertainty. The transport boundary condition at the well is a specified capture probability of 1.0. The result is a plume of capture probability extending upgradient from the well toward the ground surface, similar to a contaminant plume extending downgradient, obtained when solving the equation in the forward mode.

Use of the advection-dispersion equation for this purpose is valid, because the equation describes the physical process of advection due to a flow field, combined with dispersive spreading through the

porous medium, and it can be applied to any quantity subjected to this process (*e.g.*, solute mass, age, etc.). Here we apply this equation to a fictitious quantity that has a value of 1.0 at the well screen and tends to zero infinitely away from the well, and we choose to interpret the result as capture probability.

The capture probability concept represents a refinement of the conventional approach for delineating a capture zone, which is based on a line drawn on a map dividing an area into "inside" (capture, or 100% capture probability) and "outside" (no capture, or 0% capture probability) segments. The conventional approach can cause problems because a property owner just inside the line may face land use restrictions that his/her neighbour just outside the line would not encounter. Conceptually, a more realistic way to assess the risk of contamination would be to assign a capture probability of less than 100% to the area just inside the line, and more than 0% to the area just outside the line. This means that, for example, we may judge the chances of well contamination due to a source at some point inside the line at 75% (capture probability $P = 0.75$). The capture probability concept formalizes this straightforward approach, producing a continuous probability spectrum from 100% (at the well itself) to 0% (very far from the well).

This concept could replace the traditional "line-on-the-map" concept. However, if required for planning purposes, a line on the map can still be recovered easily from the probability distribution by choosing a capture probability contour appropriate for the problem at hand. Molson and Frind (2012) suggested the 0.5 contour on the basis of life expectancy considerations. Another option is to select a contour on the basis of mass balance between recharge and pumping (Frind et al., 2002).

It should be noted that capture probability will not predict the actual impact on a well. Capture probability simply puts a number on the risk level. It means that, for example, a contaminant source on the 0.75 probability contour will pose a higher risk of impacting the well than a source on the 0.5 contour. To determine the actual impact of a specific contaminant source on a well, forward solute transport runs or the well vulnerability method (Frind et al., 2006; Enzenhoefer et al., 2011) can be used. The well vulnerability method provides the maximum concentrations to be expected at the well, plus the arrival and exposure times, due to any source of contamination within the capture zone. This method uses the same advective-dispersive transport equation as the capture probability method, except that instead of the specified value of 1.0 at the well, a pulse is applied at either the contaminant source or the well; the resulting breakthrough curve then provides the desired information.

3.3.2 Global-scale uncertainty: Scenario analysis

Capture probability, as defined above, expresses only the local-scale component of uncertainty. The global-scale component of uncertainty can be assessed by scenario analysis involving a limited number of realistic conceptual model configurations and boundary conditions (Evers and Lerner, 1998; Poeter, 2007; West et al., 2011; also others). These scenarios can be seen as different realizations or attempts to represent a complex system, where perturbations are based on physical rather than statistical principles and follow no particular pattern. Different scenarios can be created by developing alternative conceptual models, applying different boundary conditions, changing the geometry and/or the hydraulic characteristics of hydrostratigraphic units, using different grid types or discretizations, or by using different codes.

By allowing the incorporation of alternative model structures, the robustness of model predictions can be enhanced (Refsgaard et al., 2007). The only requirement for a model scenario to be considered is that it should be a valid representation of reality based on a realistic conceptual model with reasonable parameter distributions and boundary conditions, and it should be solved using an accepted, verifiable numerical method. Because the differences between scenarios may be substantial, each scenario must be calibrated against the original field data. A successful calibration, however, is only a necessary, but not a sufficient condition for validity (Oreskes et al., 1994). As will be shown below, different scenarios can calibrate equally well to the same data.

3.3.3 Integrating multiple scenarios: the Precautionary approach

If there is more than one valid representation for a given situation, as is the case for most practical applications, it is impossible to objectively choose which is "the best" representation (Carrera and Neuman, 1986). However, simply presenting a collection of alternative capture zones arising from different scenarios/models would not be very useful in the decision-making process, and it would overload decision makers with information. Also, it would not address the critical problem of how to delineate capture zones under uncertain conditions. In order to facilitate the decision-making process, alternative capture zones must be combined or integrated in a systematic and transparent way. West et al. (2011), for example, used technical judgement in the weighing of different scenarios to arrive at a final capture zone.

A logical choice for combining or integrating the results from alternative model scenarios, which we will use here, is the precautionary approach. The precautionary approach follows the intent of the

Precautionary Principle as defined formally in the Wingspread statement (Raffensperger and Tickner, 1999): "*When an activity raises threats of harm to human health or the environment, precautionary measures should be taken even if some cause and effect relationships are not fully established scientifically*". The Precautionary Principle is often used in a regulatory context, and it generally applies to decision-making under uncertain conditions without necessarily quantifying the uncertainty. For example, one of the guiding principles of source protection in the Province of Ontario is that "*Source protection plans must be based on risk management, when risks can be estimated, and the precautionary principle when risks cannot be estimated*" (Province of Ontario, 2004).

The precautionary approach for the delineation of well capture zones, or more generally, groundwater management zones, can be considered as appropriate because an independent validation of a well capture zone is rarely possible. Tracer tests would in most situations simply take too long, monitoring would carry its own uncertainties, and furthermore, the introduction of tracers into a water supply aquifer may be undesirable. Therefore, the precautionary approach should be a defensible option in practical situations.

3.3.4 Protection versus mitigation

In the context of wellhead protection, the "precautionary measure" pertains to the inclusion or exclusion of a given area in a WHPA. This decision depends on the purpose of the decision-making exercise, where we distinguish between two objectives: (a) the protection of a groundwater resource from the threat of contamination, and (b) the mitigation of a body of groundwater that has been contaminated.

For example, let's imagine that there is doubt whether a certain point (x,y) at ground surface is inside or outside the capture zone of a given well. If the objective is to define protection zones to keep contaminants from reaching the well (*e.g.*, choosing the location for a new landfill), then the "precautionary measure" is to assume that point (x,y) is inside the capture zone. This measure preferentially overestimates the extent of the capture zone and decreases the chance of placing a potentially hazardous activity inside the true capture zone of the well.

Alternatively, the objective may be to define capture zones for the hydraulic containment of contaminated areas (*i.e.*, hydraulic barriers), or to prioritize sites for the implementation of Beneficial Management Practices or BMPs (Wassenaar et al., 2006) in order to enhance water quality at the

well. Now the "precautionary measure", in case of doubt, is to assume the given area falls outside the capture zone. This preferentially underestimates the extent of the capture zone and increases the chances that flow through the designated BMP areas will ultimately be captured by the well, benefiting the mitigation objective.

Fig. 3.1, adapted from Evers and Lerner (1998), graphically illustrates the concept. The left part of the figure shows possible capture zones generated by a number of alternative model scenarios; to the right appear the resulting management areas corresponding to either a protection-based objective or a mitigation-based objective. For a protection decision, the precautionary approach would consider the union of all alternative capture zones, while for a mitigation decision it would consider the intersection of alternative capture zones. These management areas differ in extent. Because the extent of the area subject to management measures has economic as well as environmental and social implications, the distinction between them is important. Evers and Lerner (1998) called these areas the "zone of uncertainty" and the "zone of confidence", respectively. It is important that the precautionary principle should be applied in conjunction with sound hydrogeologic interpretation. In other words, professional judgement should be exercised in the creation and selection of scenarios to be considered.

3.3.5 Mathematical formulation

The proposed integrated approach can be implemented mathematically through two simple equations. These equations combine capture probability estimations (*i.e.*, local-scale uncertainty) from multiple scenarios (*i.e.*, global-scale uncertainty), in a risk-averse manner (*i.e.*, precautionary approach). For protection decisions, the equation is:

$$P_{\mathrm{PROT}}(x, y, t_{\mathrm{C}}) = \max\left[P_1(x, y, \forall z, t_{\mathrm{C}}), P_2(x, y, \forall z, t_{\mathrm{C}}), \ \ldots \ , P_{\mathrm{N}}(x, y, \forall z, t_{\mathrm{C}})\right] \tag{3.1}$$

where $P_{\mathrm{PROT}}(x,y,t_{\mathrm{C}})$ is the maximum probability, from all scenarios, that a particle at a given point (x,y) will be captured within a time period not greater than t_{C}. For example, a $P_{\mathrm{PROT}}(x,y,80) = 0.5$ means that, for the position (x,y) on this contour, all simulations estimate that the groundwater infiltrated at point (x,y) has a probability of capture of 50% or lower, within 80 years. The resulting protection map combines the maximum estimated probabilities throughout the vertical extent of the

model domain, from the bottom to ground surface. This is also a conservative assumption, assuming that there may be vertical preferential flow paths.

For mitigation decisions, the equation to be used is:

$$P_{\mathrm{MIT}}(x,y,t_{\mathrm{C}}) = \min\left[P_1(x,y,z_{\mathrm{GS}},t_{\mathrm{C}}), P_2(x,y,z_{\mathrm{GS}},t_{\mathrm{C}}), \ \ldots \ , P_{\mathrm{N}}(x,y,z_{\mathrm{GS}},t_{\mathrm{C}})\right] \tag{3.2}$$

where $P_{\mathrm{MIT}}(x,y,t_{\mathrm{C}})$ is the minimum probability, from all scenarios, that a particle at a given point (x,y) at ground surface (z_{GS}) will be captured within a time period not greater than t_{C}. For example, $P_{\mathrm{MIT}}(x,y,80) = 0.5$ means that, for the position (x,y), all simulations estimate a probability of capture by the well of 50% or higher, within 80 years. Overestimating the probability of capture is not desirable in this case, so the values at ground surface are taken into account.

In this way, the information from all scenarios is merged into two types of maps for guiding management decisions: one for protection and one for mitigation. This reduces information overload for decision makers, increases efficiency, and makes modelling results more transparent and understandable to stakeholders, as suggested by Brugnach et al. (2007).

The methodology is based on the assumption that erring on the side of caution is desirable, and accordingly, it mathematically expresses the postulate that when making decisions subject to doubt, consider the worst-case situation amongst the available alternative interpretations of the natural system. The rationale behind this postulate, and hence this methodology, cannot be proven or disproven using physical field data. It is merely the mathematical translation of a precautionary (risk-averse) approach to combining alternative representations of well capture zones to support groundwater management decisions. Using control theory terminology, this approach attempts to be "fail-safe", defined as "a system which fails to a state that is considered safe in the particular context" (Blanke et al., 2001).

3.4 Example application: Water supply well, Waterloo Moraine

The approach outlined above was applied to delineate the protection and mitigation capture zones for one of the water supply wells that are part of a system of well fields operated by the Regional Municipality of Waterloo, Ontario, Canada. The well is located within the Waterloo Moraine (Fig. 3.2), a complex glacial aquifer system that is of importance as a source of water for the local community of over half a million people. The health of the local aquatic ecosystem also depends on the groundwater. The Waterloo Moraine has been the focus of many field and modelling studies (Martin, 1994; Callow, 1996; Martin and Frind, 1998; Frind et al., 2002; CH2M-HILL and S.S. Papadopulos & Associates, 2003; Bester et al., 2006; Frind et al., 2006; Rahman et al., 2010).

For the sustainability of groundwater resources, recharge plays a key role and its estimation is usually associated with significant uncertainty, even when averaged temporally and spatially (Stauffer et al., 2005). Although this approach can be applied to many different sources of uncertainty, we focus here on the uncertainty in the spatial distribution of recharge.

3.4.1 Waterloo Moraine model

The groundwater flow model that underlies our study is based on the original Waterloo Moraine model by Martin and Frind (1998). The conceptual model is bounded by major water courses (Grand River, Nith River and Conestogo River), and covers an area of 740 km^2 (Fig. 3.2). The model is based on the assumption that at the river boundaries, all water discharges into the river, and that regional flow crossing beneath the river is negligible. This assumption provides a no-flow model boundary around the periphery of the model. Major watercourses on the boundary and in the interior of the domain are represented by specified heads. Vertically, the model consists of 8 hydrostratigraphic layers. The original groundwater flow simulations were performed using WATFLOW (Molson et al., 2002), a 3D finite-element groundwater flow model. This code also contains a built-in automatic calibration routine (Beckers and Frind, 2001), which facilitates the calibration of multiple flow scenarios.

The present study uses the original Waterloo Moraine model with its original boundary conditions for flow, but focuses on the rectangular area shown in Fig. 3.2 for detailed capture zone simulations. Within this smaller study area, the hydraulic conductivity distribution of Martin and Frind (1998) was updated using new data provided by the Regional Municipality of Waterloo. The model discretization

was refined within the smaller area, with 29 elemental layers, giving a total of ~ 1,300,000 nodes and ~ 2,500,000 elements.

3.4.2 Alternative recharge scenarios

To assess uncertainty in the spatial distribution of recharge, three alternative recharge distributions generated by different codes were used: (1) Hydrogeosphere (Therrien et al., 2005) as applied by Jones et al. (2009), (2) GAWSER (Schroeter & Associates, 1996) in association with MODFLOW (Harbaugh et al., 2000), as applied by CH2M-HILL and S.S. Papadopulos & Associates (2003), and (3) WATFLOW. Each of these three models is based on valid theories, and, although different, the corresponding recharge distributions can all be considered as physically realistic. All are approximations because they are based on limited data.

Hydrogeosphere (HGS) is a 3D fully-integrated surface and variably-saturated subsurface flow code, including solute and heat transport. HGS adopts a rigorous approach to representing the interaction between different components of the hydrological cycle. Surface water is represented using the diffusion-wave approximation of the Saint Venant equation (Govindaraju, 1988). Unsaturated flow is simulated using the Richards equation with the van Genuchten parameterization (van Genuchten, 1980) to estimate saturation (S) and hydraulic conductivity (K) as a function of pressure head. The recharge distribution was taken from the work of Jones et al. (2009).

GAWSER is a storm-event surface water model, which was coupled to the finite-difference groundwater model MODFLOW. Unsaturated flow is not represented. This recharge distribution was taken directly from an existing study (CH2M-HILL and S.S. Papadopulos & Associates, 2003).

In WATFLOW, the recharge distribution is estimated using the recharge spreading layer (RSL), a virtual layer of porous material placed on top of the ground surface, emulating interflow in the surficial layer (Fig. 3.3). Darcian flow in the RSL is assumed. An average recharge value is specified on top of this layer; this recharge is redistributed within the RSL to avoid mounding on low-K materials. Thus the hydraulic conductivity of the recharge spreading layer controls to what extent recharge is spatially distributed. Accordingly, the hydraulic conductivity of the RSL becomes a calibration parameter.

The recharge distributions produced by these three different models are presented in Fig. 3.4 for HGS, GAWSER/MODFLOW and WATFLOW, respectively. As the original recharge distributions for HGS and GAWSER/MODFLOW did not cover the whole area of the model domain used for the

simulations, an average recharge of 250 mm/yr was assigned where recharge estimations were not available. The supply well which will be the focus of the capture zone delineation is shown in the figure.

In each of the three models, the recharge (*i.e.*, the actual downward flux that infiltrates at ground surface and eventually reaches the water table) is an internally calculated quantity that depends on the processes built into the model. Since these processes vary for the three models, the average recharge within the model area (calculated by averaging the downward fluxes) differs somewhat (212 mm/yr for HGS; 233 mm/yr for GAWSER/MODFLOW; and 255 mm/yr for WATFLOW), but the differences are small enough to allow the recharge magnitude to be discounted as a major control. Accordingly, the spatial variation of recharge is taken to be the controlling parameter.

For HGS, the generated recharge distribution (Fig. 3.4a) covers approximately the southeast quadrant of the study area. The blue areas indicate a gaining stream. Contrary to expectations, the three gravel pits within the area do not affect the recharge distribution produced by HGS. The GAWSER/MODFLOW recharge distribution (Fig. 3.4b) covers the southern part of the study area. The GAWSER/MODFLOW recharge differs significantly from that generated by HGS, on account of the very different mechanism built into this model. Recharge in this model is controlled by surface soil type and depression-focused infiltration (*i.e.*, closed-basin areas in which runoff accumulates); these mechanisms result in a high spatial variability of recharge with numerous areas of either high or low values. In particular (see Fig. 3.4b), there is a large area of low recharge near the centre of the study area, flanked to the south by areas of high recharge. WATFLOW covers the entire study area (Fig. 3.4c), controlling recharge by means of its recharge spreading layer (Fig. 3.3), which simulates interflow. For the WATFLOW simulation, a recharge value of 600 mm/yr was assigned a priori to the gravel pits. This value was obtained during calibration, using an expert estimate (P. Martin, personal communication, 2009) as a starting value. The result is a recharge distribution which is intermediate between those of HGS and GAWSER/MODFLOW. A consequence of the differing recharge distributions for the three scenarios is that the stream segments that are gaining/losing are not the same between the models.

3.4.3 Steady-state flow calibration

Three alternative steady-state flow models (one for each recharge scenario) were calibrated to match observed heads in 42 wells. To achieve calibration, the hydraulic conductivity for each hydrostratigraphic unit was allowed to vary within one order of magnitude. This range is comparable

with the error bounds for field estimation methods commonly used at this scale (Alexander et al., 2011). All three flow models were calibrated starting from the same initial hydraulic conductivity distribution. Therefore, differences in the calibrated hydraulic conductivity field are commensurate with changes in recharge, as the target calibration data set used for the three models is the same.

This process resulted in comparable calibration fits for all three scenarios, as shown in Fig. 5. The average error ranges between -2.5m (GAWSER/MODFLOW) and 2.4m (HGS), while the average absolute error ranges between 4.0m (GAWSER/MODFLOW) and 2.4m (WATFLOW). This error compares to a range in head of about 80m over the model domain. As an independent verification, an observed baseflow value for a creek located within the studied area was found to be comparable to calculated discharge estimations for all three scenarios. Because of the approximate nature of the data, it would be pointless to try to select a "best" model from the three conceptual model scenarios. Thus the conclusion from the calibration is that the three models are all acceptable, but non-unique.

3.4.4 Conventional approach to capture zone delineation: Particle tracking

The capture zone delineation focuses on the primary supply well identified in Figs. 3.4 and 3.6. Fig. 3.6 also shows additional municipal wells which are not directly considered for capture zone delineation, but which strongly influence the results for the primary well. To delineate the primary well capture zone for each of the three scenarios, the conventional backward particle tacking approach was first applied to the three recharge scenarios, using the particle tracking routine WATRAC (Frind and Molson, 2004). Particles were placed around a circle at the well and allowed to travel in the upgradient direction from the well within the 3D flow field, until they emerged at ground surface. The results are shown in Fig. 3.6. The tracks represent advective travel only, with no uncertainty due to local-scale heterogeneities taken into account.

The three sets of particle tracks extend generally from the primary supply well toward the northwest, and their shape and orientation is influenced by the other wells in the well field. A portion common to all three scenarios extends first to the north, and then curves to the west. Beyond this common portion, HGS (Fig. 3.6a) has a leg extending to the northwest, while GAWSER/MODFLOW (Fig. 3.6b) has a similar northwest tending leg, but displaced toward the east. WATFLOW (Fig. 3.6c) has no extension beyond the common portion.

Delineating a capture zone from the above particle tracking results would clearly require some judgement. If local-scale uncertainty is to be addressed, one way to accomplish this is by means of a standard Monte Carlo analysis, creating a sufficiently large number of realizations for each of the three scenarios, and applying particle tracking to each realization. Alternatively, local-scale uncertainty can also be accounted for by means of the capture probability method, which we demonstrate in the following.

3.4.5 Capture probability and scenario analysis

To apply the capture probability method, an advective-dispersive transport model in backward mode is run for each of the three calibrated scenarios. The transport code WTC (Molson and Frind, 2005) was used for this purpose. Dispersivities of 20 m, 5 m, and 0.02 m were chosen for longitudinal, horizontal transverse and vertical transverse directions, respectively, as in earlier studies of this system (Frind et al., 2002). The model was run to quasi-steady-state conditions, which was approached at 180 years. From these 3D capture probability distributions, two sets of maps were extracted: (1) the maximum capture probability over the aquifer depth for the three recharge scenarios (Fig. 3.7), obtained from the 3D model output by selecting, for each point (x,y) in the horizontal plane, the maximum value in the vertical direction, and (2) the capture probability at ground surface for the three recharge scenarios (Fig. 3.8), obtained by plotting the intersection of the 3D probability plume with the ground surface. For ease of interpretation, the 0.5 contour has been emphasized in all figures.

These figures show that, although the calibration leads to about the same fit for each scenario, the capture probability plumes obtained differ significantly between scenarios. A major influence on the shape of the plumes is on account of the wells immediately to the northwest of the primary well, which produce indentations in the capture zone for the primary well. Another group of wells farther to the northwest, however, impacts mainly the HGS (Fig. 3.7a) and WATFLOW (Fig. 3.7c) plumes. For HGS, these wells cause the plume to split into two branches extending to the northwest, while for WATFLOW, only one branch extends to the northwest. For GAWSER/MODFLOW, the wells to the northwest seem to restrain mainly the higher probability values (>0.5) for the primary well, but not the lower values, resulting in a large plume extending to the northwest.

The capture probability plumes at ground surface (Figs. 3.8a, 3.8b, and 3.8c) show basically the same trends as Fig. 3.7, except that at the surface, the plumes are somewhat smaller and more

irregular. This shows that the maximum extent of a capture zone occurs at depth, which supports the need for a 3D analysis.

The differences in the probability plumes for the different scenarios demonstrate the high sensitivity of capture probability with respect to recharge. In particular, the large size of the GAWSER/MODFLOW plume could be related to the large area of low recharge (Fig. 3.4b), which coincides with the centre of the probability plume (Fig. 3.7b) for this scenario. On the other hand, local features such as the stream or the gravel pits do not seem to have a significant effect on capture probability.

In terms of a final capture zone, it should be kept in mind that the capture zone of most interest will be the combined capture zone for all supply wells. In this combined capture zone, the indentations seen in Figures. 3.6, 3.7, and 3.8 would not occur. Considering only one well out of a group of wells in the same well field, as we have done here, results in a sharp gradient in the individual probability functions, resulting in numerical dispersion. This problem is less likely to occur when all wells in the well field are investigated together.

A high capture zone sensitivity with respect to hydrogeologic parameters has also been observed in other studies, such as Piersol (2005) and Franke et al. (1998).

3.4.6 Groundwater management areas: Protection vs. Mitigation

The two sets of maps in Figs. 3.7 and 3.8 can be used to generate two single maps delineating groundwater management areas under either the protection or the mitigation objective, using Eqs. (3.1) and (3.2). The process is schematically shown in Fig. 3.1. To generate the protection map for the primary supply well (Fig. 3.9), the maximum capture probabilities over all scenarios in Fig. 3.7 are chosen on a point-by-point basis. For the mitigation map for the same well (Fig. 3.10), the same point-by-point approach is taken, but now the minimum capture probability at ground surface over all scenarios in Fig. 3.8 is chosen. In both cases, these maps provide conservative predictions for each location based on the three selected scenarios and the type of decision to be made.

A comparison of Figures. 3.9 and 3.10 shows that the capture probability maps for protection and mitigation differ substantially for this well. While the management area for protection is about 5 km wide and extends nearly 20 km to the northwest from the well, the management area for effective mitigation is only about 1 km wide by 3 km long extending in the northerly direction. The difference in this case is primarily due to the uncertainty in the recharge distribution. Other uncertainties exist

that would lead to more scenarios and thus also have an impact on capture probability and capture zone extent.

As a final question, we may ask whether a valid capture zone can be delineated by simply merging the particle tracks from the three scenarios. The result is given in Fig. 3.11, which shows the particle tracks from Fig. 3.6, with the 0.5 probability contour from Fig. 3.9 superimposed. As is evident from the figure, the 0.5 contour provides a reasonable envelope for the particle tracks. This demonstrates that particle tracks from different scenarios can be merged to provide a capture zone that takes global-scale uncertainty into account. In the present case, however, drawing the envelope without the benefit of the 0.5 contour would require considerable judgment. Thus the capture probability approach can be seen as being less subjective and more informative than particle tracking by itself.

3.5 Discussion: Some key points

This study has raised some key points that are highly relevant in the appreciation of uncertainty in modelling.

Scenario selection: Care should be taken that only scenarios that are physically realistic and representative are included. The analysis can be only as good as the technical judgement behind the formulation and selection of these scenarios. This is a limitation of any modelling endeavour, but since this approach uses a conservative stance, for every scenario that is added, the resulting groundwater management areas can only become more conservative or remain the same. Therefore, the inclusion of one single inadequate scenario may render the final delineation excessively conservative.

Dealing with expert subjectivity: Due to the subjectivity that is typically inherent in expert judgment, different interpretations may be expected from different experts working on the same problem (*e.g.*, Beven, 1993). The proposed approach provides a framework for incorporating the uncertainty derived from different experts by combining the results in a conservative manner. This eliminates the difficult (or impossible) task to unquestionably select the "best" or “right” model among a set of alternative valid representations. Because the problem of choosing the “right” model is eliminated, this approach should reduce the potential for litigation.

"Safest decision" vs. "Optimum decision": The precautionary nature of this method leads naturally to more conservative and safer decisions than a decision based on a single scenario. But safety has a price. For protection applications, this method can lead to the imposition of restrictions in areas that may not significantly impact the well, while for mitigation applications, it may exclude areas that could possibly contribute to the well. The approach does not lead to "optimum decisions", as some statistical methods do. Instead, it aims to make the "safest decision" based on the available interpretations of the real system, in a transparent and pragmatic manner. Practitioners should keep in mind that, even with this precautionary stance, it is impossible to exhaust all relevant possible combinations of valid models. Therefore, the protection and mitigation maps do not necessarily represent the absolute worst-case predictions that can possibly be made, as there is always a possibility that an important model interpretation could be left out of the analysis (Refsgaard et al., 2007).

Costs considerations: The proposed approach does not require more data than the conventional approach; the same dataset that is used to create one scenario can be also used to generate alternative scenarios. However, multi-model analysis does require more time than single-model analysis. The additional cost will depend on whether alternative scenarios are based on different models or on modifying parameters within the same model. In any case, modelling costs are usually a small percentage of overall costs of source water protection studies.

Field data vs. modelling: It is important to keep in mind that modelling can never be a substitute for field data. The proposed method expresses uncertainty, but does not reduce it. To reduce uncertainty, additional data should be collected and incorporated in the model. For example, direct field estimations of recharge would constrain the distribution of this parameter in the model and consequently reduce model uncertainty.

3.6 Conclusions

We have attempted to provide some new insights into the problem of uncertainty in capture zone delineation for complex systems that are not readily amenable to stochastic analysis. For these systems, we propose that uncertainty be considered at two scales. At the local scale of the stratigraphic unit, the porous material may be considered heterogeneously homogeneous, and the resulting uncertainty can be represented by using the macrodispersion concept, leading to a capture probability distribution. At the larger global scale, where uncertainty is due to a variety of causes including structural uncertainty and uncertainty in the boundary conditions, uncertainty can be addressed by means of systematic scenario analysis over a number of different but physically plausible scenarios, with each being calibrated individually against field data.

Results from multiple scenarios can be integrated using the precautionary approach to delineate groundwater management areas under either of the two objectives: (1) the protection of groundwater sources, and (2) the mitigation of contaminated areas by means of remedial measures. For the first objective, the precautionary approach leads to a conservative capture zone based on the combination of all areas that might contribute to capture. For the second objective, it leads to an equally conservative capture zone based on the selection of all areas with high probability of capture that are most likely to contribute to flow to a given well. Both objectives can be covered within the same investigation.

We have shown that the spatial distribution of recharge can have a controlling impact on capture zone delineation, and thus be a major source of uncertainty. The wide range of recharge values generated by different models stresses the importance of independent recharge estimation using field methods to constrain this range, and thus to reduce uncertainty.

We have also shown that equally acceptable calibration fits can be obtained from different recharge distributions, thus illustrating non-uniqueness. In current practice, modellers tend to choose the "best" model on the basis of the calibration outcome, where the "best" model or scenario is taken to be the one with the best calibration fit to observed data, and other reasonable model representations may be discarded. Our work shows that this can lead to serious underestimation of a capture zone. By including all acceptable or valid models in the analysis, large-scale uncertainty can be accounted for by means of the precautionary approach.

Although this study has expanded the range of uncertainties that are commonly dealt with, we hope that it has also produced more clarity into its effects. Because uncertainty will remain elusive, model users and decision-makers need to be aware of the causes of uncertainty and alert in detecting its effects. This means that technical judgement will always play a role throughout the process, particularly in the selection of scenarios. It also means that in examining model results obtained under uncertainty, the first question should always be: Do the results make sense? Unfortunately, in a high-pressure consulting environment, there may not always be sufficient opportunity to ask this question.

3.7 Figures and tables

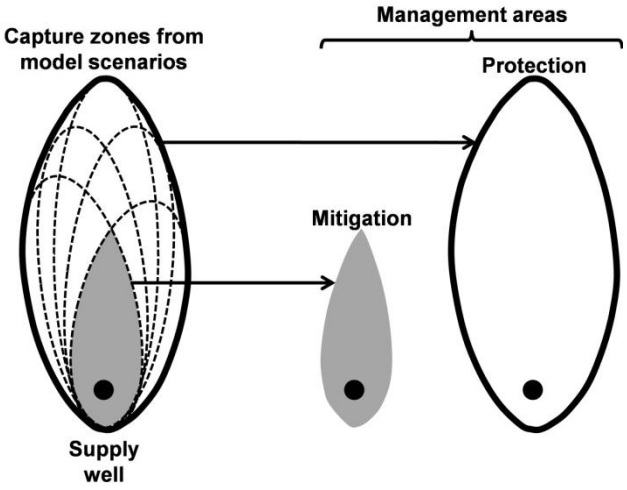

Figure 3.1. Conceptual representation of different approaches for protection and mitigation decisions (adapted from Evers and Lerner, 1998).

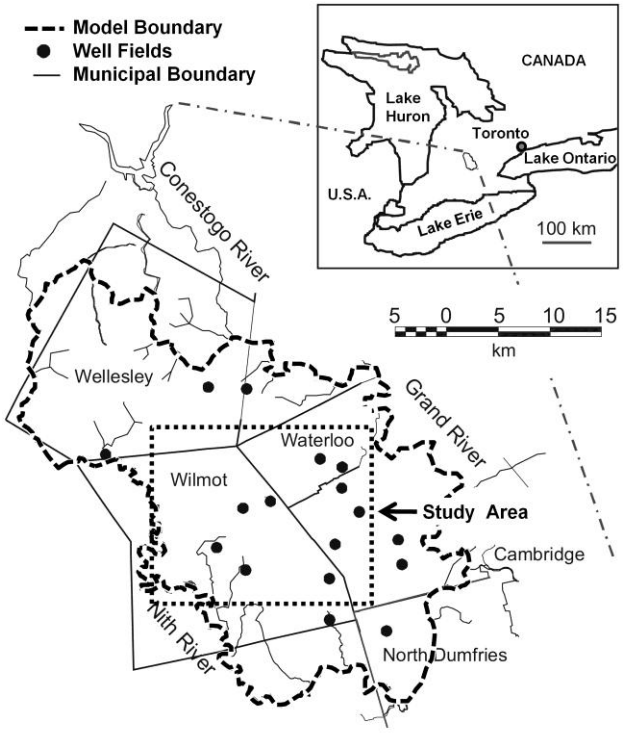

Figure 3.2. Location of study area within the Waterloo Moraine model. Well fields are comprised of one or more wells (adapted from Frind et al., 2006).

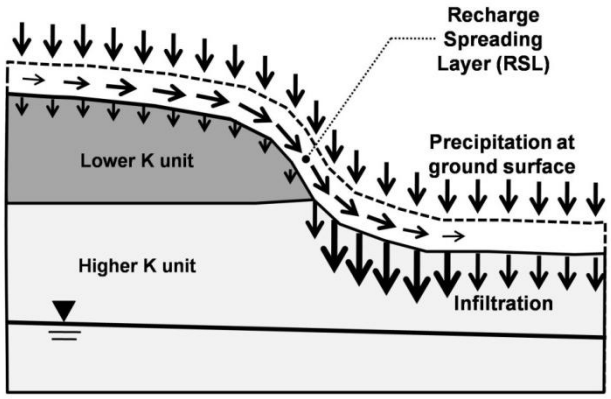

Figure 3.3. Conceptual representation of the recharge spreading layer (RSL).

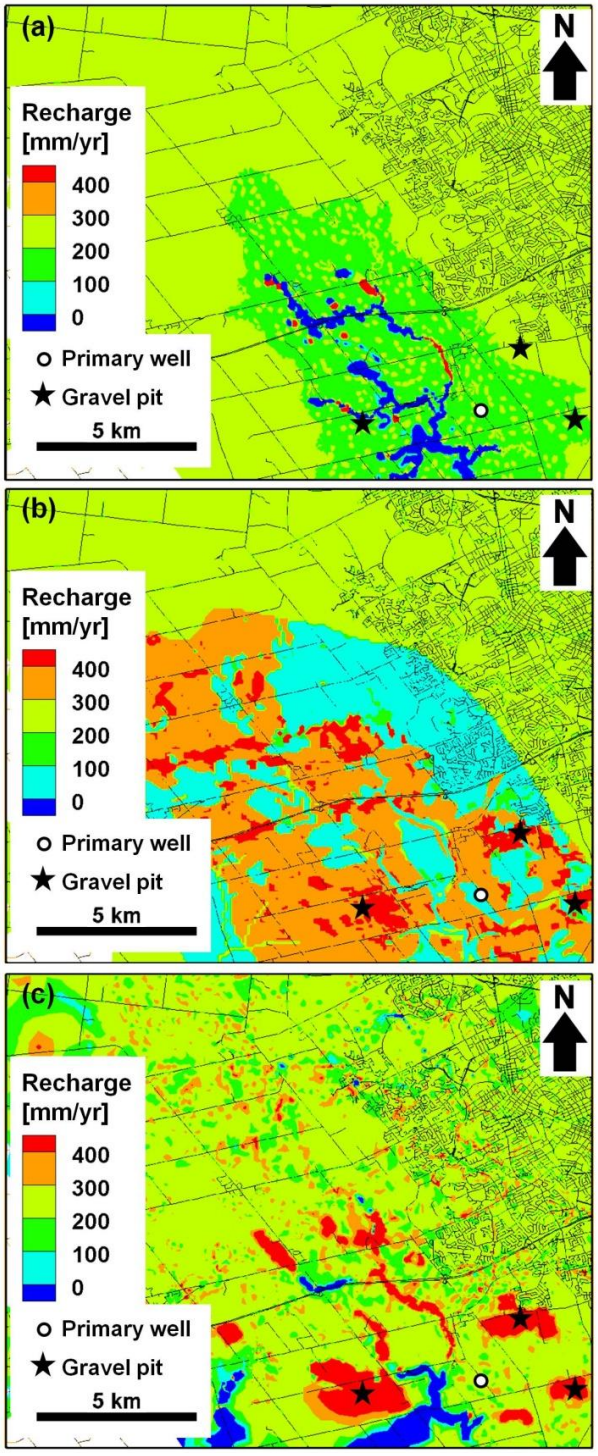

Figure 3.4. Recharge distribution estimated using (a) HYDROGEOSPHERE (from Jones et al., 2009), (b) GAWSER/MODFLOW (from CH2M-HILL and Papadopulos and Associates Inc., 2003), (c) WATFLOW.

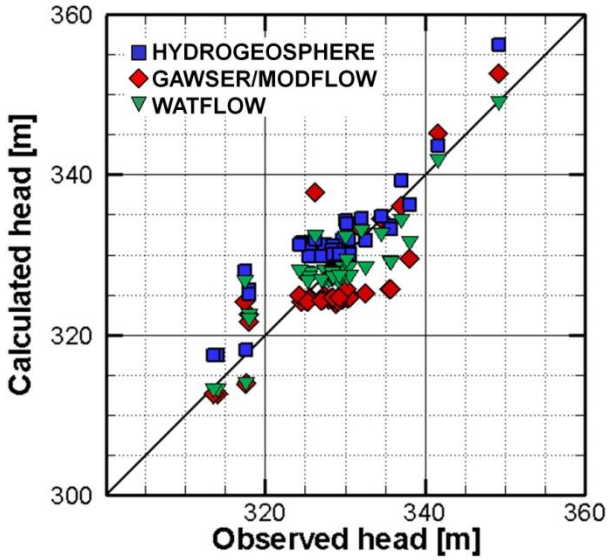

Figure 3.5. Calibration plot for three different model scenarios with different recharge distributions (HYDROGEOSPHERE, GAWSER/MODFLOW and WATFLOW).

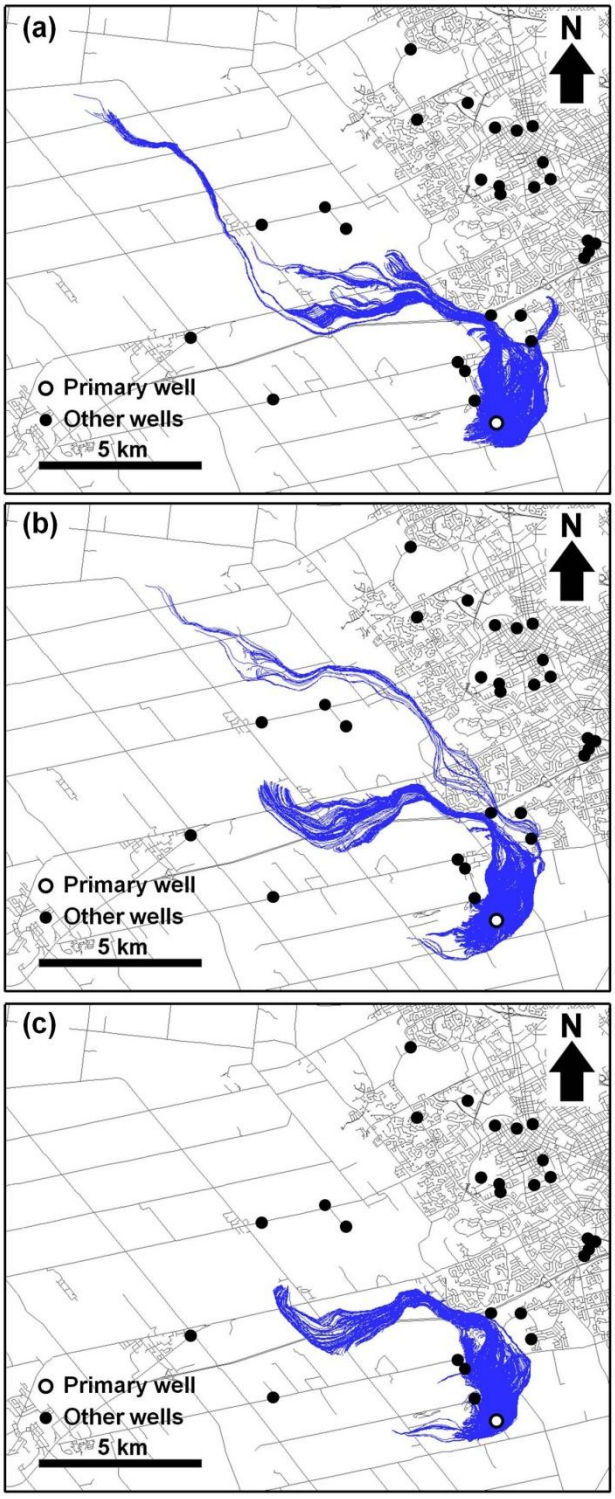

Figure 3.6. Particle tracks for primary well using recharge distributions from (a) HYDROGEOSPHERE, (b) GAWSER/MODFLOW, (c) WATFLOW.

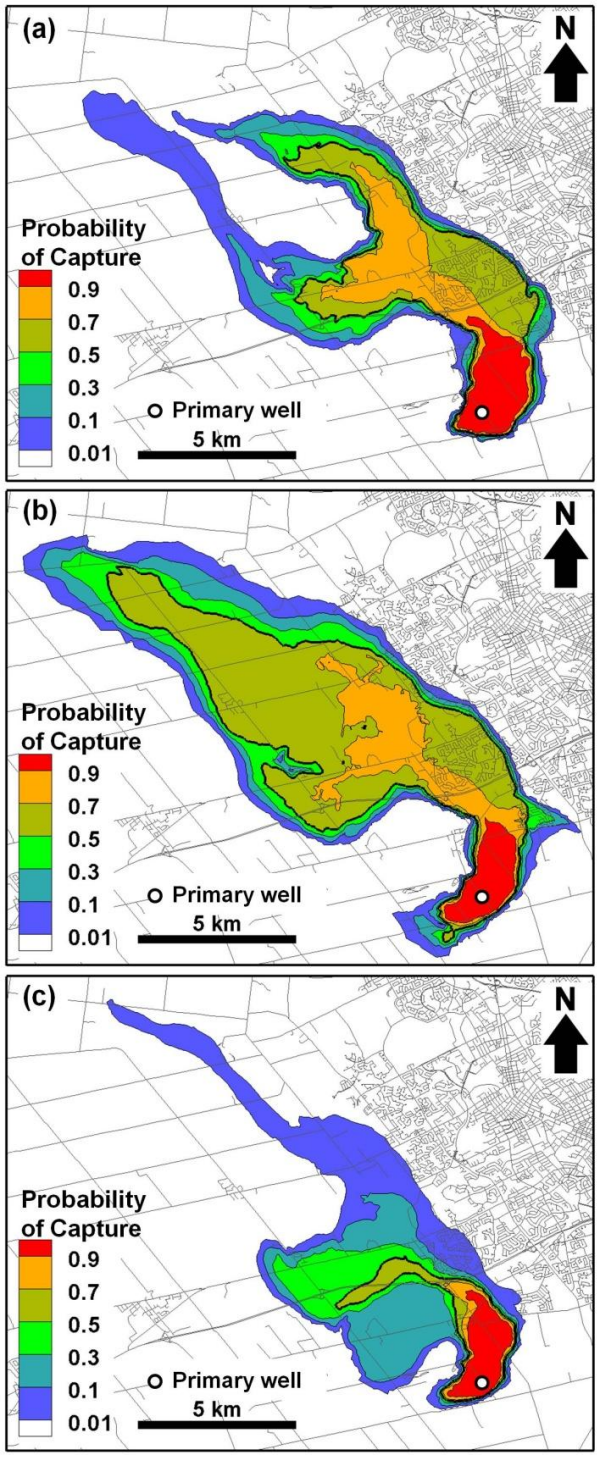

Figure 3.7. Maximum capture probability over aquifer depth using recharge distributions from (a) HYDROGEOSPHERE, (b) GAWSER/MODFLOW, (c) WATFLOW. The 0.5 contour has been emphasized.

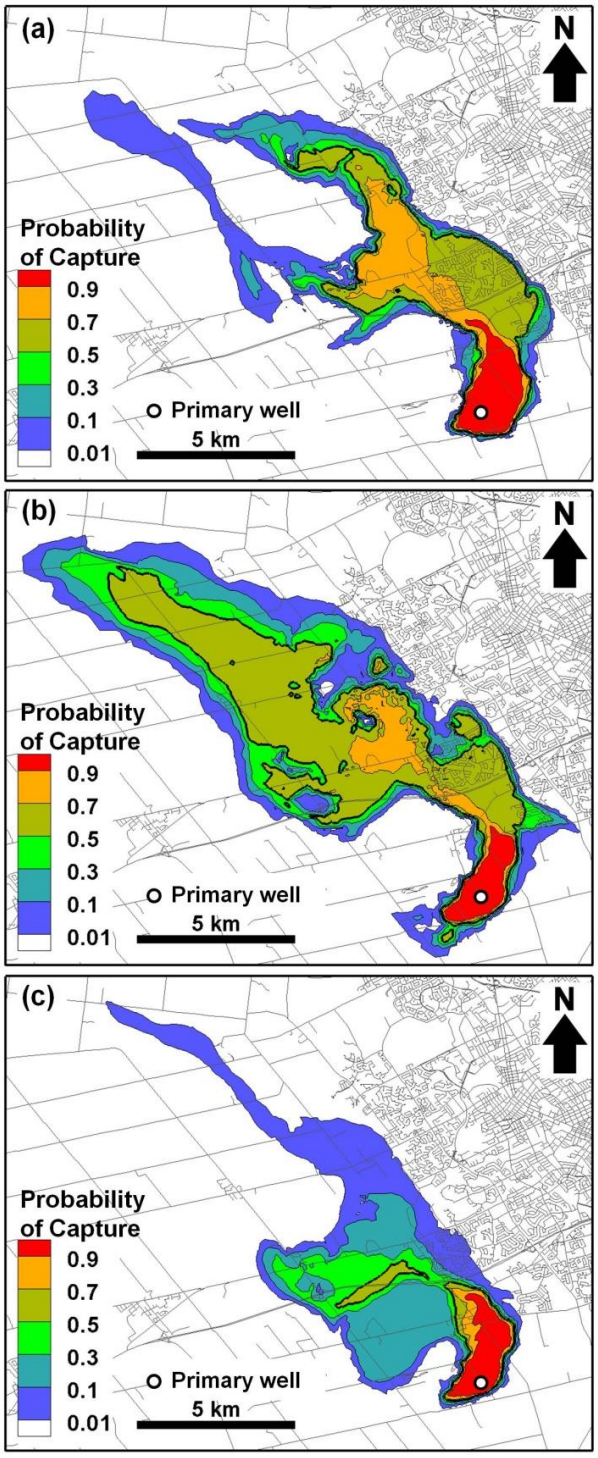

Figure 3.8. Capture probability at ground surface using recharge distributions from (a) HYDROGEOSPHERE, (b) GAWSER/MODFLOW, (c) WATFLOW. The 0.5 contour has been emphasized.

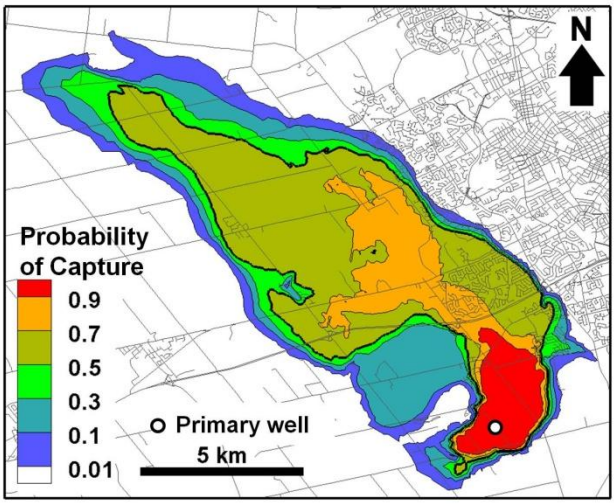

Figure 3.9. Protection map for primary supply well. The 0.5 contour has been emphasized.

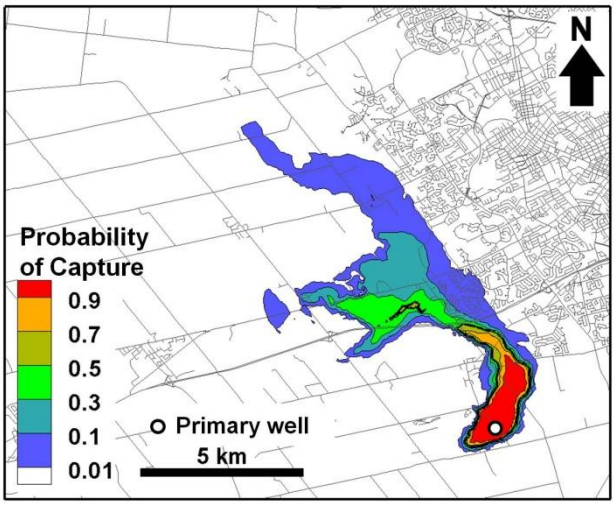

Figure 3.10. Mitigation map for primary supply well. The 0.5 contour has been emphasized.

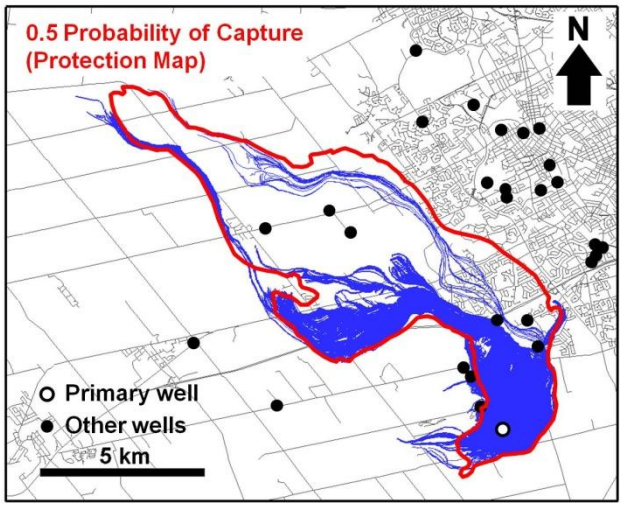

Figure 3.11. Capture zone from particle tracks, using 0.5 probability contour from protection map as envelope.

Chapter 4

Predicting the effects of Beneficial Management Practices (BMPs) on public supply wells impacted by nitrate contamination

4.1 Introduction

The availability of nitrogen is a common limiting factor for plant growth. Consequently, the application of nitrogen-based fertilizers is customary in agricultural practice. When applied in excess, the nitrogen not used by plants may leach through the root zone and contaminate groundwater resources, usually in the form of nitrate (NO_3^-). High nitrate concentrations in groundwater have public health and environmental implications and have become a common problem in many parts of the world.

One approach to address this problem is the adoption of Beneficial Management Practices (BMPs), which in this context refers to a set of measures to reduce the environmental impacts associated with agricultural activities, including nitrate leaching to groundwater. The implementation of BMPs has important societal implications and therefore their proper design must balance overall costs and benefits. However, the effects of BMPs on groundwater systems are slow and difficult to measure. Some factors that hinder the assessment of BMP performance are: (1) aquifer and contamination source properties may vary spatially and temporally over a large area, so it is difficult to isolate the effects of BMPs from all other fluctuations; (2) residence times in groundwater systems are usually long; and (3) due to the source dimensions, representative data can be expensive to collect and often are not available. Due to these complications, it is difficult to rely exclusively on direct field measurements to design and predict the effects of BMPs. In this context, numerical models can be useful to complement field efforts and provide further insights regarding BMP design and response.

In this chapter, we use a numerical model to estimate the effects of BMPs implemented in 2003 (~ 10 years ago) on nitrate concentrations at the Thornton well field, located near the City of Woodstock, ON. This case study is based on extensive field work from previous research, especially regarding recharge and nitrate loading distributions (Sebol, 2000; Golder Associates, 2001; Padusenko, 2001; Haslauer, 2005; Bekeris, 2007; Koch, 2009; Critchley, 2010; Brook, 2012). Alternative options to reduce nitrate contamination and practical aspects regarding the use of numerical models for similar cases are discussed.

In this context, the following specific objectives are pursued:

- to propose a framework to estimate the effects of BMPs in water supply wells. This framework combines multiple model settings, each with specific goals, and can be useful to design remediation strategies for similar cases;
- to compare different techniques for generation of mass loading distributions using field point measurements. The decision of which technique to use is not always straight-forward. The comparison of the results obtained from different techniques would illustrate the practical relevance of this decision;
- to investigate the effectiveness of the adoption of BMPs in selected areas as a valid strategy to improve the water quality in supply wells impacted by non-point source contaminants.

4.2 Background

4.2.1 Nitrogen and plant growth

Nitrogen is an essential nutrient for plant growth and survival. Although it constitutes the majority of the atmosphere (78% by volume of dry air), almost all nitrogen on Earth is in the form of nitrogen gas (N_2), which is inert and unavailable to most organisms (Erisman et al., 2008). Only a small fraction of the nitrogen in the atmosphere is converted by natural processes into more reactive nitrogen compounds that can be used by plants, such as nitrate (NO_3^-) or ammonium (NH_4^+). Lightning discharges and nitrogen fixation by bacteria (free-living or in symbiosis with plants) are examples of such processes. As a consequence, the availability of reactive forms of nitrogen in soils is often a limiting factor for plant growth. To increase crop production, nitrogen-based fertilizers are commonly applied in agricultural practice.

Until the first half of the twentieth century, fertilizer applications consisted mostly of recycled organic matter or limited sources of mined reactive nitrogen, such as guano or coal (Davidson et al., 2012; Sutton and van Grinsven, 2011). This situation changed dramatically since the development of the Haber-Bosch process, which allows the artificial synthesis of ammonia (NH_3) from nitrogen gas (N_2) on an industrial scale (Smil, 2001). Since the 1950s, the application of synthetic nitrogen-based fertilizers promoted significant improvements in crop yield, averting a major food crisis and enabling unprecedented population growth (Fig. 4.1). In terms of global impact, the Haber-Bosch process is arguably the most relevant invention of the 20th century (Smil, 1999) and it was referred to by Sutton et al. (2011a) as the "greatest single experiment in global geo-engineering" ever made by humans.

4.2.2 Nitrogen in groundwater

An undesired consequence of the access to abundant synthetic fertilizer is the contamination of groundwater resources. Reactive nitrogen that is not used by plants may leach through the root zone and be incorporated into groundwater, usually in the form of nitrate (NO_3^-), which is highly soluble and mobile (Almasri and Kaluarachchi, 2007). Under aerobic conditions, common in shallow aquifers, nitrate does not undergo any reactions and behaves as a conservative solute (Rivett et al., 2008). Consequently, fertilizer application in agriculture is identified as a major source of groundwater pollution (Nolan et al., 1997; Haygarth and Jarvis, 2002; EEA, 2005), although there are other anthropogenic sources that contribute to the problem, such as septic tanks and atmospheric

deposition from burning fuels. High nitrate concentrations due to agricultural activities are reported in several groundwater supplies around the world (*e.g.*, Strebel et al., 1989; Power and Schepers, 1989; Goss et al., 1998; Zhang et al., 1996), differing significantly from pristine conditions (Grizzetti et al., 2011) and above the current quality standards (Erisman et al., 2011).

High nitrate concentrations in groundwater have potential negative effects for the environment and for public health. Discharge of nitrogen-rich groundwater may cause nutrient imbalance, loss of biodiversity, eutrophication and acidification in surface water bodies (Capone and Bautista, 1985; Sutton et al., 2011, Null et al., 2012). In terms of public health, high NO_3^- concentrations in drinking water are associated with methemoglobinemia or "blue baby syndrome" (Comly, 1945; Walton, 1951) and some types of cancer (Jakszyn and González, 2006). Maximum drinking water limits for nitrate are currently 10 mg-N/L (45 mg NO_3/L) for Canada (Health Canada, 2012) and United States (USEPA, 2009), and 11.3 mg-N/L (50 mg NO_3/L) for the European Union (Official Journal of the European Communities, 1998). The World Health Organization also recommends a similar limit ($[NO_3^-]/50 + [NO_2^-]/3 < 1$, concentrations in mg/L; WHO, 2007). There is some controversy regarding the current drinking water standards for nitrate: Some recent studies suggest that it may be too strict (Avery, 1999; Powlson et al., 2008), while others argue the contrary, that the current limit may be too lenient (van Grinsven et al., 2006). Regardless of the discussion about what the exact limit should be, nitrate contamination of groundwater remains a serious concern at an international scale.

4.2.3 Beneficial Management Practices

An approach to address nitrate contamination in groundwater is to adopt agricultural practices that adjust the application of fertilizers to optimize plant uptake and minimize pollution. These practices are commonly referred to as Beneficial Management Practices (BMPs) for nutrient management (Agriculture and Agri-Food Canada, 2010; Beegle et al., 2000, Delgado and Shaffer, 2008; Wassenaar et al., 2006) or Codes of Good Agricultural Practice (European Environment Commission, 1991). The letter "B" in BMP stands for "Best" or "Better" Management Practices in some cases, and may also target other environmental impacts related with agricultural activities. The acronym "BMP" is also used in other fields of knowledge to refer to a set of good practices. Examples of areas that use this acronym are: water treatment, storm water drainage, fish farming, pesticide management, logging etc. For the purpose of this work, the focus is solely on the reduction of nitrate leaching to groundwater.

There are many costs associated with the implementation of BMPs, such as: changes in farm operation, elaboration of better nutrient management plans, infrastructure costs, improvements in handling, storage and application of fertilizers, monitoring costs and potential changes in crop yield. For the sustainable design of BMPs, these costs must be balanced against economic, environmental and public health benefits of lowering nitrate contaminations in groundwater. In other words, the design of BMPs must pass a cost-benefit analysis. To further improve BMP design, this analysis can be performed for multiple scenarios, allowing the selection of the scenario with best overall cost-benefit ratio (Bernardo et al., 1993; Yadav and Wall, 1998; AAFC, 2010; Almasri and Kaluarachchi, 2007).

Amongst the many aspects involved in this analysis (*e.g.*, legal, social, economic, operational), the groundwater system response to BMPs is an important one because of its environmental and public health implications. This response, represented by changes in groundwater and supply well concentrations, is slow and difficult to measure (Tomer and Burkart, 2003). Changes in nitrate concentrations can be delayed by long residence times, which is typical for groundwater systems (Wriedt and Bouraoui, 2009; Rivett et al., 2008; Johnston et al., 1998), or by the slow release of nitrate from the unsaturated zone and by molecular diffusion from non-active flow areas into active flow areas (Molénat and Gascuel-Odoux, 2002). Because of the long time lag between mitigation measures and overall impact on aquifer systems, decision makers cannot rely on a simple empirical approach to the problem, for example: (1) implement BMPs, (2) wait for improvements, and (3) complement with additional measures if necessary. The long time required to evaluate improvements would be impractical.

Another challenge is the identification of target or priority areas for implementation of BMPs. Nitrate in groundwater shows complex spatial and temporal patterns (Hong et al., 2007) and aquifer systems may also present some complex patterns of travel times between sources at ground surface and receptors (Cellier et al., 2011). As a result, implementing BMPs in different areas within the same field site, may have significantly different performances for the same investment. Beegle et al. (2000) argues that properly targeting BMP efforts is a key factor for a successful implementation. If the objective is to improve the water quality at a given public supply well, areas within the well capture zone should be prioritized for implementing BMPs (Evers and Lerner, 1998; Rahman et al., 2010; Sousa et al., 2013).

4.2.4 Use of numerical models to support the implementation of BMPs

To address these challenges, the use of physically-based numerical models can be useful to: (1) enhance the understanding of the aquifer system response to changes in nutrient loading; (2) make predictions to support cost/benefit analysis and the decision-making process as a whole; (3) improve monitoring and correction strategies. Models have been applied in many previous studies to interpret nitrate contamination in different scales (*e.g.*, Almasri and Kaluarachchi, 2007; Martin et al., 2006; Frind et al., 1990), to estimate BMP effects (*e.g.*, Hérivaux et al., 2013; Chesnaux et al., 2007; Molénat and Gascuel-Odoux, 2002) and to support land management decisions (*e.g.*, van den Brink et al., 2008, Almasri and Kaluarachchi, 2007).

The use of numerical models to support management decision involves general challenges that are associated with virtually all modelling efforts, such as: uncertainty, non-uniqueness, impossibility of model validation and subjectivity (Smith and Schwartz, 1981; Konikow and Bredehoeft,1992; Beven, 1993; Oreskes et al., 1994). There are also specific challenges particular to nitrate transport simulation for BMP design. Some of these specific challenges are:

(1) how to address root zone processes and combine the root zone and aquifer system scales. Both scales are important to address this problem: How much nitrogen is leached to groundwater depends on root zone scale processes. In contrast, the transport between the bottom of the root zone to receptors (*i.e.*, wells and surface water bodies) can only be understood when approached from the aquifer system scale;

(2) how to represent the time lag in the unsaturated zone on a large scale model domain (capture zone / watershed scale). As previously mentioned, the unsaturated zone acts as a buffer or storage for nitrate which delays the aquifer response to improvements in fertilizer application practices. Therefore, to properly design BMP approaches, the unsaturated zone may need to be considered explicitly. However, simulation of unsaturated zone processes requires finer discretization, which may be inefficient in larger model domains;

(3) how to deal with complex patterns of nitrate loading. One of the challenges for addressing problems involving non-point source contaminants is to characterize the contaminant source over the entire area of interest based on point field estimations. This characterization can be accomplished by using different mapping techniques. Mapping is defined, in this work, as the way by which a parameter distribution is assigned over the entire surface of interest (in this case, the ground surface). The selection of the appropriate mapping approach is not a straight-forward task.

In this context, a physically-based numerical model was developed to estimate the effects of BMPs in the Thornton well field (Woodstock, ON) and to discuss challenges involved in the application of numerical models to the design of BMPs. This work is part of a larger effort to assess the performance of changes in nutrient practices as an alternative to reduce nitrate concentrations and it relies on extensive field data from previous studies. The site and model descriptions, followed by results and discussion, are presented on the following sections.

4.3 Site description

4.3.1 Thornton well field site (Woodstock, ON)

The Thornton well field, comprised of five wells (1, 3, 5, 8, 11), is situated south of the city of Woodstock in southern Ontario, Canada (Fig. 4.2). The land use surrounding the well field is mostly agricultural (approximately 80%; Haslauer, 2005). The topography of the study site is characterized by rolling hills and drumlin features, with ground elevations ranging between 270 and 380 m above sea level (Fig. 4.3). Surface water within the study site drains to Cedar Creek, which is a tributary of the Thames River.

This well field is an important source of drinking water to the city of Woodstock, with a total pumping rate of approximately 6600 m^3/day in the period between 2006 and 2012 (Fig. 4.4). Since 1970s, an increasing trend in nitrate concentrations had been observed in the supply wells, eventually exceeding the drinking water standard of 10 mg NO_3-N/L in the 1990s. Pumping rates were then reduced, and concentrations in the supply wells have ranged between 12 and 4 mg NO_3-N/L (Fig. 4.5). The water from the Thornton well field was blended with contributions from other well fields with lower nitrate concentrations to comply with drinking water standards.

This field site has been the objective of study of many different researchers. Padusenko (2001) and Haslauer (2005) characterized the site hydrogeology. Sebol (2000) and Heagle (2000) investigated the site geochemistry and residence times based on isotope tracers. Bekeris (2007) and Koch (2007) estimated recharge and nitrate mass loadings distributions. Critchley (2010) studied the use of a cross-injection scheme to locally stimulate denitrification. Brook (2012) compared different fertilizer management strategies and estimated recharge during a melt event using temperature profiles. The site characteristics that are relevant for the modelling work presented in this chapter are summarized in the following sections.

4.3.2 Geology and hydrostratigraphy

The bedrock geology is comprised of Silurian dolostone and shale overlain by Devonian limestone. The bedrock surface is generally flat or gently rolling, sloping from north-east to south-west, with some drainage indentations (Cowan, 1975). One deep monitoring well (WO-28D) reached the limestone bedrock at 69 m below ground surface (Haslauer, 2005).

The quaternary geology of the field site is dominated by Zorra Till, which is stiff, stony and silty. This unit is underlain by Catfish Till (and possibly Port Stanley Till), which is associated with glaciofluvial sand and gravel deposits (Cowan, 1975). Some of the supply wells are located in a glaciofluvial outwash channel, which is highly permeable (*i.e.*, sand and gravel) and may act as a relatively fast connection between ground surface and water table/well screen. The field site is located in the interlobate zone, in which ice lobes displaced and mixed sediments in different directions, at different times. As a result, the hydrostratigraphical units are discontinuous and heterogeneous. The overburden thickness varies between 30 m and 80 m (Brook, 2012). Haslauer (2005) and Padusenko (2001) present more detailed summaries of the site geology.

A hydrostratigraphical model for the site (Fig. 4.6) was developed by Haslauer (2005). It is comprised of alternating aquitards and aquifers, underlain by bedrock. The top of the bedrock is treated as an additional aquifer. These aquifers/aquitards are discontinuous in certain areas, reflecting the glacial depositional history of the site. The main aquifer used for water supply is Aquifer 3, as indicated on Fig. 4.6. The regional groundwater flow direction in this aquifer is from southwest to northeast, and locally from west to east, as shown on Fig. 4.7. The potentiometric map indicates the influence of the well field in the form of depressed water levels in the upgradient direction.

4.3.3 BMP implementation

To address the problem of increasing nitrate concentrations, the County of Oxford purchased two plots of farmland (total area = 111 ha = 275 acres, Fig. 4.8) in 2003. These plots were then leased back to farmers under the condition that BMPs would be implemented. The purchased plots are located within the estimated two-year time of travel capture zone, according to an earlier study by Golder Associates (2001; Fig. 4.8) that considered travel times exclusively in the saturated zone. By decreasing nitrate loading in these areas, the objective was to eventually reduce concentrations at the supply wells.

To implement BMPs in these parcels, the amount and distribution of fertilizer to be applied was estimated based on field tests to assess existing soil nutrient and taking into account specific crop type requirements. Fertilizer application was then made with help of a global positioning system (GPS) and carefully recorded. Also, manure application was replaced by synthetic fertilizers and crops requiring lower fertilizer application rates were chosen. Bekeris (2007) estimated that the implementation of BMPs changed the average nitrogen balance (*i.e.*, nitrogen input as fertilizers minus the nitrogen removed by crops at harvest) from +26 kg-N/acre to -38 kg N/acre, for the years 2003 to 2005, while still maintaining crop yields equal or superior to the long-term average for the region. To compensate for costs associated with BMPs, the farmers received a discount on lease payments (Haslauer, 2005; Bekeris, 2007; Brook, 2012).

4.3.4 BMP area and capture zone

By comparing the area of a potential farmland considered for BMP implementation with the total well capture zone area, it is possible to have an initial idea of potential long-term improvements. Assuming steady-state conditions and an average recharge value within the capture zone, the capture zone area can be estimated by a simple conservation of mass statement, as follows: Pumping rate (Q) = Recharge (R) x Capture zone area (A_{CZ}), in consistent units. For the Thornton well field, assuming an average recharge of 470 mm/year (~ 1.29 x 10^{-3} m/day) and a total pumping rate for all wells of 6600 m^3/day, the capture zone area A_{CZ} can be estimated as ~ 5.13 x 10^6 m^2 (513 ha). This calculation does not consider uncertainty (Chapter 3) which can influence capture zone delineation and extent. It is also noted that this capture zone area is not necessarily consistent with the estimation by Golder Associates (2001; Fig. 4.8), since different boundary conditions and pumping rates were used.

The BMP area purchased by the County of Oxford (A_{BMP} = 111 ha) corresponds to ~ 20% of the total estimated capture zone area (A_{CZ} ~ 513 ha). A rough first estimate of the effects of BMPs suggests that an intervention in 20% of the capture zone should have a similar (~ 20%) potential reduction in concentrations in the well water, assuming complete interruption of mass loading in that area, homogeneous mass loading and recharge over the entire capture zone and that the system is initially in steady-state transport conditions. In the case mass loadings are expected to be reduced but not completely eliminated, the long-term reduction in concentration at the supply wells can be estimated by multiplying A_{BMP}/A_{CZ} (~ 20%) by the expected percent reduction in loading within the BMP area. For example, if mass loadings in BMP areas decrease by ~ 50%, the long term reduction in nitrate concentrations due to BMPs can be estimated as ~ 10% (= 20% x 50%). The extensive field

work performed in the Thornton well field site allows a much more sophisticated estimation of BMP effects, but this rough calculation may be useful as a first approach to the problem. It is also a reminder that the intervention in a limited part of the capture zone is not expected to completely eliminate the contamination by non-point source pollutants, but only to reduce concentrations.

4.3.5 Recharge and nitrate loading

Bekeris (2007) and Koch (2009) estimated recharge and nitrate mass loadings in several locations referred to as "Recharge Stations" (Fig. 4.8). Recharge rates were estimated by tracking the downward movement of tracers (potassium or sodium bromide, applied at ground surface) in soil cores. Soil moisture estimates from neutron moisture probes were also used for these estimations. Bekeris (2007) confirmed field recharge estimations using additional methods: one-dimensional models HELP (Schroeder et al., 1994) and SHAW (Flerchinger, 2000), zero-flux plane method (Scanlon et al., 2002) and water balances.

The same soil cores were also used to measure nitrate concentrations in pore water at different depths over a several year period. These results indicated that the implemented BMPs are effective in reducing nitrate loading to the aquifer. The estimated average nitrate loading changed from 7.5 to 3.4 g NO_3-N m^{-2} $year^{-1}$ (Bekeris, 2007; Koch, 2009). Field evidence of reduction of nitrate loading to groundwater is an important finding, because poor BMP design and performance could potentially go unnoticed for a long time, since a significant time lag is expected between the adoption of BMPs and overall improvements in nitrate concentrations in the aquifer/supply wells (Grizzetti et al, 2011).

An advantage of using soil core analysis is that the nitrate loading to groundwater can be estimated below the root zone, avoiding the simulation of the complex and transient root zone processes, which can be a major source of uncertainty (Durand et al., 2011). The groundwater upstream of the supply wells contains high dissolved oxygen concentrations (Heagle, 2000), which inhibits denitrification. Therefore, after nitrate is displaced below the root zone, it can be treated as a conservative solute. In some situations, however, some denitrification may still occur around pockets of low-K material (Green at al., 2008).

4.3.6 Groundwater age and estimated timeframe for improvements

Based on isotope tracers, Sebol (2004) estimated that the water in the main aquifer just upstream of the supply wells is less than 10 years old. Using a saturated groundwater flow model, Padusenko (2001) estimated travel times of less than 10 years for all supply wells. Adjusting these

estimates to consider the storage of nitrate in the unsaturated zone, the timeframe for changes in the supply wells following improvements in fertilizer application was estimated between 10 to 30 years. Using hand calculations and making some simplifying assumptions (*e.g.*, piston flow, no reactions, no preferential flow), Haslauer (2005) estimated this time frame to be approximately 15 years.

4.4 Model setup and calibration

4.4.1 Conceptual model

The conceptual model was based on the hydrostratigraphical model developed by Haslauer (2005) and updated using VIEWLOG (Kassenaar, 2004) to incorporate borehole data from Koch (2009). The final result is illustrated in Figure 4.6. This update involved changes in the thickness of some hydrostratigraphical units and the identification of new hydraulic connections between aquifer units, but it did not require any conceptual changes on the model proposed by Haslauer (2005).

The initial hydraulic conductivity field was based on previous distributions estimated by Haslauer (2005), following the work of Padusenko (2001), who used grain size distribution methods and single well recovery tests in both observation and supply wells. This hydraulic conductivity distribution was updated using additional slug tests performed by Critchley (2010). The ratio between hydraulic conductivities in the horizontal and vertical directions was assumed to be 1 (*i.e.*, isotropic or anisptropy ratio $K_h/K_v = 1$), although existent modelling studies in glacial aquifer systems used anisptropy ratio K_h/K_v of 10 (Martin and Frind, 1998). The use of an K_h/K_v ratio of 1 is justified by the possible presence of vertical features in the till layers that may increase the vertical conductivity.

All aquifers and aquitards were simulated as porous media. Haslauer (2005) reports that drilling the top of the bedrock showed typical behaviour of fractured media (hard, dry and sharp-edged cuttings, producing water immediately as a fracture was intercepted). However, an equivalent porous medium representation of flow for the top of the bedrock was considered appropriate, since the well field is tapping the aquifer above in the overburden and fractured flow is not expected to play a major role in the well field response to BMPs implemented on the areas purchased by the Oxford County. Below this bedrock aquifer, the medium was assumed to be impermeable.

As shown in Chapter 3, recharge can significantly influence the shape and area of capture zones. For the particular case of BMP design and assessment, recharge is recognized as an important factor for two main reasons: (1) it influences the capture zone of the Thornton well field and, consequently, the relative importance of the purchased farmlands to well water quality; and (2) it is necessary to estimate groundwater residence times and, consequently, the time lag expected between implementation of BMPs and improvements at the supply wells.

The recharge assigned to the top model boundary was based on a spatial distribution previously proposed by Padusenko (2001), which divided the site in different zones based on near-surface soil

properties, crop type and topography. For each of these zones, recharge values were estimated by Padusenko (2001) from a series of 1D water balance model simulations using the code HELP (Schroeder et al., 1994). For the current model, the zonation proposed by Padusenko (2001) was maintained, but the recharge magnitude was adjusted using multiplication factors to match field estimates from Bekeris (2007) and Koch (2009). The final result is a distribution that varies with soil properties, crop type and topography and that is consistent with estimations from tracer experiments. The obtained recharge distribution is shown on Fig. 4.12.

All groundwater flow simulations in this work were assumed as steady-state, since the time-scale of interest spans over many hydrological cycles (few years to a few decades) and seasonal variations are expected to dampen before reaching the supply wells. Therefore, storage parameters were not needed for the simulations.

Two different sets of dispersivity values were used in the transport simulations. Smaller values were assigned above the water table (Longitudinal disp. = 0.10 m; Vertical and horizontal transverse disp. = 0.05 m), and larger values for the saturated zone (Longitudinal disp. = 10.0 m; Vertical and horizontal transverse disp. = 0.5 m). A study by Frind and Hokkanen (1987) indicates that for a glaciofluvial sand aquifer the transverse vertical dispersivity should be small (between 0.005 and 0.01 m). The larger value of 0.5 m was chosen to avoid the need for a fine vertical grid discretization. Because both the flow field and the plume converge towards the well, the large adopted transverse dispersivity is not expected to affect the predicted concentrations at the well. However, the breakthrough curve and the time of arrival of a given pulse could be affected.

4.4.2 Modelling approach

To simulate flow and nitrate transport, the commercial finite-element code FEFLOW (Diersch, 2006) was used. Two important characteristics of FEFLOW for this particular application are: (1) the ability to simulate variably-saturated flow and transport, therefore accounting for nitrate storage in the unsaturated zone, and (2) the ability to simultaneously use multiple computer processors, reducing execution times.

To reduce the computational burden, numerical simulations were performed at two scales, referred to as "Larger-Scale model" and "Smaller-Scale model" (Fig. 4.9). The first one is a larger saturated flow model (3100 ha) that was used to estimate regional groundwater flow around the well field. This model was calibrated and then used to define flow boundary conditions to a smaller model domain

(700 ha), which encompasses the well field and the farm properties in which the BMPs were implemented. This Smaller-scale model was used to simulated variably-saturated groundwater flow and transport. A graphic summary of the complete modelling approach, to be explained in the following sections, is presented on Fig. 4.10.

4.4.3 Larger-scale model: Saturated flow

The updated hydrostratigraphy and hydraulic conductivity field were used to populate the Larger-scale model domain (Fig. 4.9). The boundaries of this model were defined based on the regional groundwater flow for Aquifer 3. Specified head (Type I or Dirichlet) boundary conditions were assigned along the boundaries to impose the interpreted regional groundwater flow system, interpreted from observed water level measurements. No-flow boundary conditions (Type II or Neumann) were assigned to groundwater divides and along streamlines (Fig. 4.11).

Pumping rates were taken as the average from 2006 to 2012 (Fig. 4.4). These values considered in the model are, in m^3/day: 2030.3 (Well 1), 264.3 (Well 3), 383.7 (Well 5), 1524.4 (Well 8) and 2410.1 (Well 11). Due to the proximity of the well screens and similar observed concentrations, Wells 1 and 5 were combined as a single well in model simulations, for simplicity (Well 1/5, combined pumping rate = 2414.0 m^3/day).

4.4.3.1 Flow calibration

Calibration targets were taken as the average water levels observed over 3 years (2006-2008) in monitoring wells. These water levels were monitored continuously by pressure transducers and periodically corrected by independent hand measurements. Single water level observations from pre-existing wells were also taken into consideration for calibration. These single measurements are of lower quality, but cover a wider area.

The flow calibration was made in two stages. First, the hydraulic conductivity for each aquifer/aquitard was adjusted using PEST (Doherty, 2005), an algorithm for parameter estimation which is embedded in the user interface of FEFLOW. The hydraulic conductivity values were modified by means of a multiplication factor assigned per hydrostratigraphic unit. These factors were allowed to vary within one order of magnitude during the calibration process. The anisotropy ratio was kept constant and equal to 1. The second stage of calibration consisted of a manual fine-tuning by trial-and-error to minimize calibration bias and address calibration outliers. The flow boundary conditions presented in Fig. 4.11 were also adjusted.

The calibration plot and calibration statistics for the Larger-scale saturated flow model is shown in Fig. 4.13. For the high-quality calibration targets (*i.e.*, observation wells constantly monitored), the average error and the average absolute error are -0.2 m and 1.2 m, respectively. From these targets (Table 4.1), 3 points had differences between observed and measured values above 5 m and were deemed as outliers: WO-28-1 and WO-71-S and WO-71-D. For the low-quality data (Table 4.2), calibration errors are larger (average error = -2.0 m; and average absolute error = 3.8 m) but still were considered acceptable, given that they are associated with much higher uncertainty.

In Fig. 4.14, the calculated flow field in the main aquifer (Aquifer 3) is compared with the interpolated observed hydraulic heads from: (1) all high-quality calibration targets (Fig. 4.14a) and all high-quality calibration targets with the exception of the three identified outliers (Fig. 4.14b). This comparison is useful to evaluate model calibration and to identify regions where the model fails to represent the behavior of the real system. In Fig. 4.14a, it can be seen that the model fails to capture the local flow between observation wells WO-28 and WO-71. However, if the outliers in this area are ignored, there is a relatively good match between the simulated and observed potentiometric maps in the area as a whole. This match indicates that the saturated flow model adequately captures the regional groundwater flow direction and gradient, although it does not adequately represent the local flow direction around the outliers WO-28 and WO-71. For the purpose of providing local flow boundaries for the Smaller-scale model domain, this calibration (Fig. 4.13) and simulated flow field (Fig. 4.14) were considered adequate.

4.4.4 One-dimensional model: Determining unsaturated zone discretization

One-dimensional (1D) simulations (Fig. 4.15) were performed to define the vertical discretization to be used in the unsaturated zone of the 3D Smaller-scale model. A downward solute pulse applied at ground surface was simulated in a 1D column with fixed length, but using different element thicknesses, namely: 20 m, 10 m, 5 m, 1 m, 50 cm, 25 cm, 10 cm. Breakthrough curves at the water table for all discretization scenarios were then compared. The coarsest discretization (*i.e.*, smallest computational burden) that does not generate excessive numerical dispersion was selected to develop the 3D Smaller-scale model grid.

These 1D runs were performed using the model setting illustrated in Fig. 4.15. The same software (FEFLOW) adopted for the 3D simulations was used. Soil texture (silty sand), recharge (250 mm/yr) and depth to water table (40 m) are representative of locations in the study site where significant time lag in the unsaturated zone is expected.

Flow in the unsaturated zone was simulated using the modified van Genuchten (MVG) constitutive relationships for representing saturation (S) and hydraulic conductivity (K) as a function of pressure head (Ψ). The MVG formulation is featured in FEFLOW (Diersch, 2006) and it consists of a more linear version of the equations originally proposed by van Genuchten (van Genuchten, 1980). The MVG expressions for saturation (S) and hydraulic conductivity (K) are presented below:

$$S(\psi) = \begin{cases} S_r + \dfrac{1 - S_r}{\left(1 + \left|A \cdot \psi\right|^n\right)^m} & for\ \psi < 0 \\ 1 & for\ \psi \geq 0 \end{cases} \tag{4.1}$$

$$K(\psi) = \begin{cases} K_s \cdot S_e^{\lambda}\left[1 - \left(1 - S_e^{1/m}\right)^m\right]^2 & for\ \psi < 0 \\ K_s & for\ \psi \geq 0 \end{cases} \tag{4.2}$$

where: $S(\psi)$ = saturation [-] at pressure head ψ [L], S_r = residual saturation [-], S_e = effective saturation = $(S - S_r)/(1 - S_r)$, K = hydraulic conductivity [L/T], K_s = saturated hydraulic conductivity [L/T], A = an empirical coefficient related to the inverse of air-entry pressure [L^{-1}], n is an empirical coefficient related to pore-size distribution [-], L is the empirical pore-connectivity parameter [-], assumed to be 0.5 for most soils (Mualem, 1976), m = 1 - 1/n, and $\delta \geq 1$ is an arbitrary/fitting coefficient [-]. For the Thornton well field case, parameters representative of silty sand were adopted from pedo-transfer functions (Schaap et al., 1999). The saturated hydraulic conductivity was estimated as $K_s = 5 \times 10^{-4}$ m/s and the following empirical coefficients were used: A = 3.475, n = 1.746, and $\delta = 1.1$. For simplicity, a single material was assumed throughout the whole unsaturated soil profile, which does not represent complex stratigraphic sequences in the unsaturated zone.

The model setting shown in Fig. 4.15 was used to compare solute transport using different discretizations (20 m, 10 m, 5 m, 1 m , 50 cm, 25 cm, 10 cm). Grid convergence was achieved for vertical discretization of 25 cm (*i.e.*, breakthrough curve does not change if element thickness is reduced below 25 cm). Therefore, results obtained using 10cm-thick elements were considered free from grid-induced numerical dispersion. These results were used to estimate numerical dispersion errors for other discretization scenarios, as presented in Fig. 4.16. Based on these results, the vertical discretization chosen for the 3D unsaturated zone was 1 m, which results in acceptable grid-induced numerical dispersion errors (approximately 2%). Fig. 4.17 shows a representation of both grids. In this figure, the finer discretization in the Smaller-scale model is indicated. The resulting grid properties for both the Larger-scale and Smaller-scale models are presented in Table 4.3.

4.4.5 Smaller-scale model: Variably-saturated flow and transport

After defining the discretization to be used, the calibrated Larger-scale flow solution was used to define boundary conditions for the Smaller-scale model (*i.e.*, Telescopic Mesh Refinement, Mehl et al. 2006). Only boundary conditions below the water table were exported, since the larger scale model only considers saturated flow. Above the water table, a no-flow boundary condition was assumed at the sides of the smaller scale model. After importing flow boundaries, calibration statistics were recalculated to ensure that the flow field was preserved.

Before assessing the impact of changes due to BMP, the initial distribution of nitrate in the aquifer (*i.e.*, pre-BMP conditions) was estimated using a steady-state solute transport simulation using the Smaller-scale model. Therefore, for a given set of transport boundary conditions, concentrations were allowed to reach equilibrium. Nitrate was simulated as a conservative solute, since mass loadings are representative of conditions below the root zone and there is no field evidence of significant denitrification in the main aquifer (Aquifer 3).

The use of steady-state transport in this stage implies two main simplifying assumptions, namely: (1) that nitrate contamination has been occurring for longer than groundwater residence times in this system, and (2) that the pre-BMP input of nitrate is constant in space and time over the period that encompasses the groundwater residence time. These are simplifications of the system behavior, since transit times in aquifers may vary over a wide time range, potentially predating farming in this area in at least parts of the system. Also, nitrate loadings before BMPs may have varied over the years, depending on crop types, fertilizer application practices and climatic conditions. Despite these limitations, the steady-state assumption can be considered reasonable for this case, since estimated

residence times in the main aquifer are expected to be relatively short (around 10 to 30 years, see Section 4.3.6 Groundwater age and estimated timeframe for improvements) and fertilizer application practices before the BMPs can reasonably be assumed constant over this timeframe.

On the top of the Smaller-scale model domain, the mass loading in agricultural areas was assigned as 7.5 g NO_3-N m^{-2} $year^{-1}$, which is the average pre-BMP loading estimated from soil core data (Koch, 2009). This loading was implemented as a Type I or Dirichlet boundary condition, and specified concentration values were obtained by dividing the loading 7.5 g NO_3-N m^{-2} $year^{-1}$ by the recharge magnitude in each element (*i.e.*, Specified concentration = Mass flux / Recharge, with consistent units). Since recharge varies spatially, specified concentration also changes in space.

For the woodlot and the residential area of Sweaburg, the initial recharge concentration was specified as 2.0 mg NO_3-N/L (type I), which is similar to rainwater nitrate concentrations in Ontario (Berner and Berner, 1996). By assuming rainwater values, it is implied that leaching from the woodlot area, septic tanks and fertilizer application in lawns of Sweaburg residences do not represent a major source of nitrate contamination for the Thornton well field.

On the bottom and outflow sides of the model, transport boundary conditions were assumed as specified concentration gradient equal zero (*i.e.*, Type II or Neumann). This means that there is no solute transport through diffusion across these boundaries, only through advection. Since the bottom of the model is also a no-flow boundary condition (no advection), there is no solute transport across the bottom of the domain. On the inflow sides of the model, initial concentrations values were specified based on measured concentrations in observation wells (Fig. 4.18).

4.4.5.1 Pre-BMP conditions (Steady-state transport calibration)

Transport boundary conditions were then adjusted manually to match the observed concentration values at the supply wells, prior to the implementation of BMPs. The main parameters adjusted during calibration were the inflow concentration at the sides of the model domain (Fig. 4.18), and at the woodlot and Sweaburg. Because pre-BMP nitrate loading was specified directly from field results, this loading was not adjusted during calibration.

As indicated in Fig. 4.5, nitrate concentrations are not constant and display a considerable amount of noise. Calibration targets were defined by averaging observed concentrations at the supply wells over a period of time. The definition of the period to be considered was not straight-forward: If too long, the obtained averages may include older farming practices that are not representative of

conditions when BMPs were implemented. On the other hand, if this period is too short (*e.g.*, observed concentrations at a given time), the resulting calibration targets may be excessively impacted by the data noise. After testing different durations, reasonable compromise between these two aspects was obtained by considering the average concentrations between 1999 and 2001. The obtained values to be used as calibration targets were, in mg NO_3-N/L: 10.3 (Well 1), 10.5 (Well 3), 10.1 (Well 5), 7.3 (Well 8) and 5.2 (Well 11).

The Smaller-scale model was calibrated to match pre-BMP concentrations at the supply wells. Calibration was achieved by adjusting two transport boundary conditions by trial-and-error, namely: (1) inflow concentrations at the side of the domain, and (2) inflow concentrations at the woodlot and the residential area of Sweaburg. The calibrated values for these boundary conditions are shown on Fig. 4.18 (values Pre-BMP). The resulting steady-state concentrations at the Thornton supply wells were, in mg NO_3-N/L: 10.4 (Well 1/5, targets = 10.3 and 10.1), 9.4 (Well 3, target = 10.5), 10.1 (Well 8, target = 7.3) and 8.2 (Well 11, target = 5.2). These were considered representative of pre-BMP conditions, although the simulated values overestimated concentrations at Wells 8 and 11. To achieve calibration, recharge concentration was changed to 4.0 mg NO_3-N/L, from the initial value of 2.0 mg NO_3-N/L. Also, the inflow concentration on the northwest side boundary of the model domain was specified as 22.0 mg NO_3-N/L (Fig. 4.18).

4.5 Prediction of BMP effects

After satisfactory calibration of the initial conditions, the response to concentrations at the well field to BMPs was assessed using steady-state flow and transient transport simulations. For simplicity, the change in nitrate loading from pre-BMP to post-BMP conditions was considered instantaneous, taking place in the beginning of the year 2003. Post-BMP loadings used in these simulations were estimated by Koch (2009) and are representative of the year 2008. These loadings are assumed to remain constant over time after BMPs are implemented.

Two different aspects were investigated in this stage, namely: (1) the effect of different mapping strategies to generate mass loading distributions at ground surface, and (2) the comparison of alternative BMP scenarios. These two aspects are described in the next sections.

4.5.1.1 Alternative mapping techniques for nitrate loading

To provide some insight on the issue of generating nitrate loading distributions from point estimations, four alternative mapping techniques were used to simulate post-BMP loadings within the

farmland purchased by the county of Oxford. These loadings were generated by Koch (2009) and are indicated on Fig. 4.19. They can be summarized as follows:

(1) Average: Post-BMPs nitrate loading was estimated by simply averaging point estimations.

(2) Based on field properties: This distribution was obtained by dividing the areas subjected to BMPs into different fields. Each of these fields was assigned a single nitrate loading value from one of the point estimations. The selection of the point estimation to be used was made based on a comparison between field properties (geology, topography and recharge) and properties where the measurements were made.

(3) Thiessen polygons: the area was divided into Thiessen polygons for each point estimation. Then, each area was assigned a mass loading equivalent to the corresponding point estimation.

(4) Contouring: The coordinates and mass loading for each location were used to generate a contour map covering the whole area in which BMPs were applied.

Although spatial distributions of mass loading for each of these scenarios are different, the total mass that leaches to groundwater is similar (Average: 4.3 ton NO_3-N/year; Field Properties: 4.3 ton NO_3-N/year; Thiessen: 4.1 ton NO_3-N/year; Contouring: 4.1 ton NO_3-N/year, from Koch, 2009). The comparison of the resulting breakthrough curves at the supply wells for each of these scenarios can be used to assess the uncertainty introduced by the choice of mapping technique and, consequently, provide some insight regarding the importance of selecting an appropriate mapping method.

4.5.1.2 Alternative management scenarios:

At this stage, alternative strategies to address the nitrate contamination problem were investigated. Expected benefits from these alternatives can be compared and used on the decision-making process. Particularly, these results can be used to provide a quantitative basis for cost-benefit analysis, despite the inherent model uncertainty. To illustrate this application and to provide further insight regarding the behavior of the Thornton well field in response to BMPs, the following alternative management scenarios were simulated (Fig. 4.20):

(1) Minimum Load: This scenario considers an interruption of farming activities on the plots purchased by the County of Oxford and the adoption of measures for minimizing the nitrate input to groundwater. A loading similar to that at the woodlot was assumed.

(2) Additional Areas: Simulates a situation in which BMPs are implemented in two additional farm plots indicated on Fig. 4.20. For these plots, post-BMP loadings are assumed to be the similar as the ones observed on the parcels purchased by the County of Oxford (*i.e.*, 3.4 g NO_3-N m^{-2} $year^{-1}$; Koch, 2009).

To allow a comparison with the current BMP measures, these scenarios were considered to be implemented in 2003 (*i.e.*, at the same time the real BMPs were implemented) and compared with the "Average" scenario, described on the previous section (4.5.1.1 Alternative mapping techniques for nitrate loading).

4.5.2 Short-term predictions

Using pre-BMP nitrate distribution in the groundwater system as an initial condition, the effects of BMPs were estimated using alternative mass loading mapping techniques. The results are shown in two time scales: (1) from 1999 to 2013 (~ 10 years after BMPs, Figs. 4.21 and 4.22), so that predictions can be compared with observed nitrate concentrations at the supply wells; and (2) from 2003 to 2053 (~ 50 years after BMPs, Fig. 4.23 and 4.23), to discuss long term predictions. Results from both time scales are summarized on Table 4.4.

In the shorter term (Fig. 4.21 and 4.22, Table 4.4), the following observations can be made:

(1) Simulated concentration values were not expected to change significantly for most wells, with the exception of Well 1/5: The expected change in concentration within this timeframe (10 years) is smaller than 0.5 mg NO_3-N/L, with the exception of Well 1/5, for which it is around ~ 1.0 to 1.5 mg NO_3-N/L, as shown in Table 4.4. Observed concentrations are consistent with these predictions: A more pronounced decreasing trend was only observed for Wells 1 and 5, as indicated in Fig. 4.21.

(2) Different mapping techniques did not significantly impact predictions: The maximum difference between estimated concentrations was ~ 0.5 mg/L (Well 1/5), which is negligible considering fluctuations/noise in the concentrations observed at the well.

(3) Model predictions do not capture the noise and fluctuations in the observed data: The current model setting considers a steady-state representation of flow and does not account for seasonal or annual variations in nitrate loading. Therefore, at best, it can only represent general trends in concentration. The current model is not capable of simulating abrupt changes in observed concentration data, such as changes measured in Well 3. For this well, concentrations varied abruptly

from ~ 7 mg NO_3-N/L (2007 to 2009) to ~ 11 mg NO_3-N/L (after 2009), remaining fairly constant after the change. This can also be observed in Fig. 4.22, where the mass flux for the entire well field is shown. The mass flux for each individual well was obtained by multiplying the observed concentration by the pumping rate, generating an estimate of mass of nitrate extracted per unit of time. As for the concentrations (Fig. 4.21), the simulated mass flux does not fluctuate with time as the mass flux estimated based on field data.

(4) Estimated concentration and mass flux tend to overestimate the observed trend. Estimated concentrations were ~ 1.0 to 3.0 mg NO_3-N/L higher than observed values. The predictions for Well 3 after 2009 are an exception, since observed values were underestimated by ~ 3.0 mg NO_3-N/L. The same overestimation is observed for the total mass flux (Fig. 4.22).

4.5.3 Long-term predictions

Around 50 years after BMPs were implemented, the system approaches steady state and the effects of different mass loadings can be fully observed (Figs. 4.23 and 4.24, Table 4.4). The following comments can be made about these long term estimations:

(1) Long-term concentrations were estimated to decline by ~ 2.0 (Wells 1/5 and 11) and ~ 2.5 (Well 3 and 8) from pre-BMP conditions. Final estimated concentrations were: ~ 8.5 (Wells 1/5), ~ 7.0 (Well 3), ~ 7.5 (Well 8) and ~ 6.5 (Well 11), in mg NO_3-N/L. These reductions would keep concentrations below the drinking water limit.

(2) Most changes are expected to happen between 5 and 30 years after BMPs are implemented: Concentrations are expected to start changing around 5 years after BMPs for Well 1/5, and around 10 years for the remaining wells. The majority of this reduction takes place after 20 years (Well 1/5) and 30 years (Wells 3, 8 and 11). This timeframe is consistent with earlier predictions from Padusenko (2001) and Haslauer (2005), presented on Section 4.3.6 (Groundwater age and estimated timeframe for improvements).

(3) Differences between predictions using alternative mapping techniques are negligible, especially considering all uncertainties involved in long term estimations. The maximum differences between estimated concentrations were, in mg NO_3-N/L: 0.6 (Wells 1/5), 0.7 (Well 3), 0.5 (Well 8) and 0.3 (Well 11).

In comparison with the current BMPs, the minimum loading scenario is expected to further diminish concentrations for all supply wells. Since the same area is considered, the time lag and

affected wells are the same. The only difference is the magnitude of these improvements. As shown in Table 4.5, the additional long term concentration reduction for the minimum loading scenario in comparison with the current BMP strategy is, in mg NO_3-N/L: 0.8 (Well 1/5), 0.7 (Well 3), 0.8 (Well 8) and 0.7 (Well 11).

Additional Area 1 impacts primarily Well 8. This additional area would promote a long term decrease in concentration of 1.2 mg NO_3-N/L in Well 8, in addition to the 2.2 mg NO_3-N/L reduction expected from current BMPs, resulting in a total expected reduction of 3.4 mg NO_3-N/L. The effects of BMPs in this area are expected to be relatively fast, affecting concentrations in Well 8 in less than 5 years after BMPs are implemented. In 10 years, BMPs in this area are expected to reduce concentrations in Well 8 in 1.0 mg NO_3-N/L, in addition to the 0.3 mg NO_3-N/L reduction expected from the current BMPs.

Additional Area 2 impacts mostly Well 11, promoting a long term decrease in concentration of 0.8 mg NO_3-N/L in Well 11, in addition to the 2.0 mg NO_3-N/L reduction from current BMPs (*i.e.*, total estimated long term reduction = 2.8 mg NO_3-N/L). A much longer time lag (20 to 30 years) is expected before this area starts affecting concentrations at the supply well.

Since water from different wells are blended before distribution to the public, another way to compare different scenarios is by looking at the estimated properties of the combined contributions from all wells (Table 4.6). The following values can be calculated: the total nitrate mass (or mass rate) extracted from the pumping wells, or the resulting concentration in the mixture. Alternative scenarios would provide the following combined mass extraction rates, in ton NO_3-N/year: 17.8 (average, current BMPs), 15.9 (min. loading), 16.8 (Additional Area 1), and 17.0 (Additional Area 2). These values should be contrasted with the pre-BMP rate of 22.9 ton NO_3-N/year. A different way to express this same result is to use the combined concentration from all the wells, which can be calculated by the arithmetic mean of concentrations, weighted by the pumping rate for each well. In this case, the estimated combined concentrations are, in mg NO_3-N/L: 7.4 (average, current BMPs), 6.6 (min. loading), 7.0 (Additional Areas 1 and 2), which can be compared to the pre-BMP value of 9.5 mg NO_3-N/L.

4.5.4 Suggestion for future work for the Thornton well field

The following activities would provide additional insight:

(1) Perform sensitivity analyses with respect to anisotropy and dispersivity: These parameters may impact model results and it is important to verify how much uncertainty is being introduced by these two factors. If the sensitivity to anisotropy is considered high, additional field experiments to estimate the anisotropy ratio may be justified and can be performed using the existing infrastructure.

(2) Use alternative recharge distributions: The spatial distribution of recharge is a major hydrologic driver in the system response and an important source of uncertainty. The current study adopted a single recharge distribution, which does not consider uncertainty in this parameter.

(3) Delineate well capture zones considering uncertainty: The methodology developed in Chapter 3 should be applied to delineate the overall capture zone for the well field using results from (1) and (2). Capture zone delineation is essential for understanding the system, including the estimation of the effects of BMPs.

(4) Assess alternative techniques to generate nitrate loading distributions for the entire capture zone: The current study only investigated some simple alternative mapping methods within the BMP area, which covers a relatively small part of the capture zone. For the remaining agricultural areas, an average value was chosen. This assessment can be done using more rigorous approaches (*e.g.*, Bester et al., 2005), and can include the entire capture zone. Different nitrate loadings outside the BMP area will not impact the absolute changes in concentrations due to BMPs (since these changes only depend on conditions within the BMP area). However, it is important to estimate the relative improvements due to BMPs, since it would allow a better calibration to initial conditions and providing better understanding of nitrate distribution within the capture zone.

(5) Improve uncertainty assessment: Using results from suggestions (1) to (4), model uncertainty can be better assessed by creating an envelope around estimated breakthrough curves for alternative scenarios. In this assessment, uncertainty regarding hydraulic conductivity distributions and hydrostratigraphy can also be performed.

(6) Use a transient flow model: The discrepancies between the estimated concentration trend and the noisy measurements (Fig. 4.21) indicate that the current model representation is not capturing an aspect of this system that may be important for water management. A transient model would provide some additional insight and allow the investigation of other problems such as the risk of pathogen contamination following fast infiltration events (*e.g.*, snowmelt). The TMR (Telescopic Mesh Refinement) approach used in the current model would be more cumbersome for a transient model.

4.5.5 Insights for similar problems

This case study provided some insights that may be useful for other sites with similar conditions. Some of these points are discussed below:

(1) Rough estimations of BMP effects are useful in earlier stages of work: After developing a full 3D transport model, with heterogeneous recharge and mass loading, the estimated reduction in nitrate concentration is ~ 22% (*i.e.*, [9.5 -7.4]/9.5 = 22%, values from Table 4.6). Despite the difference from the initial rough calculation based on a simple statement of conservation of mass (~ 10% reduction, Section 4.3.4), this simplified estimation can be considered useful in early stages of BMP design. Considering all the uncertainties involved, it may not be a bad approximation of the value obtained using the sophisticated model. For both cases, reliable recharge and mass loading estimates are fundamental.

(2) Soil core estimations of mass loading avoid the simulation of root zone processes and reduce model complexity and uncertainty: Field estimations of recharge and mass loading by Bekeris (2007) and Koch (2009) were fundamental for the modelling study. By estimating loadings below the root zone, nitrate was simulated as a conservative tracer. As an additional benefit, these measurements allow direct field verification of the efficiency of BMPs.

(3) This problem can be addressed by a combination of multiple model settings: Hand calculations (Chapter 2), 1D unsaturated flow and transport, 3D saturated flow in a larger scale and 3D variably-saturated flow and transport were used in this study. Models were used to assign inputs (*e.g.*, boundary conditions), define settings (*e.g.*, grid discretization) and verify results for other models. Rather than being an evolution of a single interpretation of reality, these models are concurrent representations of the problem, with different levels of sophistication and objectives. When combined appropriately, these representation provide a better understanding of the problem than what can be obtained from a single model setting.

(4) In some situations, spatially variable mass loadings can be assumed as homogeneous without compromising model results: Model results using different nitrate loading distributions within the BMP area were similar. Therefore, the choice of mapping technique did not introduce significant uncertainty for this case and a simpler approach can be used (*e.g.*, average) for further simulations. This conclusion can be generalized for similar cases provided that: (1) alternative mapping techniques result in similar total mass applied; and (2) the area in which the mass loading distributions are different is relatively small in comparison with the total capture zone area (~ 20%, for this case). Both

conditions are satisfied for this case. For other cases in which these same two conditions are met, model simulations can be simplified and contaminant loading can be assumed as a simple average, speeding up model setup and execution.

4.6 Conclusion

The current BMPs implemented on the County of Oxford property are expected to reduce overall concentration at the Thornton well field below the drinking water limit (from ~ 9.5 to ~ 7.5 mg NO_3-N/L) and can be considered as a viable approach to mitigate the problem. Concentrations trends are expected to start decreasing 5 to 10 years (*i.e.*, years 2008 to 2013) following the adoption of BMPs (*i.e.*, year 2003). The majority of improvements in water quality are expected to be realized after 20 to 30 years after BMPs were adopted (*i.e.*, years 2023 to 2033).

In case the expected improvements are not considered sufficient, other measures to reduce nitrate loading can be adopted. Some of these alternatives were simulated, for which further reductions in concentrations were estimated as ~ 0.4 to ~ 0.8 mg NO_3-N/L. These results can be used to support future decisions regarding the management of the supply well.

The modelling approach presented here provides a framework in which different model settings are applied to evaluate BMP performance and alternative management scenarios. This framework can be modified and applied to other sites in which supply wells are affected by non-point sources of contamination.

4.7 Figures and tables

Table 4.1. High-quality calibration targets and results. Absolute errors > 5m are highlighted.

Well	Easting [m]	Northing [m]	Well screen elevation [masl]	Observed head [masl]	Calculated head [masl]	Observed - Calculated [m]
WO04D-18	520116	4770379	290.0	297.6	297.3	0.3
WO04D-43	520116	4770379	265.5	295.6	296.5	-0.9
WO11-18	519657	4770437	285.9	298.9	298.2	0.7
WO11-6	519656	4770438	298.1	298.8	299.0	-0.2
WO28-1	518992	4769790	294.8	297.8	304.2	-6.4
WO28-2	518992	4769790	265.6	297.8	298.3	-0.6
WO28-4	518992	4769790	258.2	302.7	298.3	4.3
WO35	519978	4770190	296.6	297.7	297.6	0.1
WO36	520062	4770309	296.3	297.7	297.4	0.3
WO37	519849	4770359	296.6	298.1	298.4	-0.3
WO40	519548	4770560	297.0	298.7	299.4	-0.7
WO56	519759	4769719	296.9	298.3	299.0	-0.7
WO58	519345	4769788	295.7	301.8	301.5	0.3
WO60	519408	4769959	293.6	301.1	300.5	0.6
WO61	519586	4770112	296.0	299.7	299.6	0.2
WO62	519922	4770426	292.2	298.1	298.1	0.0
WO63	519850	4770359	288.6	298.1	298.4	-0.2
WO64	519884	4770191	289.2	297.8	298.1	-0.3
WO66	519684	4770484	297.3	298.8	299.0	-0.2
WO67	519488	4770318	296.4	299.9	299.7	0.2
WO68	519231	4770033	296.4	301.7	302.1	-0.3
WO69	518628	4769468	300.2	303.4	306.0	-2.6
WO70	518181	4769745	302.4	303.5	306.8	-3.3
WO71-D	519050	4770550	294.2	309.3	301.6	7.7
WO71-S	519049	4770551	303.0	309.6	301.6	7.9
WO72-D	519791	4770580	290.7	298.3	298.8	-0.4
WO72-S	519793	4770580	294.2	298.3	298.8	-0.4
WO73-D	519937	4770754	293.3	298.4	298.2	0.1
WO74-D	520056	4770156	284.3	297.5	297.3	0.2
WO74-M	520055	4770155	288.5	297.5	297.3	0.2
WO74-S	520054	4770154	291.1	297.5	297.3	0.2
WO75-D	520014	4770112	283.0	297.6	297.5	0.1
WO75-S	520015	4770112	293.1	297.6	297.5	0.1
WO76	519338	4769425	296.2	302.5	302.7	-0.3
WO02	520295	4770104	281.8	296.5	296.2	0.3
WO02-D	520134	4770067	287.1	296.5	296.9	-0.4
WO05-b	520059	4770189	286.1	297.6	297.3	0.3
WO06	520295	4769919	286.3	295.9	296.2	-0.2
WO07	520229	4770183	282.3	295.6	296.6	-1.0
WO08-D	520295	4770259	279.4	294.0	296.4	-2.4
WO09	520342	4770289	280.6	295.9	296.4	-0.5

Table 4.1. High-quality calibration targets and results. Absolute errors > 5m are highlighted (continued).

Well	Easting [m]	Northing [m]	Well screen elevation [masl]	Observed head [masl]	Calculated head [masl]	Observed - Calculated [m]
WO12	520127	4769499	296.0	296.7	296.7	0.0
WO18	520456	4769882	285.3	293.1	295.8	-2.7
WO20	520317	4769284	289.6	293.3	297.0	-3.6
WO22	520255	4769779	289.2	295.8	296.4	-0.6
WO27	520410	4770090	277.2	293.4	295.3	-1.9

Table 4.2. Low-quality calibration targets and results. Absolute errors > 5m are highlighted.

Well (MOE ID)	Easting [m]	Northing [m]	Well screen elevation [masl]	Observed head [masl]	Calculated head [masl]	Observed - Calculated [m]
28969	520014	4771803	265.1	299.7	294.1	5.6
28991	521124	4771103	257.7	290.3	292.6	-2.3
28993	521014	4771023	264.1	291.4	293.4	-2.0
28995	521294	4770663	274.4	288.3	295.2	-6.8
30127	516514	4769283	299.4	309.4	312.9	-3.5
30128	516664	4768353	255.2	290.1	299.9	-9.8
30129	516574	4768448	300.3	309.4	314.1	-4.8
30131	516514	4768403	300.2	307.5	314.1	-6.7
30172	519834	4770223	266.5	293.2	297.0	-3.8
30176	520094	4768908	248.2	293.7	299.0	-5.2
30178	519614	4768393	260.2	297.6	300.9	-3.3
30185	519304	4768123	249.7	288.6	301.7	-13.1
30207	519614	4768303	250.2	294.1	301.0	-6.9
30208	519654	4768263	260.5	302.1	301.1	1.0
30210	519574	4768243	260.2	297.8	301.2	-3.3
30212	518894	4767083	247.9	306.7	303.1	3.6
30410	520104	4772503	263.0	294.5	292.4	2.1
30411	520179	4772603	263.2	295.2	292.2	3.0
30515	520314	4770563	283.2	293.9	296.8	-2.9
30647	520134	4769473	295.8	301.1	296.8	4.3
30721	516934	4769623	256.2	306.0	296.4	9.6
30757	519764	4767973	260.2	298.1	301.4	-3.3
30804	517484	4768443	248.7	294.2	301.6	-7.4
30812	519914	4767973	260.3	296.6	301.3	-4.8
30848	519014	4770473	257.3	294.7	296.9	-2.2
30849	517914	4770823	262.3	297.1	295.0	2.1
30850	520014	4770563	254.6	289.3	296.3	-7.0
30858	519354	4768523	293.6	305.6	304.3	1.3
31003	519849	4767943	260.5	297.6	301.3	-3.8
31230	521094	4771093	257.7	290.3	292.6	-2.3
31365	520064	4770573	285.5	296.9	297.8	-0.9
31370	520974	4771283	258.4	288.9	293.3	-4.4
31454	517614	4770363	305.1	308.2	307.3	0.9
31491	519374	4768163	290.0	303.9	305.6	-1.7
31492	519434	4768203	289.6	301.1	304.8	-3.7
31547	519254	4768573	293.6	304.3	304.5	-0.2
31548	518161	4769588	254.1	296.9	298.8	-1.9
31639	519001	4768774	295.1	302.7	305.3	-2.6
32049	519474	4768183	289.3	301.3	304.8	-3.6
32147	517374	4770603	307.0	308.5	307.7	0.8
32160	520014	4768723	248.5	297.5	299.7	-2.2
32348	517914	4770803	262.2	300.6	295.0	5.6
32418	520134	4768963	247.7	297.3	298.7	-1.4

Table 4.2. Low-quality calibration targets and results. Absolute errors > 5m are highlighted (continued).

Well (MOE ID)	Easting [m]	Northing [m]	Well screen elevation [masl]	Observed head [masl]	Calculated head [masl]	Observed - Calculated [m]
32488	519794	4768103	259.9	295.3	301.1	-5.9
32496	519394	4768423	291.9	306.5	304.5	2.0
32585	519314	4768583	294.3	304.7	304.3	0.4
32586	519594	4768403	289.3	300.2	303.8	-3.6
32704	517694	4770403	304.7	307.9	306.7	1.2
32879	518374	4766923	299.6	314.9	312.5	2.4
32882	518094	4766803	297.1	314.0	313.4	0.6
32883	518414	4767103	298.6	311.1	312.0	-0.9
33310	517654	4770423	305.0	309.1	307.1	2.0
33437	517174	4767883	303.0	311.0	313.5	-2.5
33538	519934	4767880	260.5	299.1	301.4	-2.4
33633	518884	4768953	297.9	305.4	305.6	-0.1
33762	519744	4768043	250.4	295.4	301.4	-6.0
33833	518984	4768718	293.0	303.0	305.4	-2.5
33961	519399	4772173	263.4	303.5	293.2	10.3
33962	519224	4768668	259.5	298.5	300.7	-2.2
34240	516439	4768613	299.3	308.4	314.2	-5.7
34319	519917	4767905	260.5	299.4	301.3	-1.9
34347	519829	4767892	260.5	300.1	301.5	-1.4
34418	519134	4768778	292.9	303.0	304.7	-1.7
34419	519240	4768663	259.5	299.0	300.7	-1.8
34443	519377	4768128	289.9	302.4	305.6	-3.3
34551	518788	4767651	293.7	308.0	309.7	-1.7
34552	520252	4770761	255.3	293.1	295.9	-2.8
34567	519354	4770180	256.9	298.7	297.4	1.3
34584	519667	4768048	250.4	296.4	301.3	-4.9
34627	519768	4767878	260.2	300.3	301.6	-1.3
34628	519034	4768868	298.1	303.4	305.0	-1.5
34658	518939	4768872	298.4	301.7	305.4	-3.7
34815	520562	4769041	285.3	293.8	296.6	-2.8
34873	519865	4769353	293.7	302.0	297.4	4.5
35038	519214	4768687	292.7	301.6	304.5	-2.9
35149	520359	4770611	285.5	292.7	296.8	-4.1
35169	519752	4770399	292.3	295.5	298.7	-3.2
35234	519026	4768873	299.2	305.5	305.0	0.5
35345	520321	4770677	263.3	294.7	295.9	-1.1
35410	518730	4769685	299.0	303.0	305.2	-2.3
35551	519896	4768011	260.1	296.8	301.3	-4.5
35612	520965	4769875	255.0	287.8	296.1	-8.3

Table 4.3. Summary of grid properties.

Grid properties	Larger Scale Model	Smaller Scale Model
Nodes per nodal surface	5,591	10,172
Number of nodal surfaces	25	100
Total number of nodes	139,775	1,017,200
Elements per elemental layer	11,001	19,676
Number of elemental layers	24	99
Total number of elements	264,024	1,947,924

Table 4.4. Estimated concentrations at supply wells after current BMPs using different mass loading mapping techniques within BMP area.

Well	Pre-BMP Simulated conc. [mg NO_3-N/L]	10 years after BMPs (year 2013)		50 years after BMPs (year 2053)		Mass loading mapping technique
		Estimated conc. [mg NO_3-N/L]	Reduction from pre-BMP conditions [mg NO_3-N/L]	Estimated conc. [mg NO_3-N/L]	Reduction from pre-BMP conditions [mg NO_3-N/L]	
1/5	10.4	8.9	1.5	8.2	2.2	Average
		9.5	0.9	8.7	1.7	Contouring
		9.1	1.3	8.4	2.0	Field Properties
		9.5	0.9	8.8	1.6	Thiessen
3	9.4	9.3	0.1	7.2	2.2	Average
		9.3	0.1	6.8	2.6	Contouring
		9.3	0.1	7.1	2.3	Field Properties
		9.3	0.1	6.5	2.9	Thiessen
8	10.1	9.8	0.3	7.9	2.2	Average
		9.8	0.3	7.3	2.8	Contouring
		9.8	0.3	7.7	2.4	Field Properties
		9.8	0.3	7.4	2.7	Thiessen
11	8.2	7.8	0.4	6.2	2.0	Average
		7.7	0.5	6.4	1.8	Contouring
		7.8	0.4	6.4	1.8	Field Properties
		7.7	0.5	6.5	1.7	Thiessen

Table 4.5. Estimated concentrations at supply wells for alternative fertilizer managements strategies.

Well	Pre-BMP Simulated conc. [mg NO_3-N/L]	10 years after BMPs (year 2013)		50 years after BMPs (year 2053)		Alternative Scenarios
		Estimated conc. [mg NO_3-N/L]	Reduction from pre-BMP conditions [mg NO_3-N/L]	Estimated conc. [mg NO_3-N/L]	Reduction from pre-BMP conditions [mg NO_3-N/L]	
1/5	10.4	8.9	1.5	8.2	2.2	Average
		8.4	2.0	7.4	3.0	Min. Loading
		8.9	1.5	8.2	2.2	Add. Area 1
		8.9	1.5	8.2	2.2	Add. Area 2
3	9.4	9.3	0.1	7.2	2.2	Average
		9.2	0.2	6.5	2.9	Min. Loading
		9.3	0.1	7.2	2.2	Add. Area 1
		9.3	0.1	7.2	2.2	Add. Area 2
8	10.1	9.8	0.3	7.9	2.2	Average
		9.7	0.4	7.1	3.0	Min. Loading
		8.8	1.3	6.7	3.4	Add. Area 1
		9.8	0.3	7.8	2.3	Add. Area 2
11	8.2	7.8	0.4	6.2	2.0	Average
		7.6	0.6	5.5	2.7	Min. Loading
		7.6	0.6	5.9	2.3	Add. Area 1
		7.8	0.4	5.4	2.8	Add. Area 2

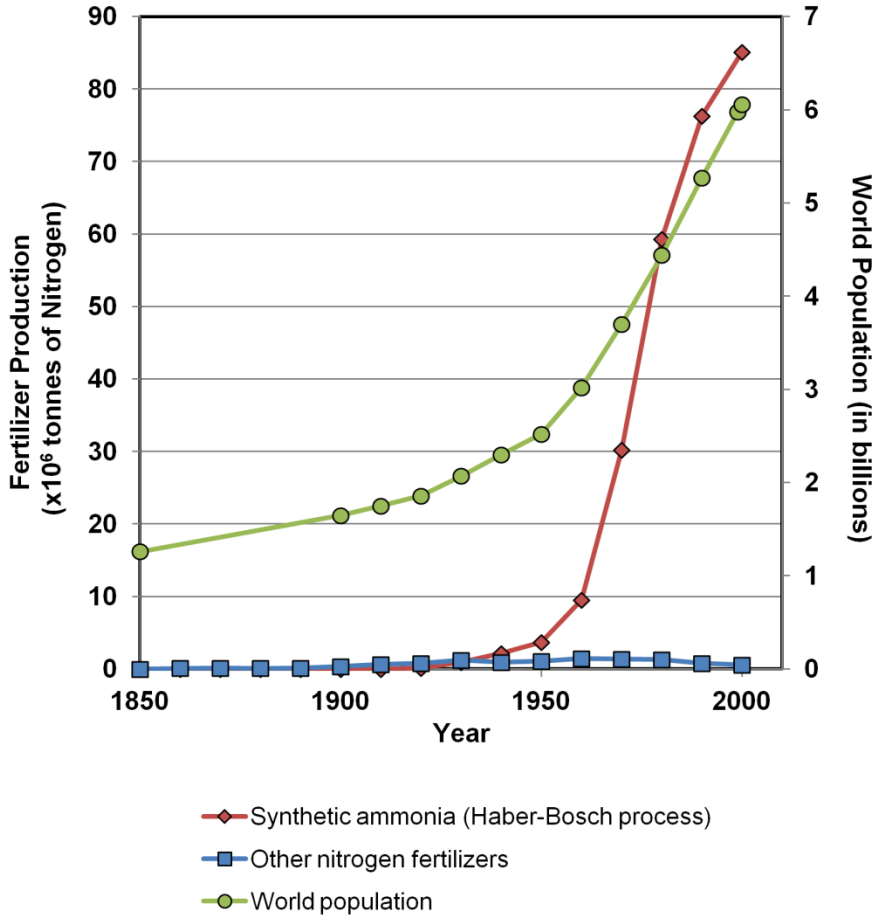

Figure 4.1. World population and nitrate fertilizer production (data from Smil, 2001).

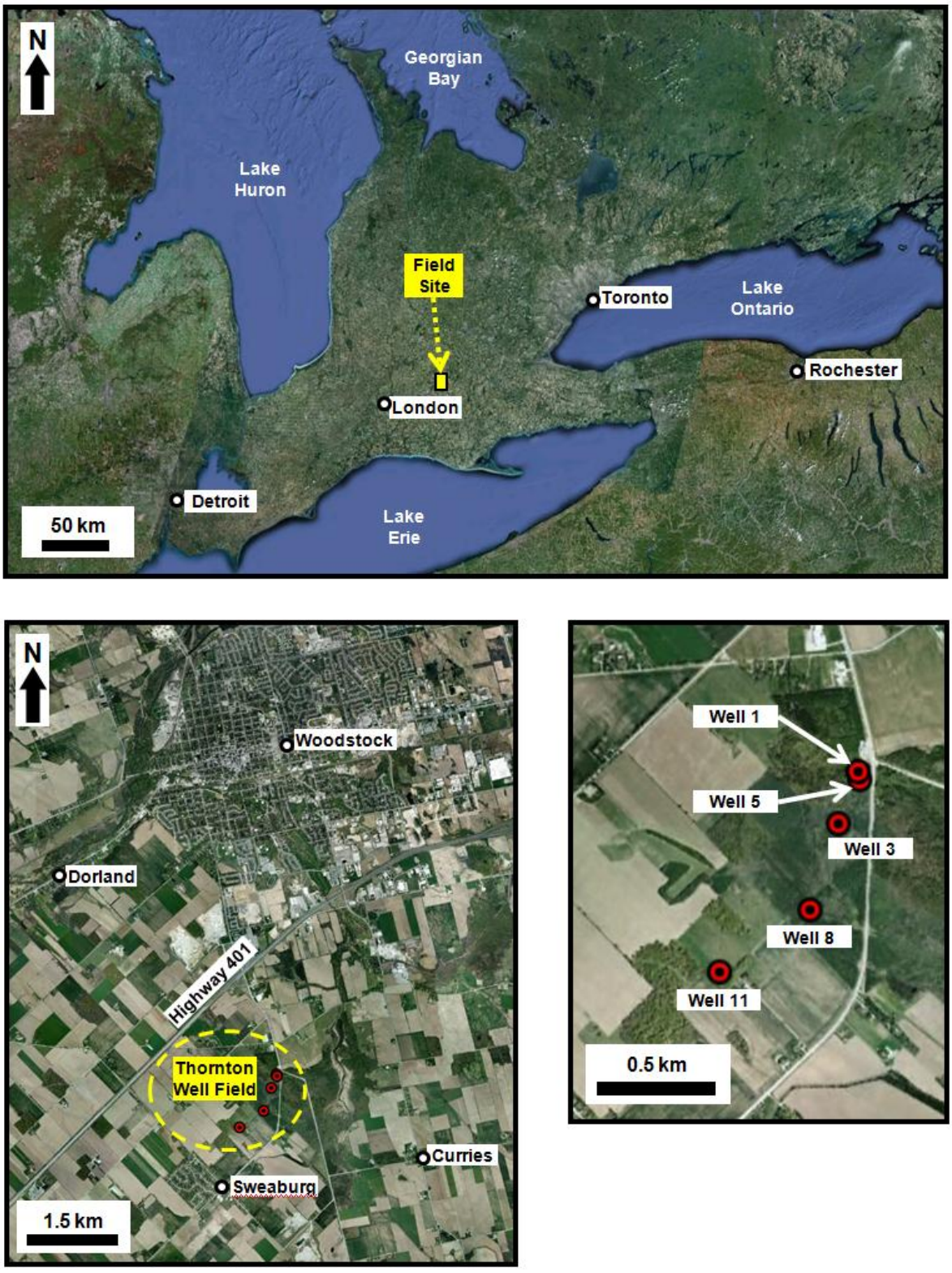

Figure 4.2. Study site location. Aerial imagery from Google Earth Pro (2013a, 2013b).

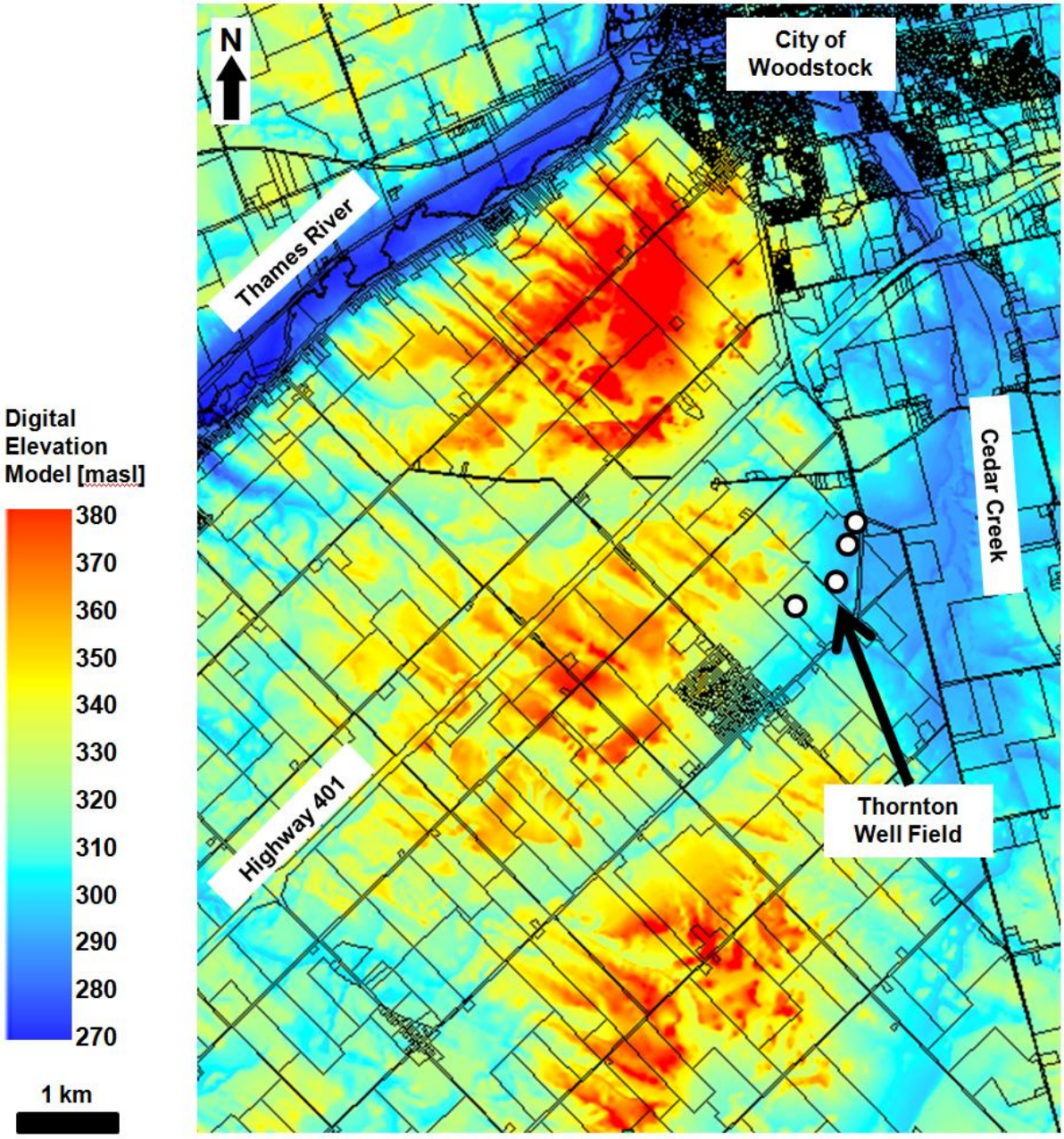

Figure 4.3. Topography of study site. Digital elevation data from County of Oxford (2005).

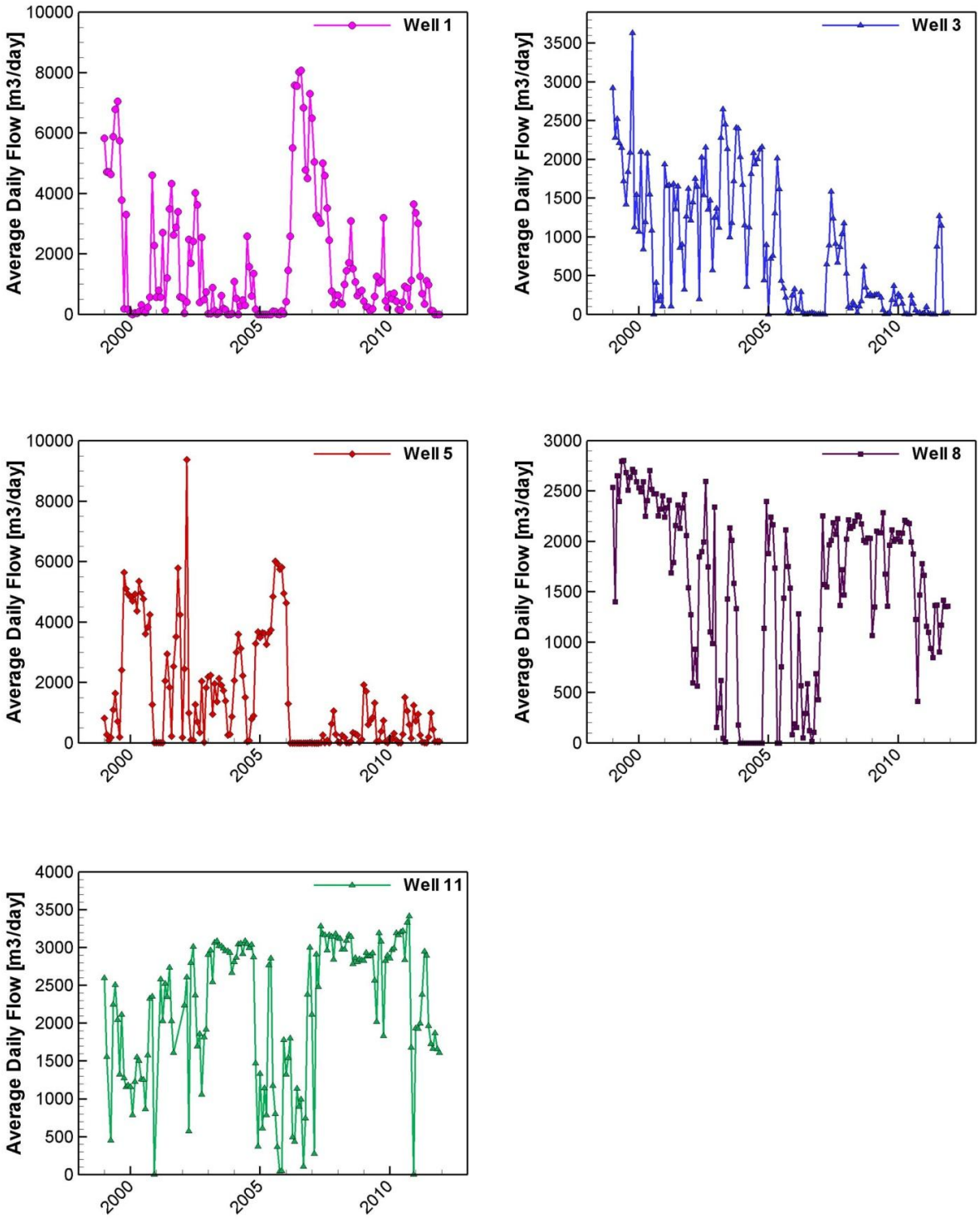

Figure 4.4. Thornton well field pumping rates from 1999 to 2011. Data provided by the County of Oxford.

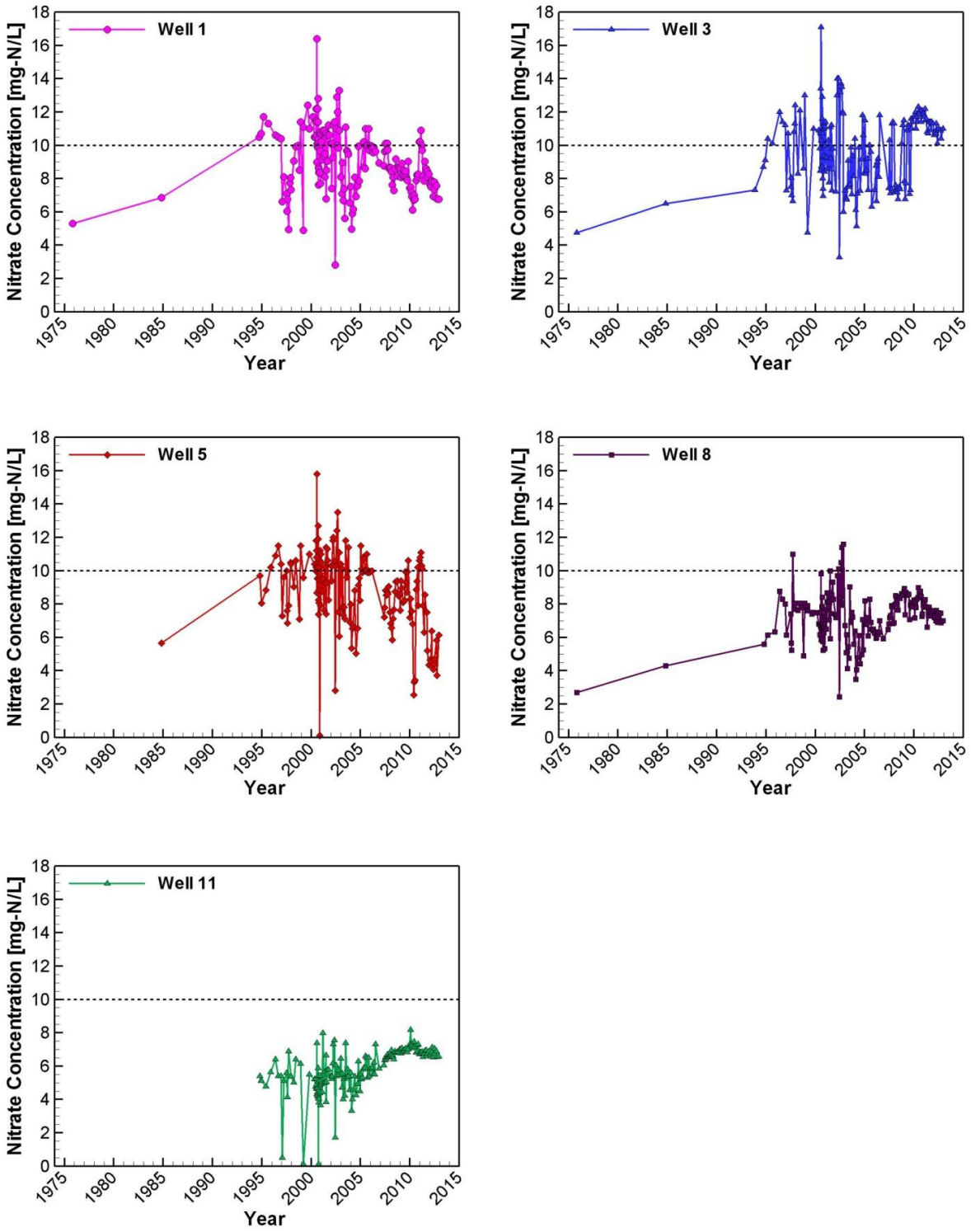

Figure 4.5. Nitrate concentrations [mg NO_3-N/L] in the Thornton well field from 1975 to 2012. Data provided by the County of Oxford.

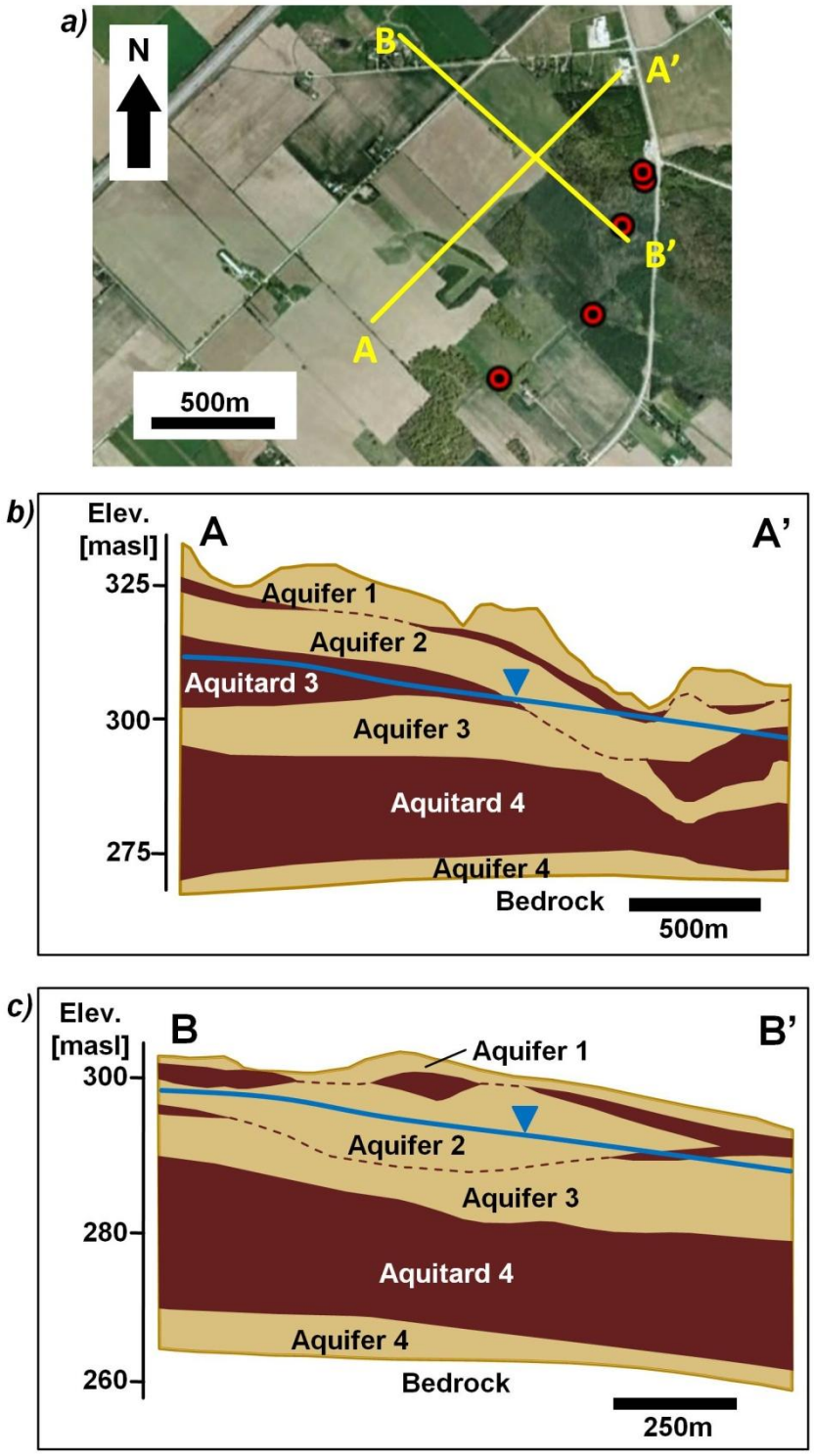

Figure 4.6. Hydrostratigraphical model: (a) Plan view; (b) and (c) Cross-sections. Contains data from Haslauer (2005), Koch (2009). Aerial imagery is from Google Earth Pro (2013b).

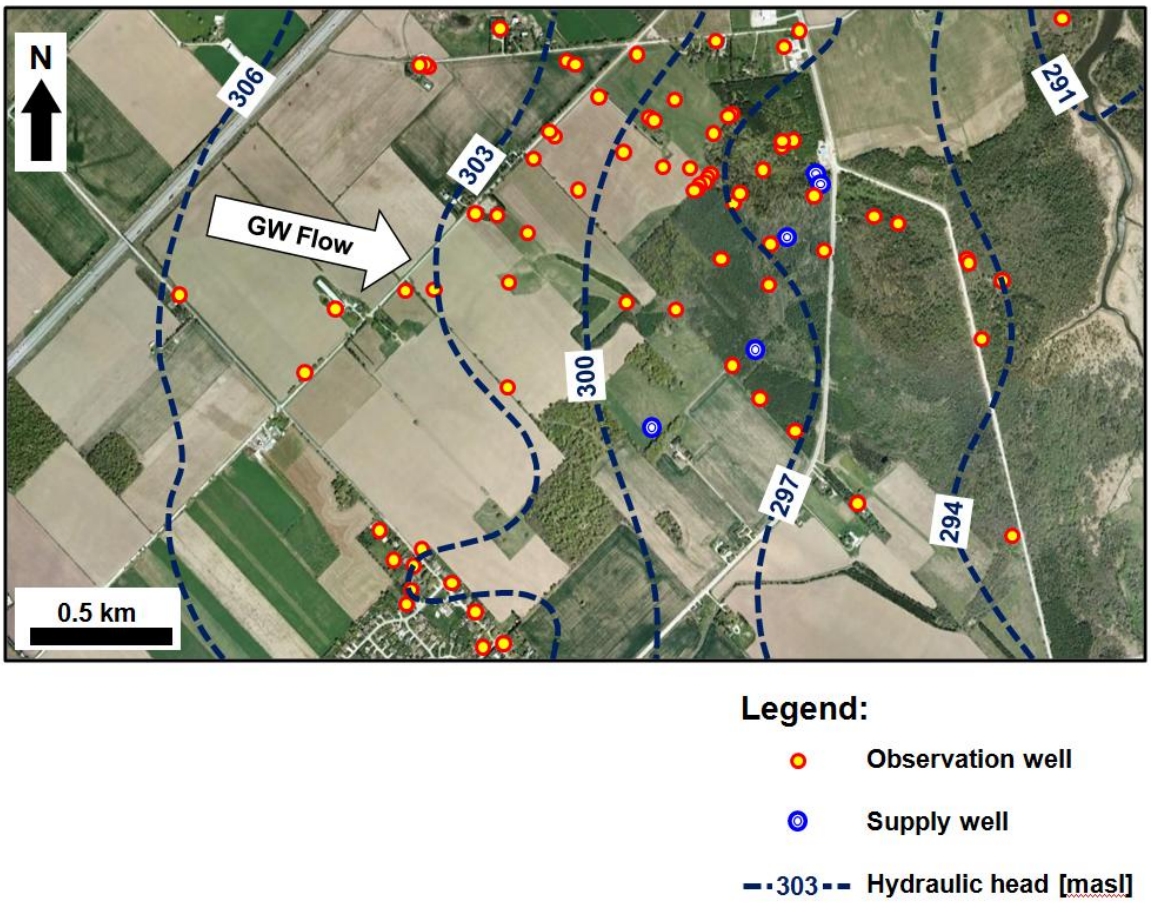

Figure 4.7. Potentiometric map for Aquifer 3 (modified from Haslauer, 2005). Aerial imagery is from Google Earth Pro (2013b).

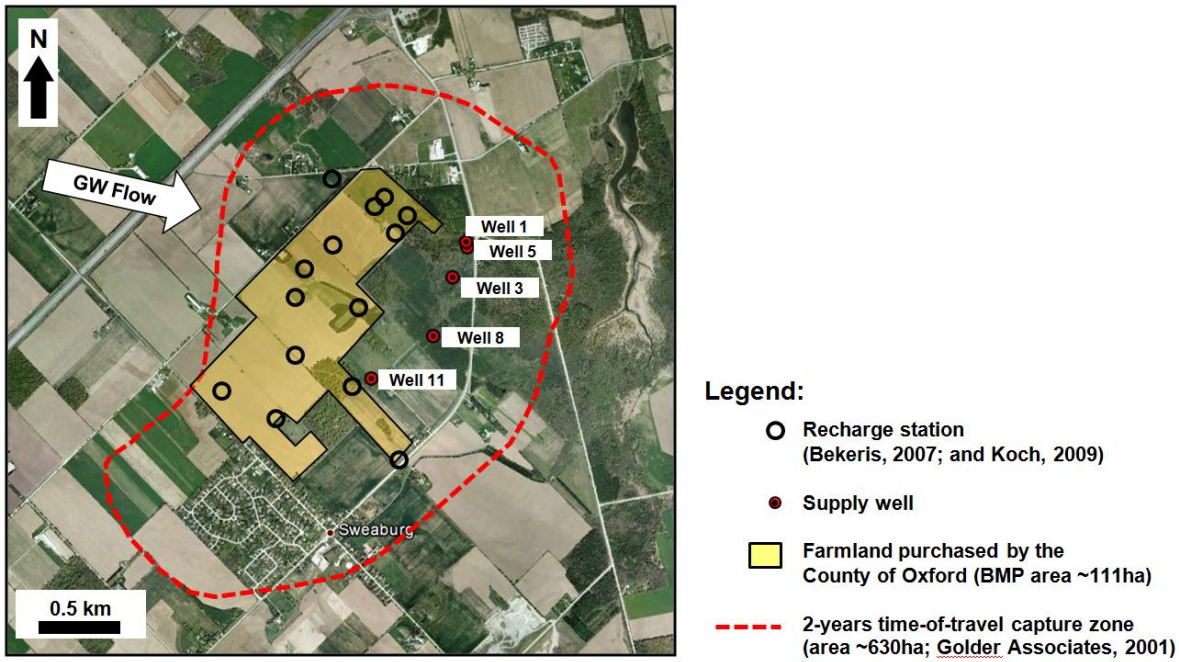

Figure 4.8. Farmlands in which BMPs were implemented and recharge estimation stations. Aerial imagery from Google Earth Pro (2013b).

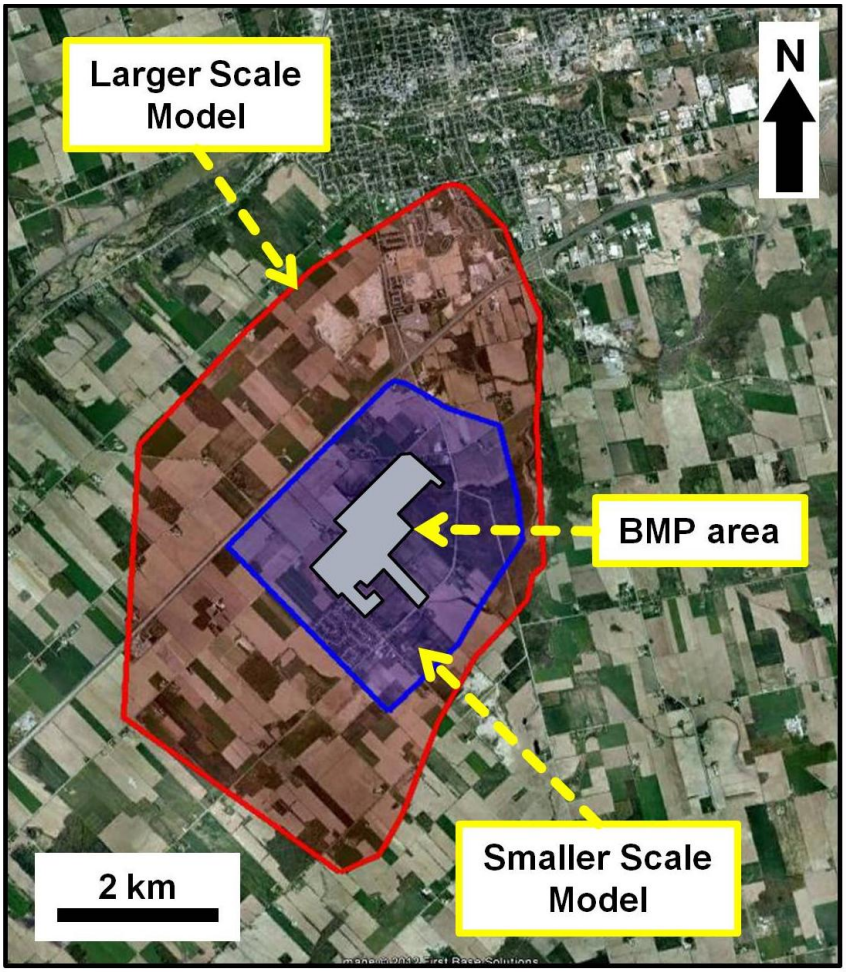

Figure 4.9. Larger-scale and Smaller-scale model domains. Aerial imagery from Google Earth Pro (2013b).

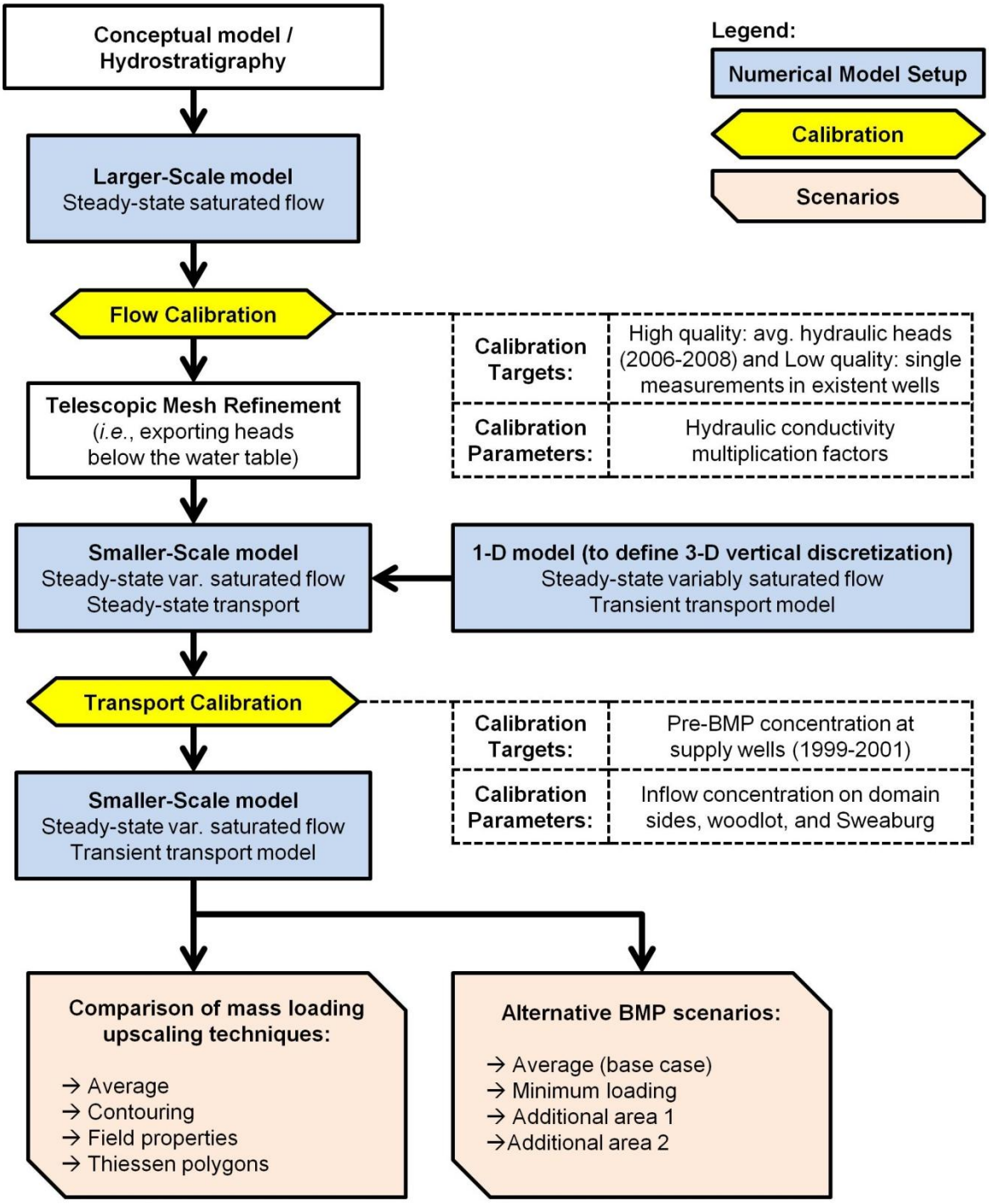

Figure 4.10. Summary of modelling approach.

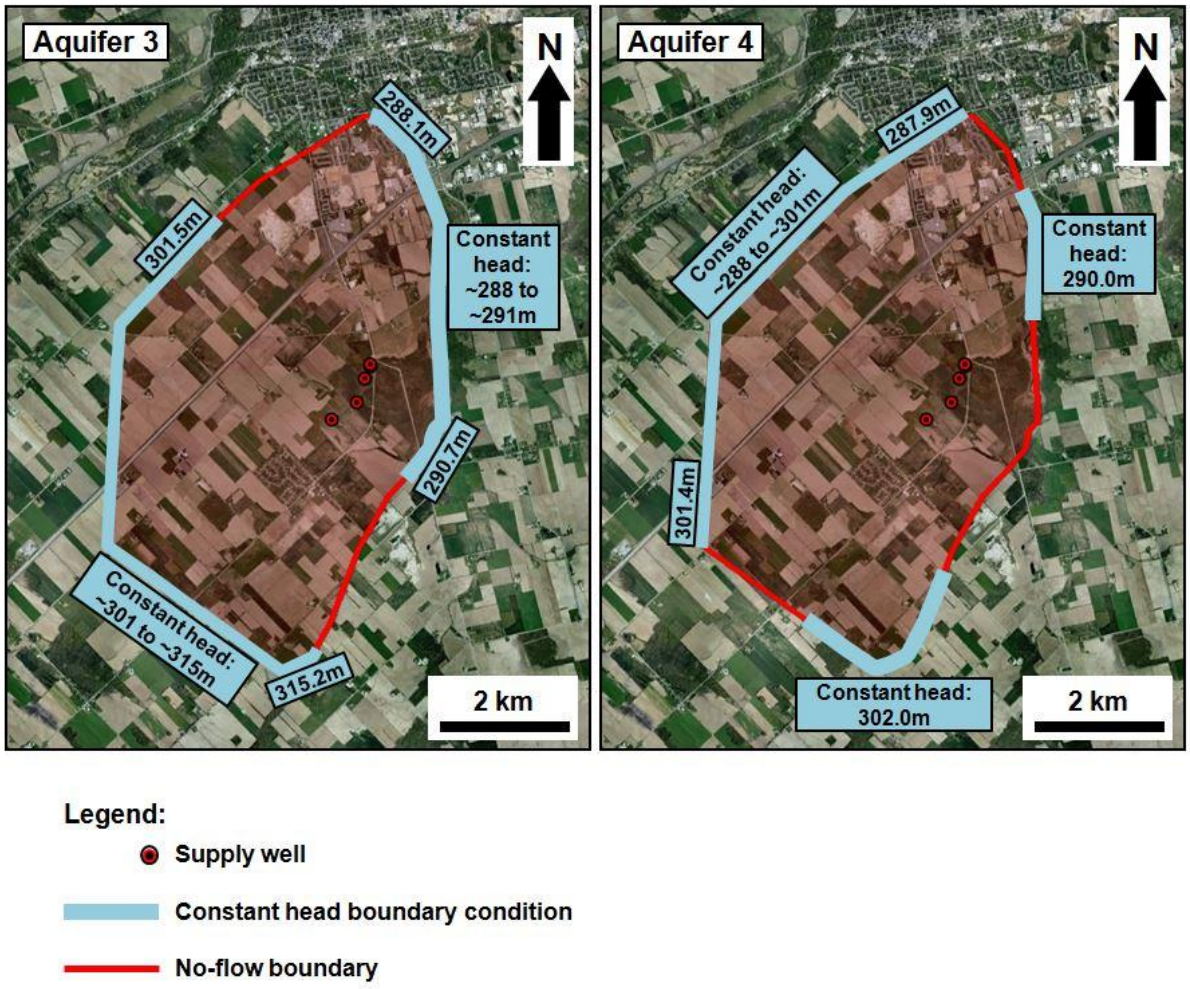

Figure 4.11. Flow boundary conditions for Larger-scale model. Aerial imagery from Google Earth Pro (2013b).

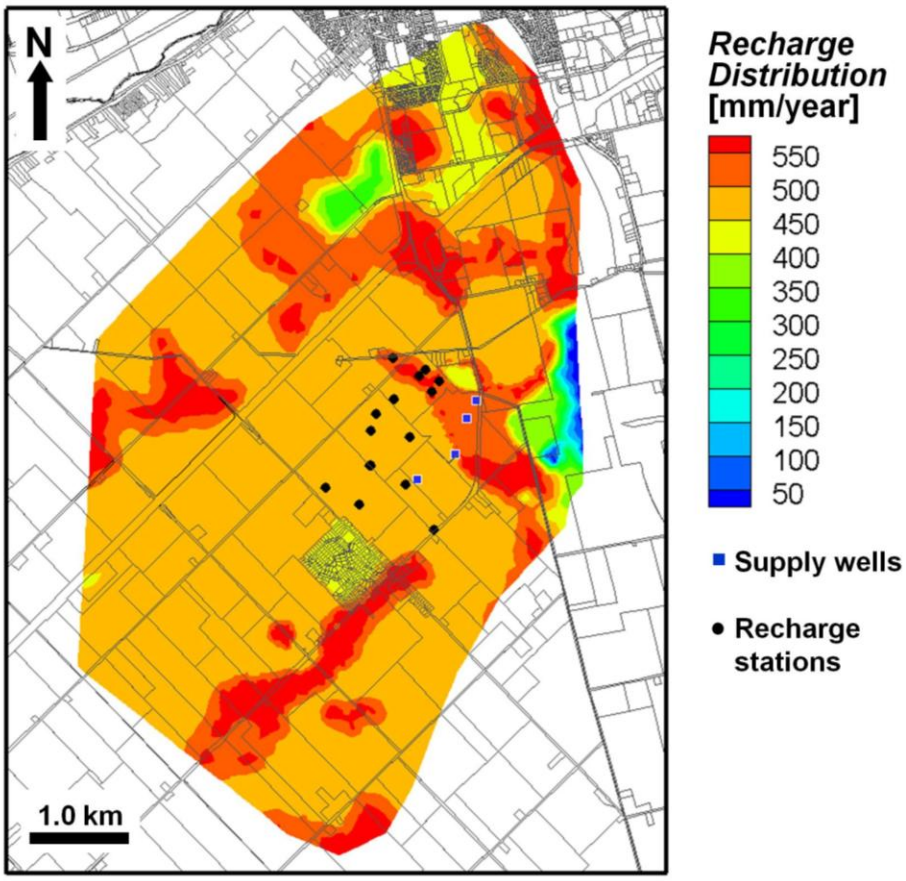

Figure 4.12. Recharge distribution (modified from Padusenko, 2001).

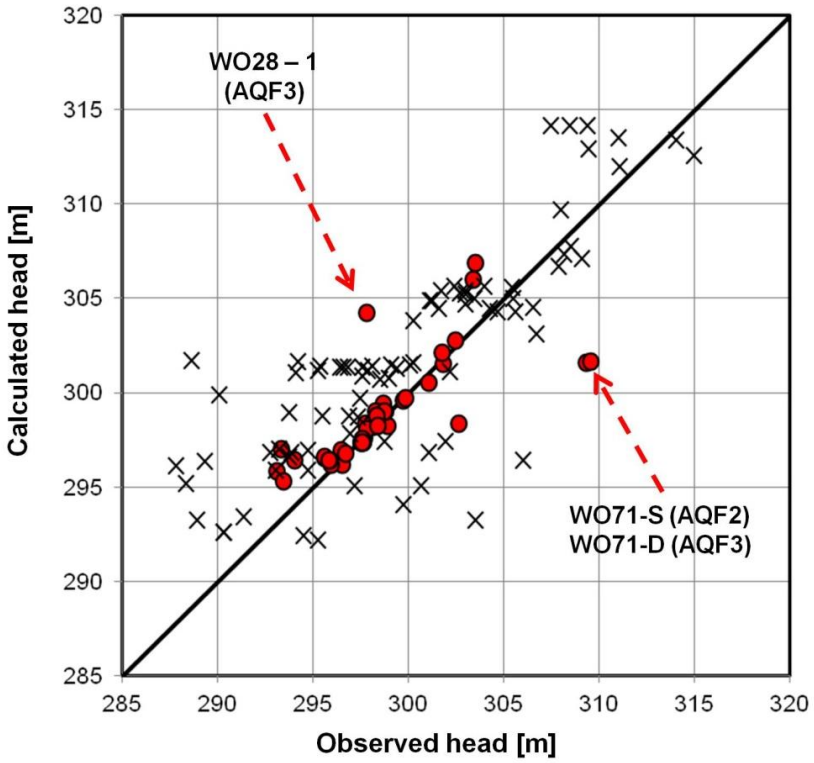

Calibration Statistics	High Quality Calibration Targets (Table 1)	Low Quality Calibration Targets (Table 2)
Average Error (m)	**-0.2**	-2.0
Average Absolute Error (m)	**1.2**	3.8
Maximum Positive Error (m)	**7.9**	9.6
Maximum Negative Error (m)	**-6.4**	-13.1
Num of Observation Points	**46**	82

Figure 4.13. Flow calibration plot (Observed heads averaged from 2006 to 2008). Calibration error is defined as "observed - calculated" hydraulic heads. High-quality data are indicated by red circles and low-quality data by crosses.

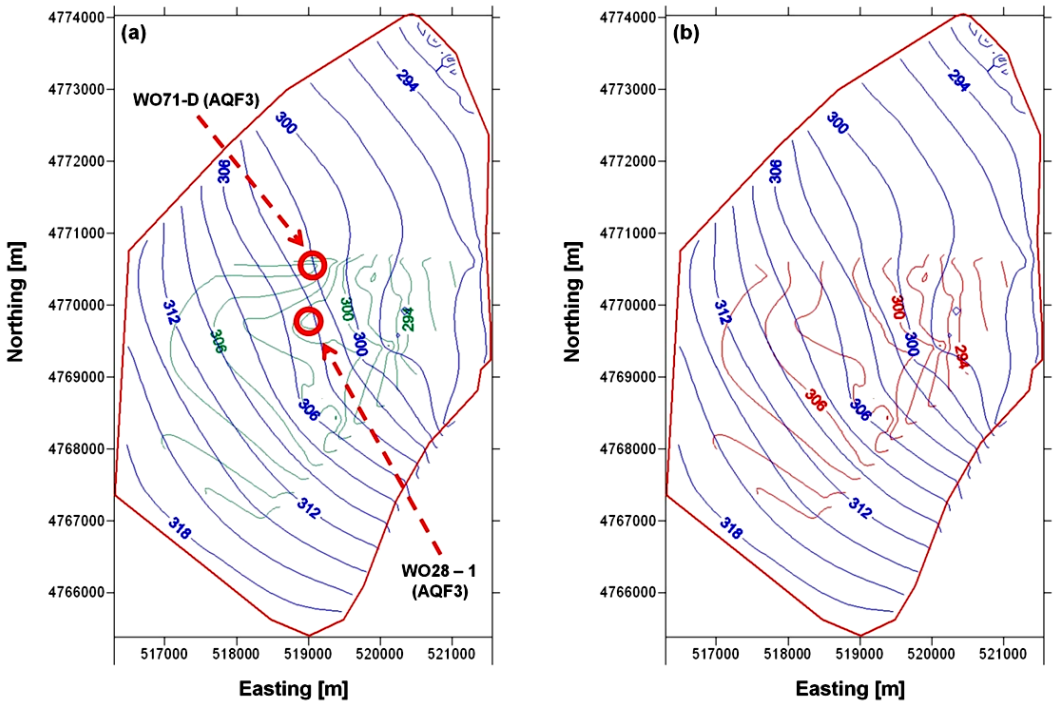

Figure 4.14. Interpolated calculated and observed hydraulic heads in Aquifer 3, (a) with and (b) without calibration outliers.

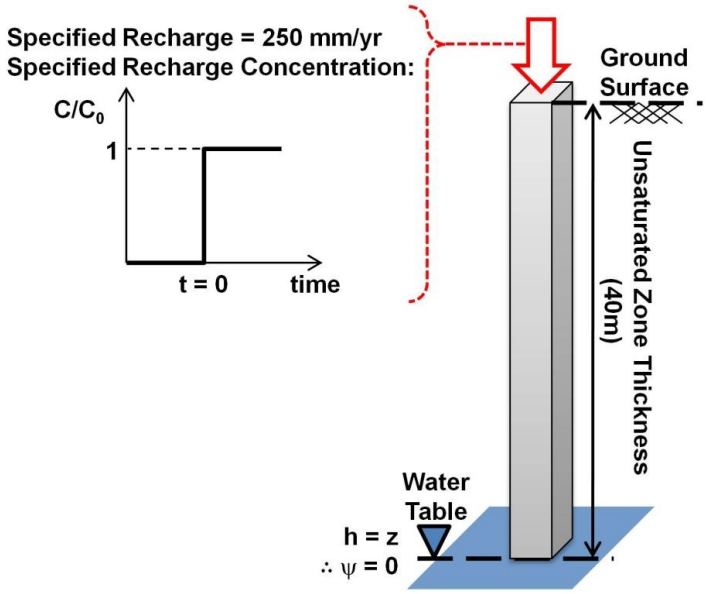

Figure 4.15. One-dimensional model setting.

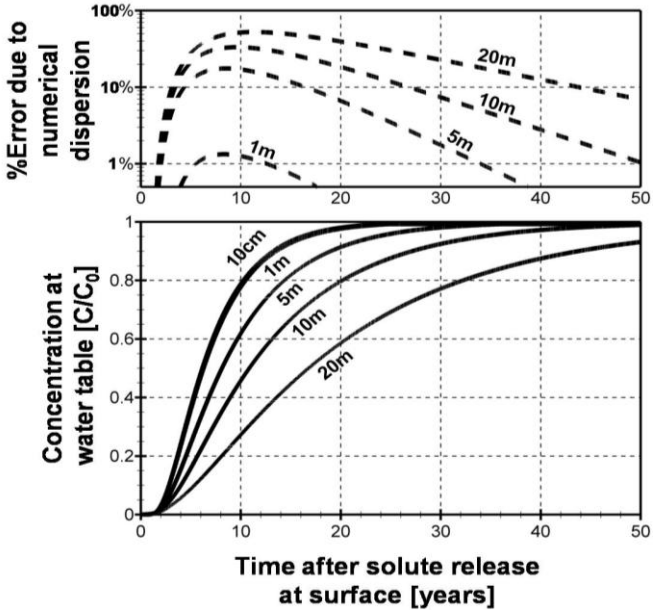

Figure 4.16. Bottom: One-dimensional model breakthrough curves at the water table in response of a solute pulse released at ground-surface; Top: Error due to grid-induced numerical dispersion as a function of time.

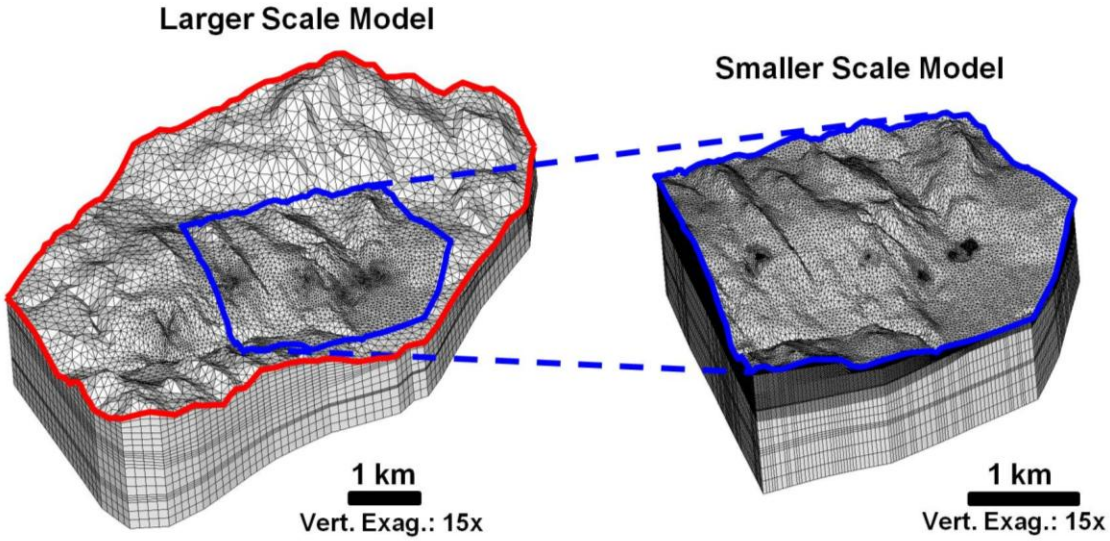

Figure 4.17. Telescopic Mesh Refinement from Larger-scale model to Smaller-scale model.

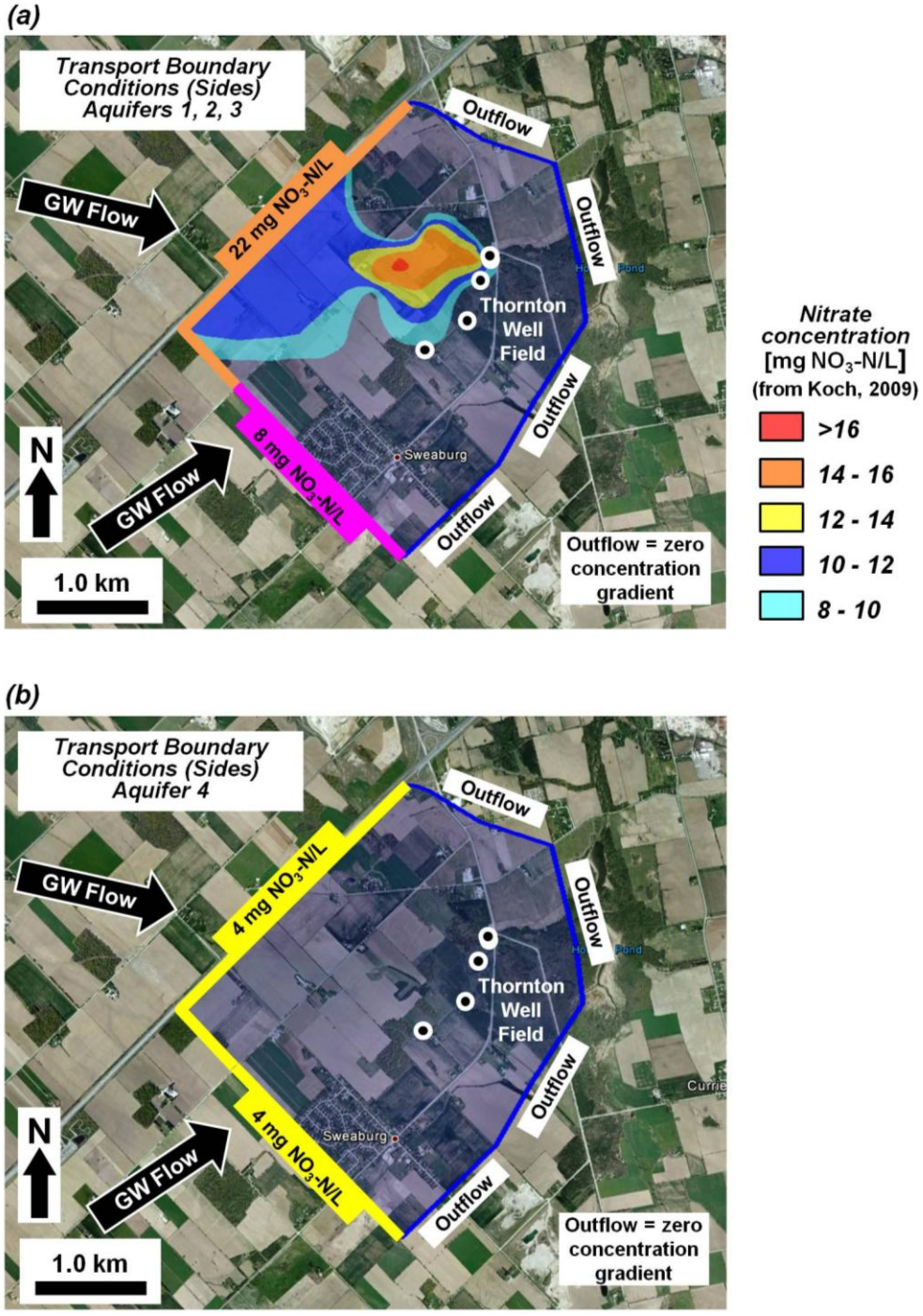

Figure 4.18. Transport boundary conditions for estimating pre-BMP conditions for: (a) Aquifers 1, 2 and 3 (showing observed nitrate plume); and (b) Aquifer 4.

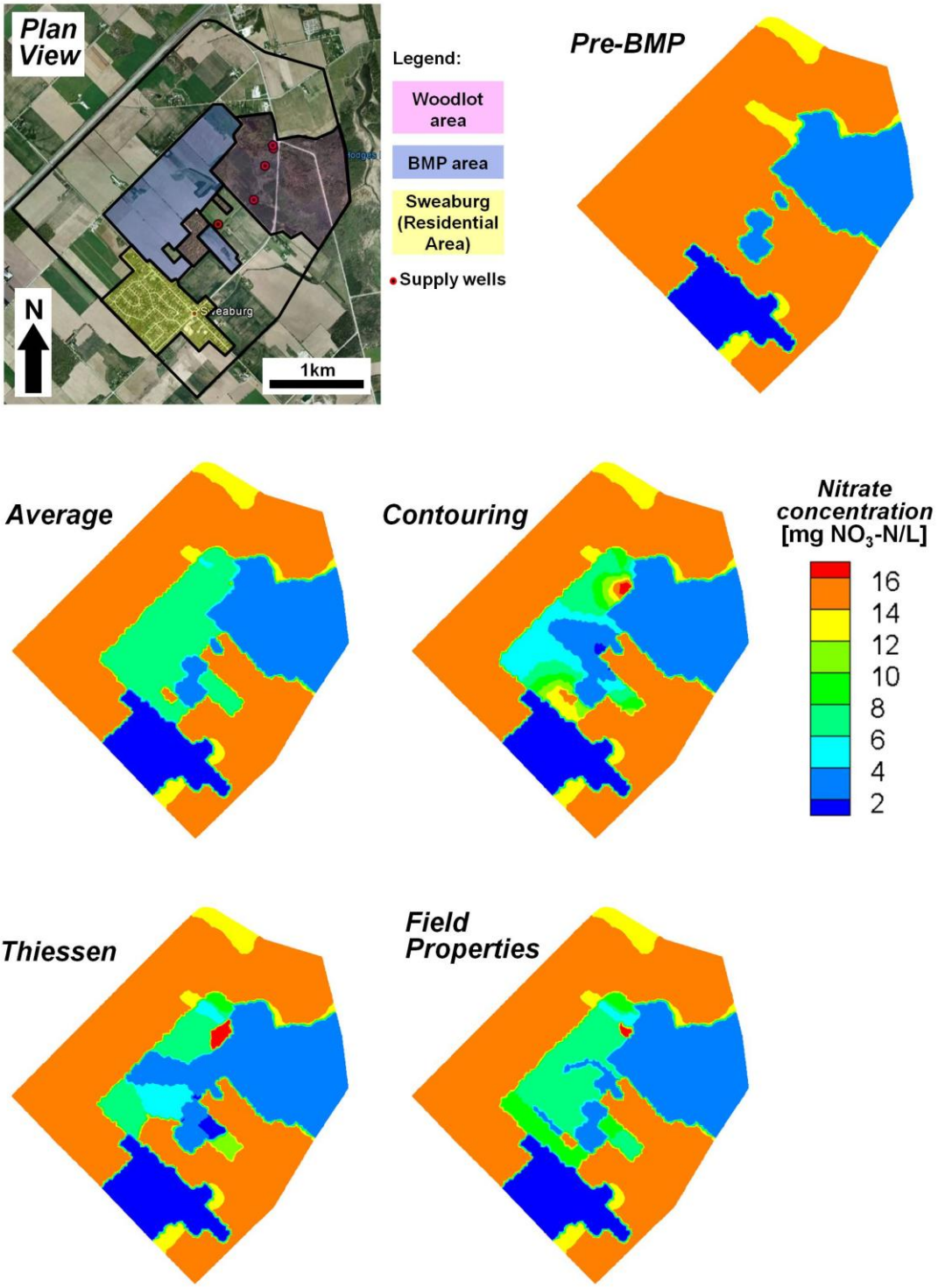

Figure 4.19. Mass loading distributions from different mapping techniques (expressed as concentration at ground surface).

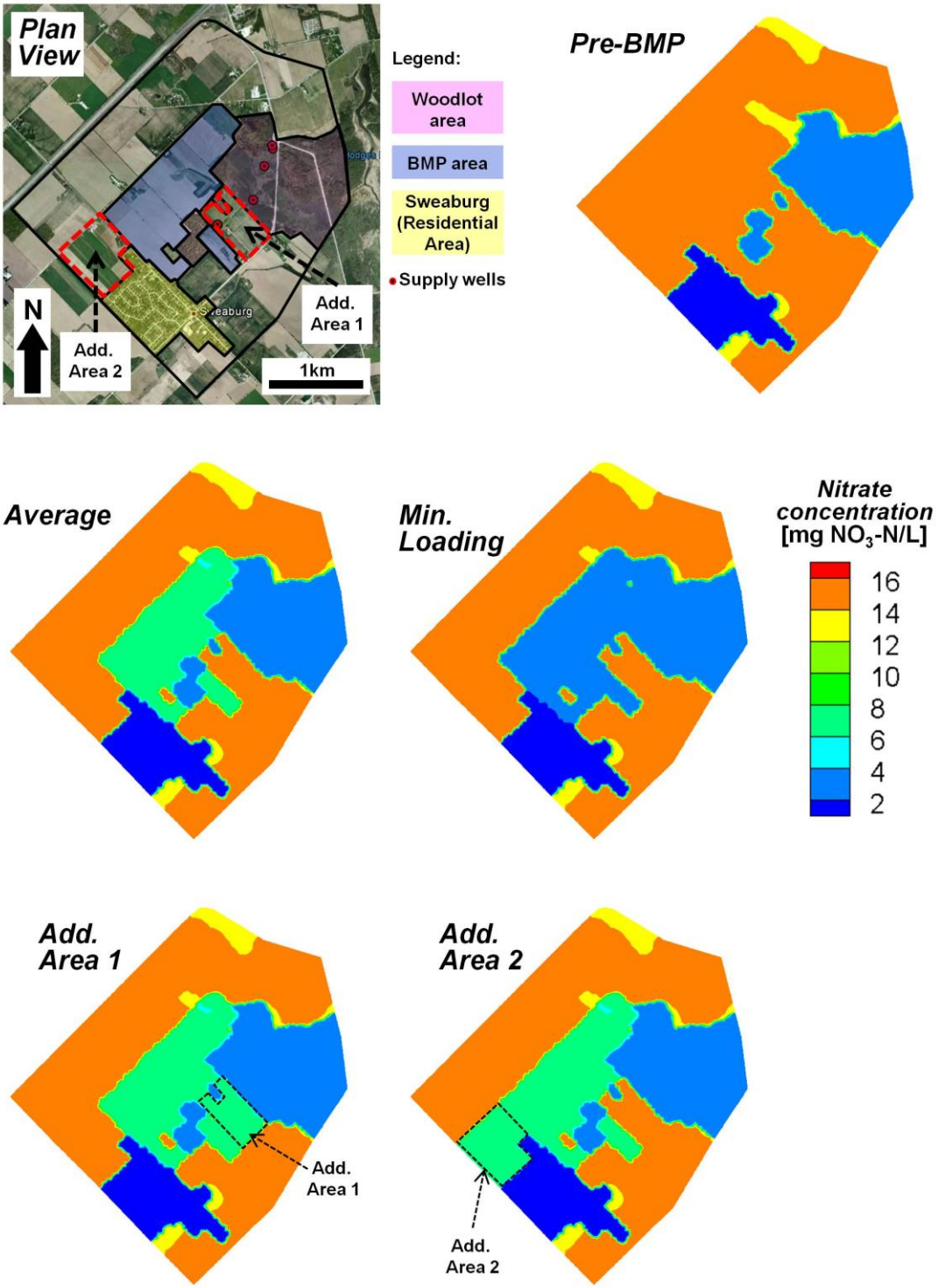

Figure 4.20. Alternative BMP scenarios.

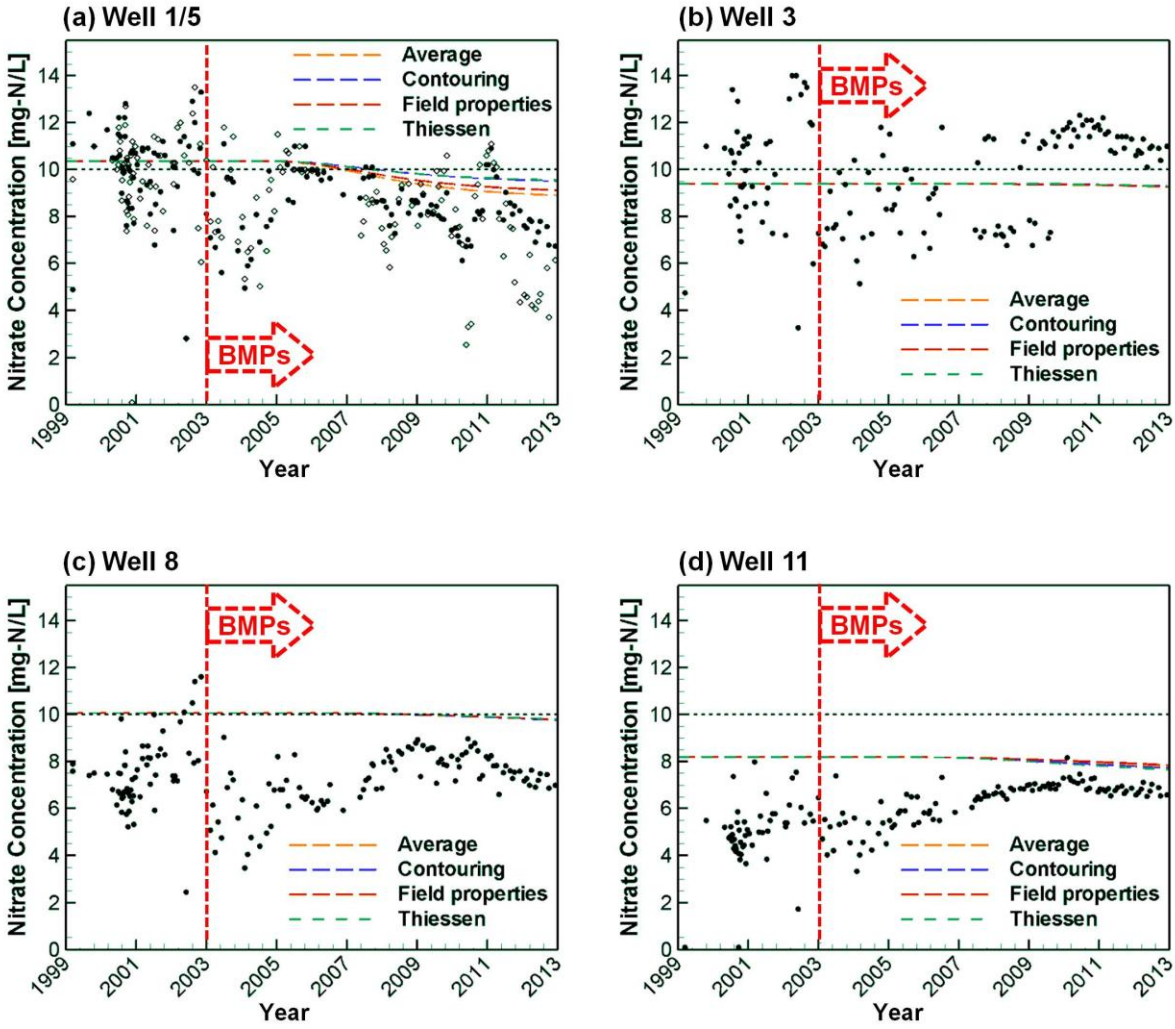

Figure 4.21. Measured (dots) and estimated (lines) nitrate concentration [mg NO_3-N/L] in the Thornton well field from 1999 to 2013. Horizontal black dashed line indicates the drinking water limit (10.0 mg NO_3-N/L). Nitrate concentration data provided by the County of Oxford.

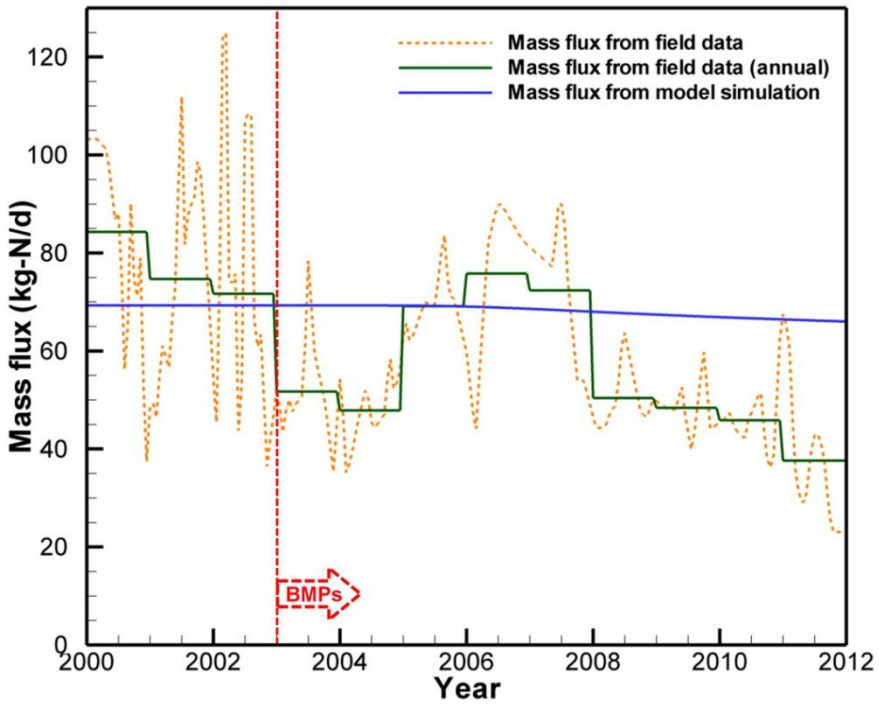

Figure 4.22. Comparison between mass fluxes estimated using field data and model predictions.

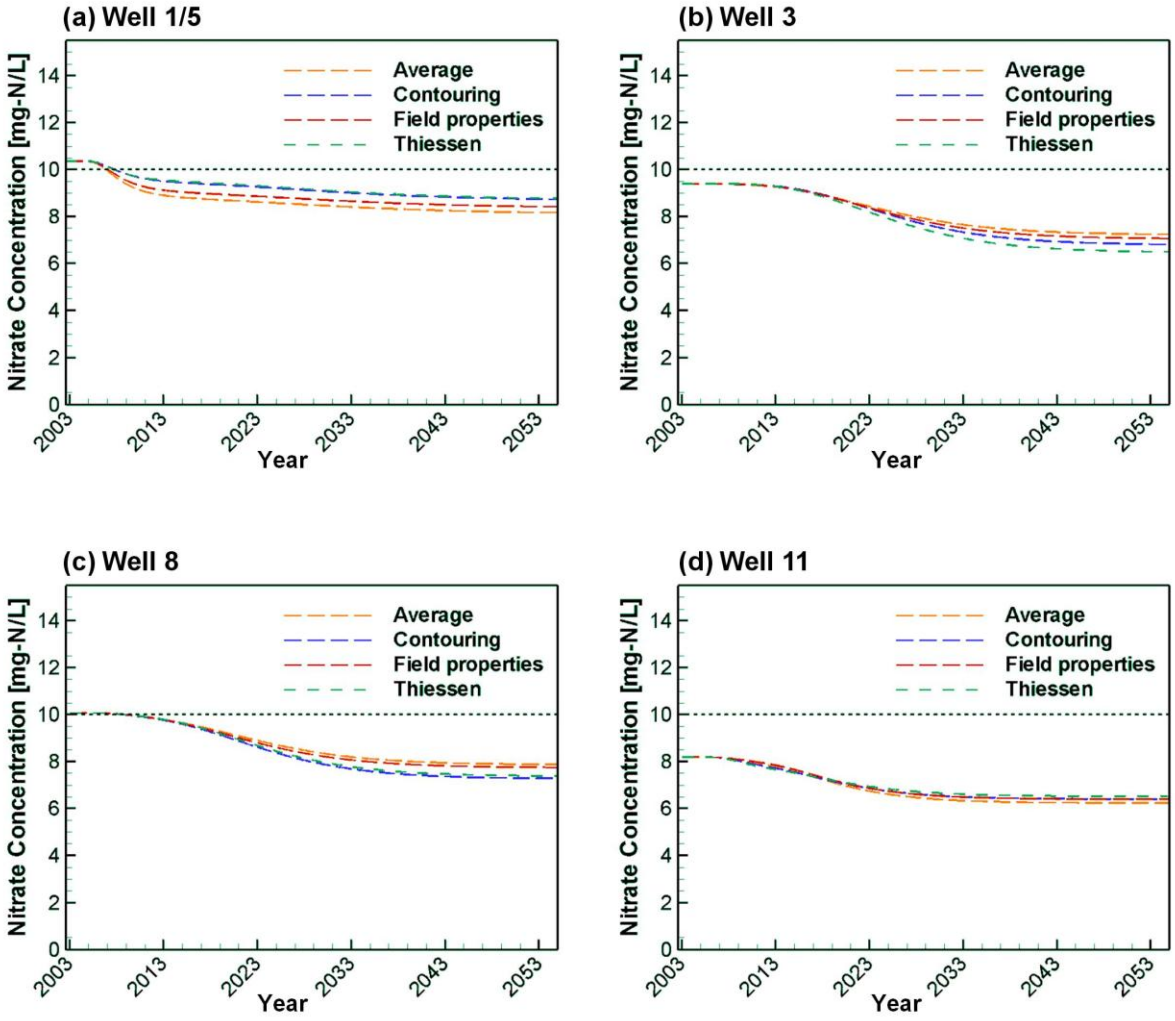

Figure 4.22. Estimated nitrate concentration [mg NO_3-N/L] in the Thornton well field from 2003 to 2053 (~ 50 years). Horizontal black dashed line indicates the drinking water limit (10.0 mg NO_3-N/L).

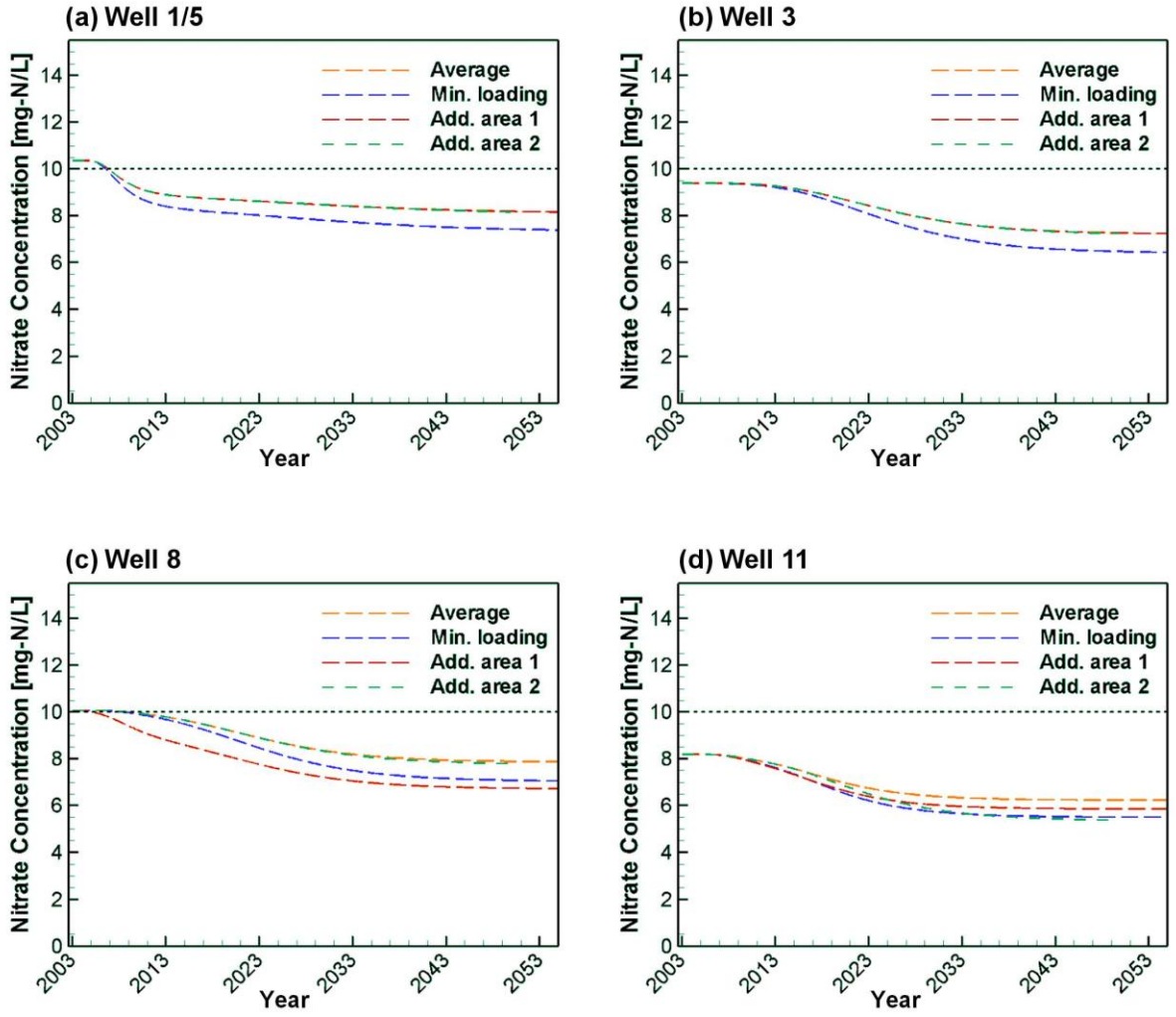

Figure 4.24. Estimated nitrate concentrations for alternative strategies to reduce nitrate concentrations [mg NO_3-N/L] in the Thornton well field from 2003 to 2053 (~ 50 years). Horizontal black dashed line indicates the drinking water limit (10.0 mg NO_3-N/L).

Chapter 5
Conclusions and recommendations

Numerical models were applied to support management decisions regarding the protection of water quality in supply wells. Three specific issues were addressed: (1) time lag in the unsaturated zone; (2) uncertainty in the capture zone delineation; and (3) effects of agricultural Beneficial Management Practices (BMPs) in supply wells. The examination of these issues in example problems provided an opportunity to discuss some applications and limitations of numerical models in source water protection. It also allowed the suggestion of specific techniques that can be useful in day-to-day modelling practice. The overall conclusions of this work are presented in two parts: (1) specific conclusions, pertaining to each particular issue; and (2) general conclusions that were common to all topics presented in this thesis.

5.1 Specific conclusions

5.1.1 Assessment of time lag in the unsaturated zone

Simplified estimations of advection travel times in the saturated and unsaturated zones can be useful to provide a quick assessment of the unsaturated zone time lag and its relative importance to the total travel time between contaminant sources and groundwater receptors. A method to assess unsaturated zone time lag was proposed to help, in early stages of investigation, the decision of whether and how to explicitly incorporate the unsaturated zone in further field and modelling efforts.

Advection travel time estimations can be made using techniques with different levels of sophistication. Simple techniques provided rough estimates of advection times, but lead to the same conclusion regarding the importance of the unsaturated zone for the studied case. The knowledge of soil properties was the critical factor in the decision, rather than the sophistication of the model used in the analysis. This conclusion is site-dependent and does not suggest that more accurate techniques are not required in this type of assessment. However, it illustrates the importance of field data and exemplifies how expedient calculations can be useful tools, especially in early stages of investigation.

5.1.2 Addressing uncertainty in capture zone delineation

A method to address capture zone uncertainty is proposed, which combines multiple scenarios of capture probability plumes, obtained using backward transport. Backward transport represents uncertainty through the macrodispersion term, creating a gradual distribution of capture probability values ranging from 100% (at the well screen) to 0% (infinitely away from the well). This distribution is more realistic and eliminates the false impression of certainty sometimes conveyed by the commonly used particle tracking method, which generates a sharp division between "inside" and "outside" the capture zone. The use of multiple model scenarios allows the analysis of types of uncertainty which are less amenable to stochastic description (*e.g.*, conceptual model, model codes, boundary condition types). The simultaneous use of more than one model contrasts with the search for a single "best" representation of reality, often seen in modelling practice. These alternative scenarios are integrated using the precautionary approach, a method familiar to decision-makers and appropriate for decisions in which a conservative (risk-averse) stance is warranted, such as issues involving public health. These alternative scenarios can be combined into two maps, considering two different management goals: (1) the protection of groundwater sources, and (2) selection of areas to be remediated.

The discussed case-study provides an example of non-uniqueness in source water protection. Although non-uniqueness is thoroughly discussed by previous researchers (*e.g.*, Beven, 1993, Oreskes et al., 1994), it is useful to have a concrete example in source water protection to illustrate this problem to decision-makers involved with source water protection management.

5.1.3 Estimating effects of Beneficial Management Practices

The adoption of BMPs in selected areas is expected to be a viable alternative to improve water quality in supply wells impacted by non-point source contaminants for the studied field site in Woodstock, ON. The presented modelling approach can be used as framework for similar cases, and for other non-point source contaminants.

For the Thornton well field, the currently adopted BMPs are estimated to reduce overall concentrations from ~ 9.5 to ~ 7.5 mg NO_3-N/L. Changes in water quality at the wells are predicted to start around 5 to 10 years after the BMPs were adopted and are expected to stabilize after 20 to 30 years. Other alternative management scenarios were simulated, with further reductions in nitrate concentration around ~ 0.4 to ~ 0.8 mg NO_3-N/L.

5.2 General conclusions

5.2.1 Reliable recharge estimations are essential

All examples discussed in this research illustrate the importance of a reliable recharge estimation for source water protection. Recharge magnitude is directly linked with the advection travel time in the unsaturated zone (Chapter 2). Recharge distribution also indicates "where" and "how much" water is recharging the aquifer and, consequently, plays an important role in shaping the well capture zone (Chapter 3). If we combine the estimates of recharge distribution with contaminant mass loading distribution, it is possible to define areas in which remediation efforts (*e.g.*, BMPs) are expected to yield the maximum benefit. Finally, recharge is connected to the residence time in the aquifer, and therefore to the time required for groundwater quality to improve in groundwater receptors (Chapter 4).

Recharge estimations using exclusively mathematical models, often seen in common practice, have the same uncertainty and non-uniqueness limitations of groundwater models. Therefore, independent field estimations of recharge are important and should be part of source water protection studies. When recharge distributions in models are constrained by field estimations, the uncertainty regarding hydraulic conductivity is also reduced, since both parameters can be independently adjusted during calibration to fit water level measurements.

5.2.2 The use of multiple model approaches should be encouraged

Another conclusion from all studied examples is that the simultaneous use of multiple model approaches can be useful in modelling practice, and should be encouraged in source water protection studies. For example, the estimation of the effects of BMPs (Chapter 4) combined 1D simulations, a larger scale 3D saturated flow model, and a smaller scale 3D variably-saturated flow and transport model. Rather than representing a continuously evolving model, they are different models altogether, combined to achieve a given modelling goal. The same is true for the different travel time estimations (Chapter 2) and alternative backward-transport capture zones (Chapter 3).

In most practical problems, there are more than one valid approach to represent reality; and it is not always straight-forward to chose the "best" one. In these cases, it is better to make management decisions based on multiple model results, which can capture different aspects of the problem, rather than trying to develop the elusive "best" model. Multiple approaches can be used to better understand parameter uncertainty, assess relative importance of processes and parameters (*i.e.*, process/parameter

sensitivity), minimize expert bias (since comparison results from different experts can be compared/integrated), define other models settings (*e.g.*, vertical discretization, Chapter 4), and check for consistency and calculation errors.

One of the main advantages is to deal with the issue of model simplicity, or alternatively, model complexity. Einstein is quoted with the phrase "Everything should be made as simple as possible, but not simpler", which is a useful guideline for developing models to represent complex natural systems, such as hydrological models. The problem is that, for most practical cases, it is difficult to define *a priori* what is the ideal level of simplification. The use of multiple model approaches with varying degrees of simplicity provides a potential solution to this conundrum. If approaches with different levels of complexity yield similar results (*e.g.*, Chapter 2), then we arrive at the useful conclusion that the additional complexity does not influence model conclusions for that particular prediction. In the case where the results are different, added complexity is justified and adding more complexity may be warranted. This knowledge can be useful to guide future field and numerical efforts.

Some practical suggestions to incorporate the use of multiple models into current modelling practice are: (1) During calibration, often practitioners have a few versions of the model that yield reasonable calibration. The common practice is to select the "best" version, usually the one with best calibration fit, and report the results only for this version. Instead, we suggest that results from all versions deemed reasonable should be reported and interpreted; (2) When analyzing model outputs, a critical question practitioners need to address is "Do these results make sense?". This is done by independently checking, usually by hand calculations, the order of magnitude of the results. These calculations are usually not reported. We suggest that simpler numerical models should be created for verification purposes, and that independent verifications should be reported in modelling studies; (3) Exposure to basic concepts and applications of different modelling strategies should be part of the training of future practitioners. They should be encouraged to work with different approaches, such as: analytical/numerical, deterministic/stochastic and even physically-based/non-physically-based (*e.g.*, artificial neural network models); (4) If the additional cost is warranted, modellers with different specialties can be hired to work simultaneously on the same problem;

A disadvantage of maintaining multiple models is the additional cost. However, given that water security and public/environmental health are at stake in source water protection decisions, it is not unrealistic to imagine that additional modelling costs would be justified in some cases. Also, additional costs can be minimized if modelling codes are developed to facilitate the maintenance of

multiple models. For example, instead of requiring the input of one parameter set (*e.g.*, recharge, dispersivity) or model setting (*e.g.*, spatial weighting), model codes should allow the selection of more than one input and automatically generate the combined output, such as multiple breakthrough curves, plumes, *etc*. This would eliminate the time-consuming and expensive task of updating several models every time a change is made. Inputs and outputs for all scenarios within a given model setting code could be contained in one single data location.

Another practical problem is to decide which results to use, amongst the multiple available interpretations. No generalizations can be made in this regard, as this decision depends on how adequately the different model representations are perceived to represent reality. This should remain a matter of professional judgment. However, there are some techniques that can help in this process. If different model representations are considered equally valid, the precautionary principle may be used, if a conservative stance is warranted. If their validity are different, some sort of weighing or averaging problem-specific technique can be used (*e.g.*, West et al., 2011; Poeter and Hill, 2007). The practitioner is also free to choose which scenarios to use, amongst many available, as long as there is a justification for it.

Another technique that is simple and useful in these cases is the use of "bounds" or "envelopes" encompassing results from different scenarios, as shown on Fig. 4.21. Bounds also indicate when there is too much prediction uncertainty and a firm conclusion cannot be made. For example, if the travel time in the unsaturated zone can range between 5% and 95% of the total travel time, a firm decision cannot be made based on these results regarding the importance of unsaturated zone time lag.

Finally, it is important to keep in mind that "quantity" does not replace "quality": The consideration of several modelling approaches only leads to an enhanced understanding of the problem if these approaches are deemed realistic.

5.3 Recommendations for future research

5.3.1 Compare techniques for generating recharge and mass loading distributions

For the estimation of BMP effects, a single recharge distribution was used, with different mass loading distributions varying only within the area in which BMPs were adopted. The next step is to use point estimates of recharge and mass loading to generate other recharge/mass loading scenarios and investigate how sensitive model predictions are to these distributions. A review and compilation of different techniques to estimate mass loading and recharge distributions would also be useful to practitioners.

5.3.2 Investigate effects of transient flow

All simulations for estimating BMP effects (Chapter 4) assumed steady-state flow conditions. Also, changes in nitrate mass loading were represented as step functions in time, instantaneously changing to an average value. Observed concentrations in the supply wells showed significant noise, which can be attributed to transient variations in the flow field and in nitrate loading at ground surface. A transient flow and transport model could be developed to represent these variations. This model can be used to investigate fast infiltration events (*e.g.*, snowmelt), which can pose a threat to well water quality. Also, the comparison of transient and steady-state predictions would be an interesting exercise to investigate the usefulness and limitations of both approaches in source water protection studies.

5.3.3 Investigate practical effects of dispersion

Many of the techniques presented in this research involved the solution of the advection-dispersion equation. This equation can be applied in source water protection problems not only to simulate solute transport, but also groundwater age, life expectancy and capture probability. In most practical large-scale problems, the required level of grid discretization to comply with the Courant and Peclet criteria would result in models that are too slow to generate results in a timely manner. More stable formulations (*e.g.*, upstream weighting), that artificially increase numerical dispersion, are often applied to deal with this issue. It would be useful to investigate the implications of artificially high numerical dispersion in source water protection problems. In other cases, the benefit from representing dispersion may not compensate the computational burden associated with solving the advection-dispersion equation. In these cases, it may be reasonable to consider advection as the only active transport process. Although there are several studies discussing different aspects of numerical

and real dispersion, there is a lack of applied guidelines to help practitioners assess and handle this process.

5.3.4 Consider other sources of uncertainty

The assessment of capture zone uncertainty (Chapter 3) only considered uncertainty induced by recharge. The logical next step is to include other sources of uncertainty (*e.g.*, hydraulic conductivity, types of numerical models, stratigraphy, location of aquitard windows, boundary conditions). This exercise would allow the comparison of the relevance of different sources of uncertainty in an example case.

References

Chapter 1 - References

Harbaugh, A.W., Banta, E.R., Hill, M.C., McDonald, M.G. 2000. MODFLOW-2000, the U.S. Geological Survey modular ground-water model - User guide to modularization concepts and the ground-water flow process, U.S. Geol. Surv. Open File Rep. 00-92, 121 pp.

Narasimhan, T. N. 2009. Groundwater: from mystery to management. Environmental Research Letters, 4(3), 1-11.

Oreskes, N., Shrader-Fechette, K., Belitz, K. 1994. Verification, validation, and confirmation of numerical models in the earth sciences. Science, New Series, Vol. 263:5147, pp. 641-646.

Pappenberger F., Beven, K.J. 2006. Ignorance is bliss: 7 reasons not to use uncertainty analysis. Water Resources Research 42(5): W05302. DOI: 10.1029/2005WR004820.

Prickett, T. A. 1979. Ground-water computer models-State of the art. Ground Water, 17(2), 167-173.

Province of Ontario 2004. Watershed-based source protection planning: a threats assessment framework. Technical experts committee report to the Minister of the Environment. Toronto: Queen's Printer for Ontario.

Province of Ontario 2006. Clean water act. Queen's Printer for Ontario.

Schoups, G., Hopmans, J.W., Tanji, K.K. 2006. Evaluation of model complexity and space–time resolution on the prediction of long-term soil salinity dynamics, Western San Joaquin Valley, California. Hydrological processes, 20(13), 2647-2668.

van den Belt, M. 2004. Mediated modeling: a system dynamics approach to environmental consensus building. Washington, DC: Island Press.

van den Brink, C., Zaadnoordijk, W. J., van der Grift, B., de Ruiter, P. C., Griffioen, J. 2008. Using a groundwater quality negotiation support system to change land-use management near a drinking-water abstraction in the Netherlands. Journal of Hydrology, 350(3), 339-356.

Chapter 2 - References

Baily, A., Rock, L., Watson, C.J., Fenton, O. 2011. Spatial and temporal variations in groundwater nitrate at an intensive dairy farm in south-east Ireland: Insights from stable isotope data. Agriculture, Ecosystems & Environment. 144, 308-318.

Baran, N., Richert, J., Mouvet, C. 2007. Field data and modelling of water and nitrate movement through deep unsaturated loess, Journal of Hydrology. 345, 27-37.

Bekeris, L. 2007. Field-scale evaluation of enhanced agricultural management practices using a novel unsaturated zone nitrate mass load approach. M.Sc. thesis, University of Waterloo.

Berkowitz, B., Silliman, S.E., Dunn, A.M. 2004. Impact of the capillary fringe on local flow, chemical migration, and microbiology. Vadose Zone Journal 3 (2), 534-548.

Beven, K., Germann, P. 1982. Macropores and water flow in soils. Water Resour. Res. 18, 1311-1325.

Bredehoeft, J. 2010. Models and model analysis. Ground Water. 48, 328.

Chesnaux, R., Allen, D.M. 2008. Simulating nitrate leaching profiles in a highly permeable vadose zone. Environmental Modeling and Assessment. 13, 527-539.

Cook, P.G., Jolly, I.D., Walker, G.R., Robinson, N.I. 2003. From drainage to recharge to discharge: Some timelags in subsurface hydrology. Water resources perspectives: evaluation, management and policy. Ed. Alsharhan, A.S., Wood, W.W., Elsevier Science, Amsterdam, pp.319-326.

County of Oxford 2011. Woodstock drinking water report - 2010 annual water system report.

Diersch, H-.J.G. 2006. FEFLOW Finite element subsurface flow and transport simulation system - reference manual, user's manual, white papers - release 5.3. WASY Institute for water resources planning and systems research. Berlin.

Fenton, O., Schulte, R.P.O., Jordan, P., Lalor, S.T.J., Richards, K.G. 2011. Time lag: a methodology for the estimation of vertical and horizontal travel and flushing timescales to nitrate threshold concentrations in Irish aquifers. Environmental Science & Policy 14, no. 4:419-431.

Fisher, L.H., Healy, R.W. 2008. Water movement within the unsaturated zone in four agricultural areas of the United States. J. Environ. Qual. 37, 1051-1063.

Freitas, J.G., Barker, J.F. 2011. Monitoring lateral transport of ethanol and dissolved gasoline compounds in the capillary fringe. Ground Water Monitoring and Remediation. DOI: 10.1111/j.1745-6592.2011.01338.x.

French, C., Wu, L., Meixner, T., Haver, D., Kabashima, J., Jury, W.A. 2006. Modeling nitrogen transport in the Newport Bay/San Diego Creek watershed of Southern California, Agricultural Water Management 81, 199-215.

Frind, E.O., Molson, J.W. 2004. A new particle tracking algorithm for finite element grids. FEM-MODFLOW Conference, Carlsbad, Czech Republic.

Haitjema, H. 2006. The role of hand calculations in ground water modeling. Ground Water. 44, 786–791.

Harbaugh, A.W., Banta, E.R., Hill, M.C., McDonald, M.G. 2000. MODFLOW-2000, the U.S. Geological Survey modular ground-water model - User guide to modularization concepts and the ground-water flow process, U.S. Geol. Surv. Open File Rep. 00-92, 121 pp.

Haslauer, C.P. 2005. Hydrogeologic Analysis of a complex aquifer system and impacts of changes in agricultural practices on nitrate concentrations in a municipal well field: Woodstock, Ontario. M.Sc. thesis, University of Waterloo.

Hill, M.C. 1998. Methods and guidelines for effective model calibration: U.S. Geological Survey Water-Resources Investigations Report 98-4005, 90 p.

Hill, M.C. 2006. The practical use of simplicity in developing ground water models. Ground Water. 44, 775-781. http://www.county.oxford.on.ca/Portals/_county/News/Woodstock 2010 .pdf, 2011. Access date: 2011/08/17.

Iital, A., Pachel, K., Deelstra, J. 2008. Monitoring of diffuse pollution from agriculture to support implementation of the WFD and the Nitrate Directive in Estonia. Environmental Science & Policy 11, 185-193.

Jackson, B.M., Browne, C.A., Butler, A.P., Peach, D., Wade, A.J., Wheater, H.S. 2008. Nitrate transport in Chalk catchments: monitoring, modelling and policy implications Environ. Sci. Policy 11, 125– 135.

Jackson, B.M., Wheater, H.S., Mathias, S.A., McIntyre, N., Butler, A.P. 2006. A simple model of variable residence time flow and nutrient transport in the chalk Journal of Hydrology 330, 221-234.

Koch, J.T. 2009. Evaluating regional aquifer vulnerability and BMP performance in an agricultural environment using a multi-scale data integration approach. M.Sc. thesis, University of Waterloo.

Kronvang, B., Anderson, H.E., Borgesen, C., Dalgaard, T., Larsen, S.E., Bogestrand, J., Blicher-Mathiasen, G. 2008. Effects of policy measures implemented in Denmark on nitrogen pollution of the aquatic environment. Environ. Sci. Pollut. 11, 144-152.

Lerner, D.N., Harris, R.C. 2009. The relationship between land use and groundwater resources and quality. Land Use Policy 265, S265–S273.

Meals, D.W., Dressing, S.A., Davenport, T.E. 2010. Lag time in water quality response to best management practices: A review. Journal of Environmental Quality 39 (1), 85-96.

Molson, J.W., Beckers, J., Frind, E.O., Martin, P.J. 2002. WATFLOW 3D version 4.0, A three-dimensional groundwater/surface water flow model, users guide. Ontario, Canada: Department of Earth Sciences, University of Waterloo.

Mualem, Y. 1976. A new model predicting the hydraulic conductivity of unsaturated porous media. Water Resour. Res. 12, 513–522.

Official Journal of the European Communities. 2000. Directive 2000/60/EC of the European Parliament and of the Council of 23 October 2000 establishing a framework for community action in the field of water policy, 72 pp.

Padusenko, G.R. 2001. Regional hydrogeologic evaluation of a complex glacial aquifer system in an agricultural landscape: Implications for nitrate distribution. M.Sc. thesis, University of Waterloo.

Pollock, D.W. 1994. A particle tracking post-processing package for MODFLOW, the U.S. Geological Survey Open-File Report. User's Guide for MODPATH/MONPATH-PLOT, version 3.

Province of Ontario 2006. Assessment report: Draft guidance module 3, Groundwater vulnerability analysis. Ministry of the Environment. Toronto: Queen's printer.

Refsgaard, J.C., Henriksen, H.J. 2004. Modelling guidelines – terminology and guiding principles, Advances in Water Resources. 27, 71–82.

Scanlon, B.R., Healy, R.W., Cook, P.G. 2002. Choosing appropriate techniques for quantifying groundwater recharge. Hydrogeology Journal. 10, 18–39.

Shaap, M.G., Liej, F.J., van Genuchten, M.Th. 1999. A bootstrap-neural network approach to predict soil hydraulic parameters. In: M. Th. van Genuchten, F.J. Liej and L. Wu, Editors, Characterization and Measurements of the Hydraulic Properties of Unsaturated Porous Media, University of California at Riverside, Riverside, CA, USA. pp. 1237–1250.

Sophocleous, M. 2011. On Understanding and Predicting Groundwater Response Time. Ground Water. doi: 10.1111/j.1745-6584.2011.00876.x.

Therrien, R., McLaren, R.G., Sudicky, E.A., Panday, S.M. 2005. HydroGeoSphere: A three-dimensional numerical model describing fully-integrated subsurface and surface flow and solute transport, Groundwater Simulations Group, University of Waterloo, Waterloo, Ont., Canada. 322 pp.

Tosaki, Y., Tase, N., Sasa, K., Takahashi, T., Nagashima, Y. 2011. Estimation of groundwater residence time using the 36Cl bomb pulse. Ground Water 49, 891–902.

van Genuchten, M. Th. 1980. A closed-form equation for predicting the hydraulic conductivity of unsaturated soils. SoilSci. Soc. Am. J. 44, 892-898.

Wayland, K.G., Hyndman, D.W., Boutt, D., Pijanowski, B.C., Long, D.T. 2002. Modelling the impact of historical land uses on surface-water quality using groundwater flow and solute-transport models. Lakes & Reservoirs: Research and Management 7(3):189-201.

Chapter 3 - References

Alexander, M., Berg, S.J., Illman, W.A. 2011. Field study of hydrogeologic characterization methods in a heterogeneous aquifer, Ground Water, 49(3), 365-383, doi:10.1111/j.1745-6584.2010.00729.x.

Beckers, J., Frind, E.O. 2001. Simulating groundwater flow and runoff for the Oro Moraine aquifer system. Part II. Automated calibration and mass balance calculations, J Hydrol, 243(1-2), 73-90.

Bester, M.L., Frind, E.O., Molson, J.W., Rudolph, D.L. 2006. Numerical investigation of road salt impact on an urban wellfield. Ground Water, 44(2):165–175.

Beven, K. 1993. Prophecy, Reality and Uncertainty in Distributed Hydrological Modeling, Adv Water Resour, 16(1), 41-51.

Blanke, M., Staroswiecki, M., Wu, N.E. 2001. Concepts and methods in fault-tolerant control, P Amer Contr Conf, 2606-2620.

Brugnach, M., Tagg, A., Keil, F., de Lange, W.J. 2007. Uncertainty matters: Computer models at the science-policy interface, Water Resour Manag, 21(7), 1075-1090.

Burnham, K.P., Anderson, D.R. 2002. Model selection and multi-model inference—A practical information-theoretic approach: New York, Springer-Verlag, 488 p.

Callow, I. P. 1996. Optimizing aquifer production for multiple wellfield conditions in Kitchener, Ontario. M.Sc. Thesis, Dept. of Earth Sciences, University of Waterloo, Ontario, Canada.

Camp, C. V., Outlaw, J.E. 1998. Stochastic approach to delineating wellhead protection areas, J Water Res Pl-Asce, 124(4), 199-209.

Carrera, J., Neuman, S. 1986. Estimation of aquifer parameters under transient and steady-state conditions: 2. Uniqueness, stability and solution algorithms, Water Resour. Res., 22(2), 211– 227.

CH2M-HILL, and Papadopulos & Associates 2003. Alder Creek groundwater study: Final report prepared for the Regional Municipality of Waterloo.

Enzenhoefer, R., Nowak, W., Helmig, R. 2011. Probabilistic exposure risk assessment with advective-dispersive well vulnerability criteria. Advances in Water Resources, 36:121-132, http://dx.doi.org/10.1016/j.advwatres.2011.04.018.

Esling, S.P., Keller, J.E., Miller, K.J. 2008. Reducing capture zone uncertainty with a systematic sensitivity analysis, Ground Water, 46(4), 570-578.

Evers, S., Lerner, D.N. 1998. How uncertain is our estimate of a wellhead protection zone? Ground Water 36:49–57.

Feyen, L., Beven, K., de Smedt, F., Freer, J. 2001. Stochastic capture zone delineation within the generalized likelihood uncertainty estimation methodology: conditioning on head observations. Water Resour. Res. 37(3):625-638. ISSN: 0043-1397.

Franke, O.L., Reilly, T.E., Pollock, D.W., LaBaugh, J.W. 1998. Estimating areas contributing recharge to wells. USGS Circular 1174. USGS, Reston, Virginia.

Franzetti, S., Guadagnini, A. 1996. Probabilistic estimation of well catchments in heterogeneous aquifers. J. Hydrol. 174(1-2):149-171.

Frind, E.O., Molson, J.W. 2004. A new particle tracking algorithm for finite element grids. FEM-MODFLOW Conference, Carlsbad, Czech Republic.

Frind, E.O., Molson, J.W., Rudolph, D.L. 2006. Well vulnerability: A quantitative approach for source water protection. Ground Water, 44(5):732–742.

Frind, E.O., Muhammad, D.S., Molson, J.W. 2002. Delineation of three-dimensional capture zones in complex multi-aquifer systems. Ground Water, 40(6), 586-589.

Frind, E.O., Sudicky, E.A., Schellenberg, S.L. 1987. Micro-scale modelling in the study of plume evolution in heterogeneous media. Stochastic Hydrology and Hydraulics, 1(4):263 279.

Gelhar, L.W., Axness, C.L. 1983. Three-dimensional stochastic analysis of macrodispersion in aquifers. Water Resources Research, 19(1):161–180.

Govindaraju, R.S., Jones, S.E., Kavvas, M.L. 1988. On the Diffusion Wave Model for Overland Flow 1. Solution for steep slopes, Water Resour. Res., 24(5), 734–744.

Harbaugh, A.W., Banta, E.R., Hill, M.C., McDonald, M.G. 2000. MODFLOW-2000, the U.S. Geological Survey modular ground-water model - User guide to modularization concepts and the ground-water flow process, U.S. Geol. Surv. Open File Rep. 00-92, 121 pp.

Jones, J.P., Sousa, M.R., Frind, E.O., Rudolph, D.L. 2009. Determining the influence of surface, unsaturated and saturated processes on source water protection strategies: a multi-model study.

GeoHalifax 2009 - 62nd Canadian Geotechnical Conference & 10th Joint CGS/IAH-CNC Groundwater Conference. September 20-24, 2009, Halifax, NS, Canada.

Kunstmann, H., Kinzelbach, W. 2000. Computation of stochastic wellhead protection zones by combining the first-order second-moment method and Kolmogorow backward equation analysis. Journal of Hydrology 237, no. 3–4: 127–146.

Martin, P.J. 1994. Modelling of the North Waterloo multi-aquifer system. M.Sc. Thesis, Department of Earth and Environmental Sciences, University of Waterloo.

Martin, P.J., Frind, E.O. 1998. Modeling a complex multi-aquifer system: The Waterloo Moraine. Ground Water 36(4), 679–690.

Molson, J.W., Beckers, J., Frind, E.O., Martin, P.J. 2002. WATFLOW 3D version 4.0, A Three-Dimensional Groundwater/Surface Water Flow Model, Users Guide. Ontario, Canada: Department of Earth Sciences, University of Waterloo.

Molson, J.W., Frind, E.O. 2005. WTC: The Waterloo Transport Code, a 3D advective-dispersive mass transport and groundwater age model, User Guide, Version 3.0, University of Waterloo and Université Laval, Canada.

Molson, J.W., Frind, E.O. 2012. On the use of mean groundwater age, life expectancy and capture probability for defining aquifer vulnerability and time-of-travel zones for source water protection. J. Contam. Hydrol. (2011), doi:10.1016/j.jconhyd.2011.06.001

Neuman, S.P. 2003. Maximum likelihood Bayesian averaging of uncertain model predictions. Stochastic Environmental Research and Risk Assessment 17, 291-305.

Neupauer, R.M., Wilson, J.L. 1999. Adjoint method for obtaining backward-in-time location and travel time probabilities of a conservative groundwater contaminant. Water Resources Research, 35(11):3389–3398.

Oreskes, N., Shrader-Fechette, K., Belitz, K. 1994. Verification, Validation, and Confirmation of Numerical Models in the Earth Sciences. Science, New Series, Vol. 263:5147, pp. 641-646.

Pappenberger, F., Beven, K.J., 2006. Ignorance is bliss: 7 reasons not to use uncertainty analysis. Water Resources Research 42(5): W05302. DOI: 10.1029/2005WR004820.

Piersol, J. 2005. Evaluating groundwater supply, sustainable capacity, and pollution threats for an urban well field in a semi-arid coastal region: Aguadulce, Panama. M.Sc. Thesis, Department of Earth Sciences, University of Waterloo.

Poeter, E. P., Hill, M.C. 2007. MMA, a computer code for multi-model analysis, U.S. Geol. Surv. Tech. Methods, TM6-E3, 113 pp.

Poeter, E., 2007. "All Models are Wrong, How Do We Know Which are Useful?" – Looking Back at the 2006 Darcy Lecture Tour. Ground Water, Vol. 35:4, 390-391. doi: 10.1111/j.1745-6584.2007.00350.x

Poeter, E.P., Anderson, D.R. 2005. Multi-model ranking and inference in ground-water modeling: Ground Water, v. 43, no. 4, p. 597–605.

Province of Ontario 2004. Watershed-based Source Protection Planning: A Threats Assessment Framework. Technical Experts Committee Report to the Minister of the Environment. Toronto: Queen's Printer for Ontario.

Province of Ontario 2006. Clean Water Act. Queen's Printer for Ontario.

Raffensperger, C., Tickner, J. 1999. Protecting Public Health and the Environment: Implementing the Precautionary Principle. Island Press, Washington, DC.

Rahman, R., Frind, E.O., Rudolph, D.L. 2010. Assessing the Impact of Beneficial Management Practices for controlling nitrate concentrations in well water. GQ10, Proc. 7th International Groundwater Quality Conference, Zurich, Switzerland. IAHS Publ. 342, 2011, 326-329.

Refsgaard, J.C., Henriksen, H.J., Harrar, W.G., Scholten, H., Kassahun, A. 2005. Quality assurance in model based water management - review of existing practice and outline of new approaches, Environ. Modell. Softw., 20(10), 1201-1215.

Refsgaard, J.C., van der Sluijs, J.P., Hojberg, A.L., Vanrolleghem, P.A. 2007. Uncertainty in the environmental modelling process - A framework and guidance, Environ. Modell. Softw., 22(11), 1543-1556.

Schroeter & Associates 1996. GAWSER: Guelph All-Weather Sequential Events Runoff Model, Version 6.5, Training Guide and Reference Manual.

Singh, A., Mishra, S., Ruskauff, G. 2010. Model averaging techniques for quantifying conceptual model uncertainty. Ground Water, 48:701–715.

Stauffer, F., Guadagnini, A., Butler, A., Hendricks Franssen, H.J., van de Wiel, N., Bakr, M., Riva, M., Guadagnini, L. 2005. Delineation of Source Protection Zones Using Statistical Methods Water Resour. Manage. 2005, 19 (2) 163– 185.

Sudicky, E.A. 1986. A natural gradient experiment on solute transport in a sand aquifer: Spatial variability of hydraulic conductivity and its role in the dispersion process. Water Resour. Res. 22, 2069-2082.

Therrien, R., McLaren, R.G., Sudicky, E.A., Panday, S.M. 2005. HydroGeoSphere: A three-dimensional numerical model describing fully-integrated subsurface and surface flow and solute transport, Groundwater Simulations Group, Univ. of Waterloo, Waterloo, Ont., Canada, 322 p.

U.S. Environmental Protection Agency 1987. Guidelines for delineation of wellhead protection areas. Office of Water, Report EPA 4405—93-001.

U.S. Environmental Protection Agency 1997. State Source Water Assessment and Protection Programs Guidance: Final Guidance. Office of Water, Report EPA-816-R-97-009.

van Genuchten, M.Th. 1980. A closed-form equation for predicting the hydraulic conductivity of unsaturated soils. Soil Sci. Soc. Am. J. 44:892-898.

van Leeuwen, M., de Stroet, C., Butler, A., Tompkins, J. 1998. Stochastic determination of well capture zones. Water Resour. Res. 34(9):2215-2233. ISN: 0043-1397.

Varljen, M.D., Shafer, J.M. 1991. Assessment of uncertainty in time-related capture zones using conditional simulation of hydraulic conductivity. Ground Water 29, no. 5: 737–748.

Vassolo, S., Kinzelbach, W., Schäfer, W. 1998. Determination of a well head protection zone by inverse stochastic modeling. Journal of Hydrology, 206.

Wassenaar, L.I., Hendry, M.J., Harrington, N. 2006. Decadal Geochemical and Isotopic Trends for Nitrate in a Transboundary Aquifer and Implications for Agricultural Beneficial Management Practices, Environmental Science & Technology, 40 (15): 4626-4632.

West, A.C.F., Stratton, B., Watt., S. 2011. Incorporating Uncertainty into Delineation of Wellhead Protection Areas: A General Discussion and Some Examples. GeoHydro 2011 - Joint meeting of the Canadian Quaternary Association and the Canadian Chapter of the International Association of Hydrogeologists. August 28-31, 2011, Quebec City, QC, Canada.

Wheater, H.S., Tompkins, J.A., van Leeuwen, M., Butler, A.P. 2000. Uncertainty in groundwater flow and transport modelling - a stochastic analysis of well protection zones, Hydrol. Processes 14, 2019-2029.

Ye, M., Meyer, P. D., Neuman, S. P. 2008. On model selection criteria in multimodel analysis, Water Resour. Res., 44, W03428, doi:10.1029/2008WR006803.

Ye, M., Neuman, S.P., Meyer, P.D. 2004. Maximum likelihood Bayesian averaging of spatial variability models in unsaturated fractured tuff: Water Resources Research, v. 40, W05113, doi:10.1029/2003WR002557.

Chapter 4 - References

Agriculture and Agri-Food Canada 2010. Watershed Evaluations of Beneficial Management Practices (WEBs), Toward Enhanced Agricultural Landscape Planning, Four-year Review (2004/5-2007/8).

Almasri, M. N. and Kaluarachchi, J.J. 2007. Modeling nitrate contamination of groundwater in agricultural watersheds. Journal of Hydrology. 343(3-4): 211–229. doi:10.1016/j.jhydrol.2007.06.016

Avery A.A. 1999. Infantile methemoglobinemia: reexamining the role of drinking water nitrates. Environ Health Perspect. 1999;107:1–8.

Baily, A., Rock, L., Watson, C.J., Fenton, O. 2011. Spatial and temporal variations in groundwater nitrate at an intensive dairy farm in south-east Ireland: Insights from stable isotope data. Agriculture, Ecosystems & Environment. 144, 308-318.

Beegle, D.B., Carton, O.T., Bailey, J.S. 2000. Nutrient management planning: Justification, theory, and practice. Journal of Environmental Quality 29:72-79.

Bekeris, L. 2007. Field-Scale Evaluation of Enhanced Agricultural Management Practices Using a Novel Unsaturated Zone Nitrate Mass Load Approach. Master's thesis, University of Waterloo.

Bernardo, D.J., Mapp, H.P., Sabbagh, G.J., Geleta, S., Watkins, K.B., Elliott, R.L., & Stone, J.F. 1993. Economic and environmental impacts of water quality protection policies: 2. Application to the Central High Plains. Water resources research, 29(9), 3081-3091.

Berner E.K., R.A. Berner. 1996. Global Environment: Water, Air, and Geochemical Cycles, Prentice Hall, NJ.

Beven, K., 1993. Prophecy, reality and uncertainty in distributed hydrological modeling. Adv Water Resour, 16(1), 41-51.

Böhlke, J. K. 2002. Groundwater recharge and agricultural contamination. Hydrogeology Journal, 10(1), 153-179.

Brook, J. M. 2012. Evaluating Innovative Nutrient Management Options and Seasonal Groundwater Recharge Dynamics in an Agricultural Source Water Protection Area.

Capone D.G., Bautista M.F. 1985. A groundwater source of nitrate in nearshore marine sediments. Nature 313: 214–216.

Cellier, B., Bouraoui, F., Billen, G. et al. 2011. Nitrogen as a threat to European water quality. In: The European Nitrogen Assessment, ed. M. A. Sutton, C. M. Howard, J. W. Erisman et al. Cambridge University Press.

Chesnaux, R., Allen, D.M., Graham, G. 2007. Assessment of the impact of nutrient management practices on nitrate contamination in the Abbotsford-Sumas Aquifer. Environmental science & technology, 41(21), 7229-7234.

Comly H.H. 1945. Cyanosis in infants caused by nitrates in well-water. JAMA 129:112–116. Reprinted in 1987, JAMA. 1945;257(20):2788–2792.

County of Oxford 2005. Digital Elevation Model; 10m by 10m cell size [computer file]. Woodstock, ON.

County of Oxford 2009. Summary Reports for Municipalities - Schedule 22 of Regulation 170/03. Woodstock Well Supply. Certificate of Approval # 2490- 7FJJFH. Electronic Source: http:// www.county.oxford.on.ca/Portals/county/News/ WoodstockSum08.pdf, 2009. Access date: 2009/05/25

Cowan,W.R. 1975. Quaternary Geology of the Woodstock Area – Southern Ontario; Geological Report 119. Tech. Rep., Ontario Ministry of Natural Resources, Division of Mines, 1975.

Critchley, C.E. 2010. Stimulating In Situ Denitrification in an Aerobic, Highly Conductive Municipal Drinking Water Aquifer

Davidson, E.A., David, M.B., Galloway, J.N., Goodale, C.L., Haeuber, R., Harrison, J.A., ... Snyder, C.S. 2012. Excess Nitrogen in the U. S. Environment: Trends, Risks, and Solutions. Issues in Ecology, (15).

Delgado, J.A., Shaffer, M.J. 2008. Nitrogen Management Modeling Techniques: Assessing Cropping Systems/Landscape Combinations. Book Chapter In R.F. Follett and J.L. Hatfield (eds) Nitrogen in the Environment: Sources, Problems and Management. pp. 539-570. Elsevier Science, New York, USA.

D'Elia C.F., Webb K.L., Porter, J.W. 1981. Nitrate rich groundwater inputs to Discovery Bay, Jamaica: a significant source of N to local coral reefs? Bull. Mar. Sci. 3: 903-910.

Diersch, H-.J.G. 2006. FEFLOW - Finite Element Subsurface Flow and Transport Simulation System - Reference manual, User's Manual, White Papers - Release 5.3. WASY Institute for Water Resources Planning and Systems Research. Berlin; 2006.

Doherty, J. 2005. PEST: Model Independent Parameter Estimation. User Manual, Fifth Edition. Watermark Numerical Computing, Brisbane, Australia.

Durand, P., Breuer, L., Johnes, P. J., Billen, G., Butturini, A., Pinay, G., van Grinsven, H., Garnier, J., Rivett, M. 2011. Nitrogen processes in aquatic ecosystems. In: The European Nitrogen Assessment, ed. M. A. Sutton, C. M. Howard, J. W. Erisman et al. Cambridge University Press., 126-146.

EEA, 2005. The European environment — State and outlook 2005. State of the environment report. European Environment Agency, Copenhagen.

Erisman, J. W., Sutton, M. A., Galloway, J., Klimont, Z., Winiwarter, W. 2008. How a century of ammonia synthesis changed the world. Nature Geoscience, 1, 636–639.

Erisman, J. W., van Grinsven, H., Grizzetti, B., Bouraoui, F., Powlson, D., Sutton, M. A., Bleeker, A., Reis S. 2011. The European nitrogen problem in a global perspective. In: The European Nitrogen Assessment, ed. M. A. Sutton, C. M. Howard, J. W. Erisman et al. Cambridge University Press.

European Environment Commission 1991. Council Directive 91/676/EEC of 12 December 1991 concerning the protection of waters against pollution caused by nitrates from agricultural sources. Official Journal L, 375(31), 12.

Evers, S., Lerner, D.N. 1998. How uncertain is our estimate of a wellhead protection zone? Ground Water 36:49–57.

Flerchinger, G.N. 2000. The Simultaneous Heat and Water (SHAW) Model: Technical Documentation. Technical Report NWRC 2000-9, Northwest Watershed Research Center, USDA Agricultural Research Service, Boise, Idaho.

Frind, E.O., Duynisveld, W.H.M., Strebel, O., Boettcher, J. 1990. Modeling of multicomponent transport with microbial transformation in groundwater: The Fuhrberg case. Water Resources Research, 26(8), 1707-1719.

Frind, E.O., Hokkanen, G.E. 1987. Simulation of the Borden plume using the alternating direction Galerkin technique. Water Resources Research, 23(5), 918-930.

Galloway, J. N., Townsend, A. R., Erisman, J. W., Bekunda, M., Cai, Z., Freney, J. R., Martinelli, L.A., Seitzinger, S. P., Sutton, M. A. 2008. Transformation of the nitrogen cycle: recent trends, questions, and potential solutions. Science, 320(5878), 889-892.

Golder Associates 2001. Phase II Groundwater Protections Study – County of Oxford: Volume I. Tech. Rep., 2001.

Google Earth Pro 2013a. Southern Ontario, Canada. 43° 32’ 23.33”N, 80° 35’ 15.94”W, Eye alt 677.61km. CNES/Spot 2013, NOAA 2013, Terrametrics 2013. Google earth v7.0.1.8244. [May 30, 2013].

Google Earth Pro 2013b. Woodstock, Ontario, Canada. 43° 05’ 15.56”N, 80° 45’ 21.72”W, Eye alt 12.31km. First Base Solutions 2013. Google earth v7.0.1.8244. [May 30, 2013].

Goss, M. J., Barry, D. A. J., Rudolph, D. L. 1998. Contamination in Ontario farmstead domestic wells and its association with agriculture:: 1. Results from drinking water wells. Journal of Contaminant Hydrology, 32(3), 267-293.

Green, C.T., Puckett, L.J., Böhlke, J.K., Bekins, B.A., Phillips, S.P., Kauffman, L.J., ... Johnson, H.M. 2008. Limited occurrence of denitrification in four shallow aquifers in agricultural areas of the United States. Journal of environmental quality, 37(3), 994-1009.

Grizzetti, B., Bouraoui, F., Billen, G. et al. 2011. Nitrogen as a threat to European water quality. In: The European Nitrogen Assessment, ed. M. A. Sutton, C. M. Howard, J. W. Erisman et al. Cambridge University Press.

Haslauer, C.P. 2005. Hydrogeologic Analysis of a Complex Aquifer System and Impacts of Changes in Agricultural Practices on Nitrate Concentrations in a Municipal Well Field: Woodstock, Ontario. Master’s thesis, University of Waterloo.

Haygarth, P.M., Jarvis, S.C. 2002. Agriculture, Hydrology, and Water Quality. CAB International Publishing, Oxford, NY.

Heagle, D.J. 2000. Nitrate Geochemistry of a Regional Aquifer in an Agricultural Landscape: Woodstock, Ontario. Master’s thesis, University of Waterloo.

Health Canada 2012. Guidelines for Canadian Drinking Water Quality Summary Table. Prepared by the Federal-Provincial-Territorial Committee on Drinking Water of the Federal-Provincial-Territorial Committee on Health and the Environment. August 2012.

Hérivaux, C., Orban, P., Brouyère, S. 2013. Is it worth protecting groundwater from diffuse pollution with agri-environmental schemes? A hydro-economic modeling approach. Journal of Environmental Management, 128, 62-74.

Jakszyn, P.; González, C.A. 2006. Nitrosamine and related food intake and gastric and oesophageal cancer risk: A systematic review of the epidemiological evidence. World Journal of Gastroenterology 12: 4296–4303.

Kassenaar, D. 2004. Viewlog. Computer Program by Earth FX, Toronto, version 3.0, 2004.

Koch, J.T. 2009. Evaluating Regional Aquifer Vulnerability and BMP Performance in an Agricultural Environment Using a Multi-Scale Data Integration Approach. Master's thesis, University of Waterloo.

Konikow, L. F., Bredehoeft, J. D. 1992. Ground-water models cannot be validated. Advances in water resources, 15(1), 75-83.

Martin, C., Molenat, J., Gascuel-Odoux, C., Vouillamoz, J.M., Robain, H., Ruiz, L., ... Aquilina, L. 2006. Modelling the effect of physical and chemical characteristics of shallow aquifers on water and nitrate transport in small agricultural catchments. Journal of Hydrology, 326(1), 25-42.

Martin, P.J., Frind, E.O. 1998. Modeling a complex multi-aquifer system: The Waterloo Moraine. Ground Water 36(4), 679–690.

Mehl, S., Hill, M. C., Leake, S. A. (2006). Comparison of local grid refinement methods for MODFLOW. Ground water, 44(6), 792-796.

Molénat, J., Gascuel-Odoux, C. 2002. Modelling flow and nitrate transport in groundwater for the prediction of water travel times and of consequences of land use evolution on water quality. Hydrological Processes, 16(2), 479-492.

Mualem, Y. 1976. A new model predicting the hydraulic conductivity of unsaturated porous media. Water Resour. Res. 12, 513–522.

Nolan, B.T., Ruddy, B.C., Hitt, K.J., Helsel, D.R. 1997. Risk of Nitrate in Groundwaters of the United States A National Perspective. Environmental science & technology, 31(8), 2229-2236.

Null, K.A., Dimova N.T., Knee, K.L., Esser, B.K., Swarzenski, P.W., Singleton, M.J., Stacey, M., Paytan, A., 2012. Submarine Groundwater Discharge-Derived Nutrient Loads to San Francisco Bay: Implications to Future Ecosystem Changes. Estuaries and Coasts (2012) 35:1299–1315. DOI 10.1007/s12237-012-9526-7

Official Journal of the European Communities 1998. Directive 98/83/EC on the quality of water intended for human consumption. Official Journal of the European Communities. European Union. 1998; L330: 32-54.

Oreskes, N., Shrader-Fechette, K., Belitz, K. 1994. Verification, validation, and confirmation of numerical models in the earth sciences. Science, New Series, Vol. 263:5147, pp. 641-646.

Padusenko, G.R. 2001. Regional Hydrogeologic Evaluation of a Complex Glacial Aquifer System in an Agricultural Landscape: Implications for Nitrate Distribution. Master's thesis, University of Waterloo.

Power, J., Schepers, J.S. (1989). Nitrate contamination of groundwater in North America. Agriculture, ecosystems & environment, 26(3), 165-187.

Powlson, D.S., Addiscott, T.M., Benjamin, N., Cassman, K.G., de Kok, T.M., van Grinsven, H., ... Van Kessel, C. 2008. When does nitrate become a risk for humans? Journal of environmental quality, 37(2), 291-295.

Rahman, R., Frind, E.O., Rudolph, D.L. 2010. Assessing the Impact of Beneficial Management Practices for controlling nitrate concentrations in well water. GQ10, Proc. 7th International Groundwater Quality Conference, Zurich, Switzerland. IAHS Publ. 342, 2011, 326-329.

Rivett, M.O., Buss, S.R., Morgan, P., Smith, J.W., Bemment, C.D. 2008. Nitrate attenuation in groundwater: A review of biogeochemical controlling processes. Water Research, 42(16), 4215-4232.

Scanlon, B.R., Healy, R.W., Cook, P.G. 2002. Choosing appropriate techniques for quantifying groundwater recharge. Hydrogeology Journal. 10, 18–39.

Schroeder, P.R., Aziz, N.M., Lloyd, C.M., Zappi, P.A. 1994. The Hydrologic Evaluation of Landfill Performance (HELP) Model: User's Guide for Version 3, EPA/600/R-94/168a, September 1994, U.S. Environmental Protection Agency Office of Research and Development, Washington, DC.

Sebol, L.A. 2000. Determination of Groundwater Age Using CFC's in Three Shallow Aquifers in Southern Ontario. Master's thesis, University of Waterloo.

Shaap, M.G., Liej, F.J., van Genuchten, M.Th. 1999. A bootstrap-neural network approach to predict soil hydraulic parameters. In: M. Th. van Genuchten, F.J. Liej and L. Wu, Editors, Characterization and Measurements of the Hydraulic Properties of Unsaturated Porous Media, University of California at Riverside, Riverside, CA, USA. pp. 1237–1250.

Smil, V. 1999. Detonator of the population explosion. Nature 400, 415.

Smil, V. 2001. Enriching the Earth: Fritz Haber, Carl Bosch and the Transformation of World Food Production (MIT Press,Cambridge, MA, 2001).

Smith, L., Schwartz, F.W. 1981. Mass transport: 2. Analysis of uncertainty in prediction. Water Resources Research, 17(2), 351-369.

Sousa, M.R., Frind, E.O., Rudolph, D.L. 2013. An integrated approach for addressing uncertainty in the delineation of groundwater management areas, Journal of Contaminant Hydrology, Volume 148, May 2013, Pages 12-24

Strebel, O., Duynisveld, W.H.M., Böttcher, J. 1989. Nitrate pollution of groundwater in western Europe. Agriculture, ecosystems & environment, 26(3), 189-214.

Sutton, M.A., Howard, C.M., Erisman, J.W., Billen, G., Bleeker, A.,Grennfelt, P., van Grinsven, H. and Grizzetti, B., 2011. The European Nitrogen Assessment: Sources, effects and policy perspectives. Cambridge, Cambridge University Press, 2011. ISBN: 97811070061.

Tomer, M.D., Burkart, M.R. 2003. Long-term effects of nitrogen fertilizer use on ground water nitrate in two small watersheds. Journal of Environmental Quality, 32(6), 2158-2171.

U.S. Environmental Protection Agency 2009. National Primary Drinking Water Regulations. EPA 816-F-09-004. May 2009.

Ulén, B., Johansson, G., Simonsson, M. 2008. Changes in nutrient leaching and groundwater quality during long-term studies of an arable field on the Swedish south-west coast. Nordic Hydrology.

Volume: 39 Number: 1, pp 63-77.van Genuchten, M.Th. 1980. A closed-form equation for predicting the hydraulic conductivity of unsaturated soils. Soil Sci. Soc. Am. J. 44:892-898.

van Grinsven, H.J.M., Ward, M.H., Benjamin, N., de Kok, T.M. 2006. Does the evidence about health risks associated with nitrate ingestion warrant an increase of the nitrate standard for drinking water? Environmental Health:A Global Access Science Source 5, 26.

Walton G. 1951. Survey of literature relating to infant methemoglobinemia due to nitrate-contaminated water. Am J Public Health. 1951;41:986–996.

Wassenaar, L.I., Hendry M. J., Harrington N. 2006. Decadal Geochemical and Isotopic Trends for Nitrate in a Transboundary Aquifer and Implications for Agricultural Beneficial Management Practices, Environmental Science & Technology, 40 (15): 4626-4632.

WHO 2007. Public Water Supply and Access to Improved Water Sources. World Health Organization. Geneva.

Wriedt, G., Bouraoui, F. 2009. Towards a large scale assessment of water availability in Europe, European Commission Joint Research Centre, Luxembourg.

Yadav, S., Wall, D. 1998. Benefit-cost analysis of best management practices implemented to control nitrate contamination of groundwater. Water Resources Research 34(3):doi: 10.1029/97WR01981. issn: 0043-1397.

Zhang, W.L., Tian, Z.X., Zhang, N., Li, X.Q. 1996. Nitrate pollution of groundwater in northern China. Agriculture, Ecosystems & Environment, 59(3), 223-231.

Chapter 5 - References

Beven, K., 1993. Prophecy, reality and uncertainty in distributed hydrological modeling. Adv Water Resour, 16(1), 41-51.

Oreskes, N., Shrader-Fechette, K., Belitz, K. 1994. Verification, validation, and confirmation of numerical models in the earth sciences. Science, New Series, Vol. 263:5147, pp. 641-646.

Poeter, E. P., Hill, M.C. 2007. MMA, a computer code for multi-model analysis, U.S. Geol. Surv. Tech. Methods, TM6-E3, 113 pp.

West, A.C.F., Stratton, B., Watt., S. 2011. Incorporating uncertainty into delineation of wellhead protection areas: A general discussion and some examples. GeoHydro 2011 - Joint meeting of the Canadian Quaternary Association and the Canadian Chapter of the International Association of Hydrogeologists. August 28-31, 2011, Quebec City, QC, Canada.